

Copyright

by

Nicole Marie Bergmann

2005

The Dissertation Committee for Nicole Marie Bergmann certifies that this is the approved version of the following dissertation:

Molecularly Imprinted Polyacrylamide Polymers and Copolymers with Specific Recognition for Serum Proteins

Committee:

Nicholas A. Peppas, Supervisor

Lisa Brannon-Peppas

Krishnendu Roy

Lynn Loo

Christine Schmidt

**Molecularly Imprinted Polyacrylamide Polymers and Copolymers with
Specific Recognition for Serum Proteins**

by

Nicole Marie Bergmann, B.S.; B.M.E.

Dissertation

Presented to the Faculty of the Graduate School of

the University of Texas at Austin

in Partial Fulfillment

of the Requirements

for the Degree of

Doctor of Philosophy

The University of Texas at Austin

December, 2005

**To My Loving Family,
For Your Constant Support, Understanding, and Patience.**

ACKNOWLEDGEMENTS

I would like to thank Professor Nicholas Peppas for his constant support during the course of my Ph.D. His advice, encouragement, and most of all unwavering support were of immense help, and I will always be indebted to him. Nicholas, I will never forget your support at Purdue, and my time at Texas was the best of my life. Thanks for bringing us with you.

I would also like to thank Lisa Brannon-Peppas for providing professional advice on many different topics, including how to handle the faculty search. I am also grateful to my dissertation committee members: Professors Krishnendu Roy, Christine Schmidt, and Lynn Loo for their support.

I feel extremely fortunate to have worked with some wonderful colleagues during my graduate studies: Kristy, Lala, Jennifer, Ebru, Christina, Bumsang, Mark, Dave, Jay, Zach, Hunter, Brock, Dan, Terry, Omar, Gianfranco, Elena, and, Giovanna. To Don especially, thank you for your help with the SEM imaging. It became an integral part of this work. Tracy, thanks for the much-needed help with FTIR and DSC and for the patience with my incessant questions. You have been my lifeline to sanity these final months, and I am so glad that we have become close. Finally, to John Huynh, the (w)undergrad, I could not have finished this thesis without your help. You are the hardest worker and brightest student that I have ever seen. Love ya, buddy. I wish you nothing but the best. I know you will be successful in whatever you do.

I would also like to thank my friends for standing by me through tough times. Wilsaan, you were always my rock to lean on, and I will forever treasure your friendship. You'll get there soon, I promise. *Love and Dance (Not Hate and Don't Dance)* is right around the corner. Mary, your e-mails and humor never ceased to brighten my dark days. All I had to do was think of the magical yellow poncho if I wanted to smile. DW, my success as a researcher was formed in

your lab, and I owe my love of TE largely to you. Congrats on the tenure. You deserve every award and accolade you get.

PKJ, you are the best friend anyone could ever ask for. You have stuck by me in good times and bad. Everything this thesis is, I owe to you. This would not be complete if not for your wonderful patience and support. You are my soulmate and best friend.

Finally, I would like to dedicate this work to my family (who probably deserves this Ph.D. as much as I do) for their immense patience and understanding. I love you more than words can express. Dad, when times got hard, your tough love and steady advice set me straight. Mom, your tenderness and wonderful hugs always calmed my nerves. Scott, you are not just my big brother, you were my inspiration to pick myself up the many times I fell. Through you, I saw how to fight through adversity without becoming bitter (No small feat). To the members of my extended family, here for me in person and in spirit, I will always be indebted. I believe that such loving support makes me the luckiest person in the world. This degree is for all of you. I love all you guys.

Molecularly Imprinted Polyacrylamide Polymers and Copolymers with Specific Recognition for Serum Proteins

Publication No. _____

Nicole Marie Bergmann, Ph.D.

The University of Texas at Austin, 2005

Supervisor: Nicholas A. Peppas

Using molecular imprinting, polyacrylamide polymers were created with recognition for serum proteins in aqueous solution. By dissolving the protein in solution with functional monomers containing electrostatic groups, polymers with specific recognition sites for the macromolecule were created. The presence of three functional monomers that are anionic, cationic, and hydrogen-bond donating gave imprinted P(MAA-DMAEMA-Aam)MIP polymers that exhibited a ~200% increase in recognition to lysozyme template as compared to recognition by non-imprinted control. In addition, the P(MAA-DMAEMA-Aam)MIP polymer exhibited a 20% increase in recognition to chicken lysozyme template compared to the human lysozyme and a 30% increase over the similarly sized macromolecule, cytochrome c. These results gave proof of the formation of a network with specific cognitive sites for the template.

In addition, the overall macroscopic properties of protein imprinted gels were examined using scanning electron microscopy, where definite morphological differences were observed between the MIP polymers and the controls. Fourier Transform Infrared Spectroscopy determined that the presence of template had no effect upon the overall gel composition, while differential scanning calorimetry was used to determine the molecular weight between crosslinks of MIP polymers and controls.

As an investigation of controlled drug delivery system, gels were also loaded with lysozyme, and the release of the protein was calculated. Imprinted gels exhibited a longer sustained release over controls, with P(MAA-DMAEMA-Aam)MIP polymers exhibiting the slowest release, where only ~80% of the protein was released after 72 h. This is compared to P(MAA-DMAEMA-Aam)C gel that exhibited ~100% release after 36 h. In all cases, released lysozyme retained enzymatic activity. The gels also exhibited good *in vitro* biocompatibility when in contact with 3T3 fibroblasts.

This work forms the foundation of fabricating polymer gels with specific recognition to macromolecules. We feel these networks hold promise as recognition components in the next generation of biomaterials and drug delivery systems. Using specific chemical groups that mimic functionalities recognized by natural macromolecules, completely synthetic materials with specific selectivity for a target ligand can be designed. It is believed that such materials can be incorporated into biosensors, responsive drug delivery systems, or other diagnostic devices requiring the detection of specific molecules.

TABLE OF CONTENTS

CHAPTER 1: INTRODUCTION	1
REFERENCES CITED	3
CHAPTER 2: BACKGROUND-MOLECULAR IMPRINTING OF POLYMERIC MATERIALS 5	
2.1 MOLECULAR RECOGNITION	5
2.2 NATURAL RECOGNITION SYSTEMS	5
2.2.1 <i>Molecular Recognition in Proteins</i>	5
2.2.2 <i>Molecular Recognition in the Immune System</i>	6
2.2.3 <i>Cellular Molecular Recognition</i>	8
2.3 ENGINEERING BIOMATERIALS WITH MOLECULAR RECOGNITION	9
2.3.1 <i>Early Biomaterial Attempts</i>	9
2.3.2 <i>Strategies for Biomolecular Recognition</i>	12
2.4 BIOMATERIALS	13
2.4.1 <i>Natural Biomaterials</i>	13
2.4.2 <i>Synthetic Polymers as Biomaterials</i>	14
2.5 MOLECULAR RECOGNITION USING SYNTHETIC POLYMER NETWORKS	18
2.6 MOLECULAR IMPRINTING	18
2.6.1 <i>Molecular Imprinting Principles</i>	19
2.6.2 <i>Molecular Imprinting in Natural Molecules</i>	20
2.6.3 <i>Covalent Imprinting in Polymers</i>	21
2.6.4 <i>Non-Covalent Imprinting in Polymers</i>	22
2.7 OBSTACLES IN LARGE MOLECULAR WEIGHT TEMPLATE IMPRINTING	28
2.7.1 <i>Diffusional Limits in Large Molecular Weight MIPs</i>	29
2.7.2 <i>Limits of Protein Dissolution</i>	30
2.8 APPLICATIONS OF MIP TECHNOLOGY	31
2.8.1 <i>Imprinted Hydrogels as Carriers for Controlled Release</i>	31
2.8.2 <i>Intelligent Gels: Environmentally Responsive DDS</i>	32
2.8.3 <i>MIP Hydrogels as Sensing/Actuating Elements in DDS</i>	37
2.9 FIGURES	41
2.10 REFERENCES CITED	50
CHAPTER 3: OBJECTIVES	70
CHAPTER 4: FABRICATION OF ACRYLAMIDE-BASED MIP POLYMERS .72	
4.1 INTRODUCTION	72
4.1.1 <i>Acrylamide-Based Hydrogels</i>	72
4.1.2 <i>Lysozyme as a Template Protein</i>	75
4.1.3 <i>MIP in Acrylamide-Based Hydrogels</i>	76
4.2 MATERIALS AND METHODS	78

4.2.1	<i>Fabrication of Lysozyme MIP Polymers</i>	78
4.2.2	<i>Equilibrium and Dynamic Recognition Studies</i>	79
4.2.3	<i>Specific Recognition Studies</i>	80
4.2.4	<i>Presence of Ionic Strength on Recognition Properties</i>	80
4.2.5	<i>Effects of pH on Recognition Properties</i>	81
4.3	RESULTS AND DISCUSSION	81
4.3.1	<i>Equilibrium Recognition Studies</i>	82
4.3.2	<i>Dynamic Recognition Studies</i>	83
4.3.3	<i>Specific Recognition of MIP Polymers</i>	84
4.3.4	<i>Ionic and pH Effects upon Recognition</i>	85
4.4	CONCLUSIONS	86
4.5	REFERENCES CITED	100
CHAPTER 5: MATERIALS CHARACTERIZATION OF ACRYLAMIDE-BASED MIP POLYMERS		103
5.1	INTRODUCTION	103
5.1.1	<i>Scanning Electron Microscopy of Polymers</i>	103
5.1.2	<i>FTIR Analysis of Polymer Networks</i>	105
5.1.3	<i>DSC Analysis of Polymers</i>	108
5.2	MATERIALS AND METHODS	110
5.2.1	<i>Polymer Preparation for SEM</i>	110
5.2.2	<i>Polymer Preparation for FTIR</i>	111
5.2.3	<i>Polymer Preparation for DSC</i>	111
5.3	RESULTS AND DISCUSSION	112
5.3.1	<i>SEM Analysis of MIP Polymer Networks</i>	112
5.3.2	<i>Determination of Chemical Composition Using FTIR</i>	117
5.3.3	<i>Chemical Composition of MIP Polymers Compared to Controls</i>	119
5.3.4	<i>DSC Determination of MIP Polymer Properties</i>	119
5.4	CONCLUSIONS	123
5.5	REFERENCES CITED	145
CHAPTER 6: INVESTIGATION OF ACRYLAMIDE-BASED MIP POLYMERS AS DRUG DELIVERY SYSTEMS		150
6.1	INTRODUCTION	150
6.1.1	<i>Hydrogels for Drug Administration</i>	151
6.1.2	<i>Polymers with Ionic Functional Groups for Controlled Release</i>	153
6.1.3	<i>MIP Polymers as IDDS</i>	154
6.2	MATERIALS AND METHODS	155
6.2.1	<i>Loading of MIP Polymers with Lysozyme</i>	155
6.2.2	<i>Release of Lysozyme from Hydrogels</i>	155
6.2.3	<i>Enzymatic Activity of Lysozyme Released</i>	155
6.3	RESULTS AND DISCUSSION	156

6.3.1	<i>Lysozyme Loading in the Hydrogels</i>	156
6.3.2	<i>Lysozyme Release from MIP Polymers</i>	157
6.3.3	<i>Ezymatic Activity of Released Lysozyme</i>	158
6.4	CONCLUSIONS	159
6.5	REFERENCES CITED	164
CHAPTER 7: INVESTIGATION OF CYTOCOMPATIBILITY OF ACRYLAMIDE-BASED MIP POLYMERS		168
7.1	INTRODUCTION	168
7.1.1	<i>Advantages of in vitro Studies</i>	168
7.1.2	<i>Swiss 3T3 Fibroblasts and in vitro Cell Culture</i>	169
7.2	MATERIALS AND METHODS	170
7.2.1	<i>Handling Procedure for Frozen Cells</i>	170
7.2.2	<i>Subculturing Procedure</i>	171
7.2.3	<i>Medium Renewal</i>	172
7.2.4	<i>Cryopreservation of 3T3 cell lines</i>	173
7.2.5	<i>Cytotoxicity Evaluation</i>	173
7.3	RESULTS AND DISCUSSION	175
7.4	CONCLUSIONS	175
7.5	FIGURES	176
7.6	REFERENCES CITED	184
CHAPTER 8: CONCLUSIONS		185
ALL REFERENCES CITED		188
VITA		216

Chapter 1: Introduction

In nature, molecular recognition occurs via the very specific interaction of functional groups present on two different molecules. The molecular interactions have evolved to the extent that a target ligand can be bound by a macromolecule in a pool of thousand of other potential targets with similar structure. For example, enzymes utilize specific amino acids to bind ligand molecules and trigger enzymatic degradation. The amino acid sequence in the ligand-binding site is both complementary in chemical functionality to the target and spatially arranged three-dimensionally in a very ordered way to obtain high specificity.

Following nature's cues, synthetic polymers can be designed to mimic natural recognition events. Because almost any chemical functionality can be introduced into a polymer backbone, any interaction in nature can be targeted. The interactions can also be subsequently "frozen" in place via crosslinking of the polymer network to create a three-dimensional recognitive cavity. Thus, a polymeric, biomimetic network with high specificity to a target ligand can be formed.

A completely synthetic system that can recognize specific target molecules could be a powerful recognition element in a wide range of applications. For example, such a system could target undesirable analytes in the blood such as cholesterol or viruses. The binding of this molecule would

effectively remove it from the bloodstream and, as such, act as an as an artificial drug for disease treatment. In addition, a biomimetic polymer could be incorporated into a therapeutic device to act as a recognition element. A possible platform for this technology could be as part of a targeted drug delivery system to deliver a drug in response to analyte binding. Other applications include biosensors to monitor analyte levels or highly sensitive assays to diagnose diseases.

When designing biomimetic, recognitive systems, a few key challenges must be met:

- i. the interactions formed between the target molecule and the network must exhibit high stability, and the network must be able to recognize the target ligand over structurally similar molecules;
- ii. because the biomimetic system will be used in a biological setting, the network must retain recognition properties in an aqueous, environmentally complex solution;
- iii. the target molecule must be able to diffuse into the bulk network in a rapid manner and;
- iv. suitable platforms in which recognitive polymers can be utilized must be investigated.

Hydrogels are insoluble, crosslinked polymers that absorb large amounts of water. These materials have shown great promise as platforms for biomimetic

recognitive systems. These polymers have a high degree of chemical design flexibility, and, as such, many different types of biomimetic systems have been fabricated. By tailoring chemical groups, research groups have fabricated hydrogels that can respond to changes in the surrounding environment¹⁻⁷. In addition, the introduction of biological groups into the polymer backbone can create biomimetic polymers with properties similar to biologic tissue. These gels have applications in tissue engineering and biomaterials. Thus, hydrogels hold great promise as the next generation of synthetic, recognitive systems in a wide array of applications.

In this work, highly-crosslinked hydrogel networks based on polymers with electrostatic attractive groups for a template protein were prepared and developed. The use of different kinds of interactions and different materials, material properties, and polymer characteristics were investigated. Platforms for the use of these recognition-based hydrogels for biomimetic systems were discussed.

References Cited

1. Lowman, A. M.; Morishita, M.; Kajita, M.; Nagai, T.; Peppas, N. A., Oral Delivery of Insulin Using pH-Responsive Complexation Gels. *J. Pharm. Sci.* **1998**, 88, (9).

2. Peppas, N. A.; Huang, Y.; Torres-Lugo, M.; Ward, J. H.; Zhang, J., Physicochemical Foundations and Structural Design of Hydrogels in Medicine and Biology. *Annu. Rev. Biomed. Eng.* **2000**, 2, 9-29.
3. Brazel, C. S.; Peppas, N. A., Synthesis and Characterization of Thermo- and Chemomechanically Responsive Poly(N-Isopropylacrylamide-co-Methacrylic Acid) Hydrogels. *Macromolecules* **1995**, 28, 8016-8020.
4. Leobandung, W. L.; Peppas, N. A. In *Temperature-Sensitive Particulate Systems Containing Poly(Ethylene Glycol)*, AICHE, Los Angeles, CA, 2000; Los Angeles, CA, 2000; p 199h.
5. Peppas, N. A.; Zhang, J., Diffusional Behavior in pH- and Temperature-Sensitive Interpenetrating Networks Used in Drug Delivery. In *Biomaterials and Drug Delivery Systems Towards the New Millenium*, Park, K. D.; Kwon, I. C.; N.Yui; Yeong, S. Y.; Park, K., Eds. Seoul, Korea, 2000; pp 87-96.
6. Vakkalanka, S. K.; Brazel, C. S.; Peppas, N. A., Temperature and pH-Sensitive Terpolymers for Modulated Delivery of Streptokinase. *J. Biomed. Materials Sci., Polym. Ed.* **1996**, 8, 119-129.
7. Zhang, J.; Peppas, N. A., Molecular Interactions in Poly(Methacrylic Acid)/Poly(N-Isopropyl Acrylamide) Interpenetrating Polymer Networks. *J. Appl. Polym. Sci.* **2001**, 82, 1077-1082.

Chapter 2: Background-Molecular Imprinting of Polymeric Materials

2.1 Molecular Recognition

The ability of a molecule to selectively recognize a target molecule in a vast pool of similar molecules is essential to biological and chemical processes. Molecular recognition occurs when two molecules are both geometrically and chemically complementary—that is when they can both "fit together" spatially as well as bind to each other using non-covalent forces, including hydrogen bonds, electrostatic interactions, hydrophobic interactions, and weak metal coordination¹. Examples of this process include the binding of an enzyme to a substrate², a drug to a biological target^{3, 4}, antigen/antibody recognition in the immune system^{5, 6}, and the formation of messenger RNA from DNA templates⁷. Thus, molecular recognition can be thought of as the driving force behind all life processes.

2.2 Natural Recognition Systems

2.2.1 Molecular Recognition in Proteins

Proteins are heteropolymers consisting of long, unbranched chains of amino acids. Most proteins in the human body consist of roughly 200-300 amino acids⁸. Every body system relies on proteins, and how proteins recognize other molecules is integral to those systems. For example, protein recognition is important in musculo-skeletal movement, enzyme catalysis in digestion, and the

uptake of therapeutic drugs into cells and tissues. The most characterized example of protein molecular recognition is the avidin-biotin complex⁹.

Avidin is a tetrameric glycoprotein that has four subunits and has a molecular weight of ~66,000 Da⁹. Biotin, also known as Vitamin H, is a naturally occurring molecule found in every living cell. Each of the four tetrameric regions of avidin specifically bind to one biotin molecule, and this binding is believed to be the strongest non-covalent binding by a protein to a molecule in nature ($K_a=10^{15} \text{ M}^{-1}$)¹⁰. It is thought that specific lysine and tryptophan residues in avidin (specifically Trp 70 and Trp 110, and Lys 45 and 94) have a high attraction to the carboxylic acid group of biotin^{7, 9, 11}. It is this molecular affinity and the spatio-chemical orientation that make the avidin-biotin complex one of the most-studied non-covalent recognition systems in all of molecular biology.

2.2.2 Molecular Recognition in the Immune System

The most widely recognized system of molecular recognition occurs in the immune system of higher order organisms in the form of antigen/antibody recognition. Antibodies are globular proteins that have evolved to express specific binding sites that recognize and capture foreign materials in the bloodstream. These foreign materials, termed antigens, can range from simple proteins to large bacteria and viruses. Antibodies are composed of linear strands of amino acids consisting of two identical polypeptide "heavy" chains (55 kDa)

and two identical polypeptide "light" chains (25 kDa) that are linked by disulfide bridges to form a "Y" structure¹² (Figure 2.1). At the N-terminus of the chains lies the variable region which contains an amino acid sequence that can recognize a particular portion of an antigen, deemed the epitope. It is not only the amino acid sequence that leads to recognition but also the orientation of the binding pocket created by heavy and light chains (Figure 2.2). The recognition between the epitope of an antigen and the variable region of an antibody occurs via electrostatic forces, hydrogen bonds, Van der Waals Forces, hydrophobic forces, or a combination of all these non-covalent interactions¹³ (Figure 2.3). This complexation via the antibody C-terminus activates the phagocytic cell to engulf and destroy the antigen.

Antibodies must therefore be able to recognize an immense number of different structures, and the variable region's flexibility in amino acid sequence allows for a huge number of possible chemical targets. As such, some researchers have estimated that the human immune system contains between 10^7 and 10^9 different antibody structures¹⁴. Many researchers are now attempting to mimic this epitope binding to create artificial antibodies for the treatment of disease¹⁵. Mosbach and colleagues^{16, 17} have considered using these "artificial antibodies" as screening of libraries for potential new drugs, as enzyme inhibitors, and as targets for protein binding.

2.2.3 Cellular Molecular Recognition

In addition to molecular recognition by proteins, cells of the body rely on this process in many cellular events. Next to proteins, the most fundamental structural elements of the body are the cells and the extracellular matrix (ECM) that they secrete for anchorage. The ECM can be widely viewed as the backbone that comprises tissues and organs, but it should not be viewed as merely providing strength and physical support. The ECM is now believed to be intricately involved in the events that lead to the eventual formation of tissue. It is composed of a fibrillar and an amorphous component¹⁸. These two broad components interact with cells via cell surface receptors and other membrane proteins. The interaction of cells with each other (cell-cell interactions) and the interaction of cells with their environment (cell-ECM interactions) have a particularly high molecular specificity. A complex recognition process is required for most cellular process including cell division, ECM secretion, motility, and apoptosis¹⁹.

Cell-ECM interactions can determine everything from cell differentiation and cell growth to cell orientation and the secretion of other molecules by the cell¹⁸. For instance, ECM interactions such as stress forces due to injury or disease can cause cytoskeletal rearrangement in cells leading to changes in protein expression and nuclear events. The cell may divide to produce more cells for tissue formation, and the cell may also differentiate into a more specific

cell phenotype. Concurrently, ECM cues can lead to a production and release of matrix molecules in a dynamic loop. These matrix molecules form an anchorage place for newly divided cells which will act with the ECM in this loop to lead to the formation of natural tissue.

Communication of a cell within its environment takes place primarily through receptors called integrins. Integrins are heterodimeric proteins with two membrane-spanning subunits that are connected to the microfilament network contained in the cytoplasm¹⁹. Integrins bind specifically to certain amino acid sequences found in proteins via Van der Waals forces, hydrogen bonding, and ionic attraction. An example of an integrin target sequence is the RGD (arginine, glycine, aspartic acid) region that makes up many cellular adhesive proteins. The adhesive proteins in turn bind to solid substrates, the ECM, or even other cells.

2.3 Engineering Biomaterials with Molecular Recognition

2.3.1 Early Biomaterial Attempts

As biological research has expanded and a greater understanding of the mechanisms of biological molecules has been revealed, researchers have tried to replicate molecular recognition behavior with synthetic molecules. The most famous initial attempt at creating an artificial biological material was performed at the beginning of the 20th century—specifically during World War II. Due to the high number of battlefield casualties in this war, many surgeons began

experimenting with replacing native tissues with artificial materials in an attempt to reduce battlefield mortality²⁰. Although all of these attempts were unsuccessful for various reasons, the idea of replacing a lost tissue with synthetic materials endured. Romanced by the thought of creating new organs along with the observance of tissue growth around a silk suture, Arthur B. Voorhees from Columbia University surgically replaced canine blood vessels with parachute nylon²¹. Voorhees believed that the material possessed suitable properties that mimicked the properties of blood vessels—including an elastic nature and a distinct hydrophobicity—that would stop the adherence of platelets and hence hinder clot formation. However, this material proved unsuitable as a replacement as thrombi eventually formed in vessels, leading to death. Nonetheless, Voorhees hypothesized that with a better understanding of the interactions of materials and the human body, better biomaterials could be possibly created.

After these initial material attempts, scientists creating biomaterials realized that materials must foremost be biocompatible, meaning the material would not illicit an immune response from the body. Many of the early catheters and pacemakers were designed with this goal in mind²². These materials were passive materials that were designed to interact with the body as little as possible, thus minimizing an immune response. However, due to the formation of a fibrous tissue capsule around the implants, these materials ultimately

failed²². It was believed the capsule formation was due to the fact these materials did not interact with the body.

Due to these limited successes, many researchers hypothesized that biomaterials could better be accepted by the body if the material itself could actively interact with body by mimicking certain physiological processes. Scientists working in the biomaterials area are beginning to apply the principles of cell transplantation, material science, and engineering to construct biological substitutes that will restore and maintain normal function in diseased and injured tissues. Much of the work in biomaterials has been focused on fabricating replacement materials that have components similar to the natural ECM of native tissues. The main function of the ECM is to serve as a template for cell and protein attachment and act as a degradable support structure for new tissue ingrowth. Most replacement ECMs attempt to mimic the behavior of natural biologic tissue, but the replacement ECM cannot be oversimplified. If the scaffold cannot provide important developmental signals to the cells on the biomolecular level, cells will not recognize the artificial ECM as a suitable material for attachment and proliferation, and thus, tissue regeneration will fail. This is why most of the initial attempts in biomaterials creation were unsuccessful.

2.3.2 Strategies for Biomolecular Recognition

Biomaterial scientists attempt to address molecular recognition of materials by cells (more aptly named biomolecular recognition) with two different major design strategies. The first method is to make the material bioactive by incorporating relevant biological molecules such as growth factors and or even whole cells into biomaterial carriers so that these molecules can be released from the material and trigger or modulate new tissue formation²³. Burdick and Anseth²⁴ have been attempting to deliver cells and growth factors in unison from injectable polymer matrices that are then UV polymerized to form a matrix. The gel acts both as a drug delivery device to deliver growth factors directly into the wound bed and as an anchorage point for cells. This group has shown viability of encapsulated cells over 3 weeks, and osteoblasts encapsulated by this method begin secreting native ECM molecules into the matrix. However, these materials are polymerized in situ, and toxicity issues could arise with the injection of acrylate monomers and oligomers into the body.

The other approach toward biomolecular recognition involves physically or chemically modifying biomaterials to incorporate specific cell-binding peptides. Cell-binding peptides are short amino acid sequences of much longer native ECM proteins that have been identified as able to incur specific, predictable interactions with cell receptors. Incorporating peptides into these materials can potentially mimic the signaling dynamic between ECM and cells in tissues. The

most studied cell adhesion peptide, RGD, has been widely used to encourage fibroblasts and other cells to adhere to polymer matrices in order to encourage tissue formation²⁵. In addition, materials that are not adhesive to cells will attract and bind cells if signaling peptides are incorporated on the surface²⁶. Nguyen and West²⁷ have incorporated protease peptide sequences into materials that can be broken down by cellular enzymes. However, it is difficult to uniformly cover polymers with peptides, and the use of peptides in humans and the resulting immunogenic response to these materials is still uninvestigated. In addition, the uses of peptides in synthetic structures can limit the feasibility of any material as an “off-the-shelf” product due to concerns about peptide degradation over time.

2.4 Biomaterials

To date, many artificial materials have been attempted as biomaterials, but many of these structures have met with only limited success. Since Voorhees’ initial attempt with parachute nylon, both synthetic and natural materials have been attempted as a replacement for native tissue.

2.4.1 Natural Biomaterials

Some research groups have focused on the use of natural materials such as collagen scaffolds as a completely natural replacement ECM. Collagen, a large component of the ECM, is naturally degraded by metalloproteases and serine proteases, allowing for its degradation to be locally controlled by cells

present in the surrounding tissue²⁸. Collagen has been investigated for many uses, and it has shown some promise in the replacement of injured cartilage and blood vessels. Frenkel and colleagues²⁹ transplanted allogenic chondrocytes in collagen matrices into rabbits and showed that the regeneration of articular cartilage was possible. Kobashi and Matsuda³⁰ formed circular tubes for blood vessel replacements using collagen seeded with smooth muscle cells. These grafts show good biocompatibility, but they cannot withstand the pulsatile flow of the bloodstream. This work illustrates one of the main problems faced using this material; natural collagen lacks rigidity, and cell-seeded constructs of collagen must be immobilized so physical forces do not destroy the material. In addition, immunogenic response hampers these materials, physical and chemical composition of collagen can vary in animal sources leading to unpredictable tissue formation, and protocols can be irreproducible from experiment to experiment³¹.

2.4.2 Synthetic Polymers as Biomaterials

2.4.2.1 *Poly(lactic) and Poly(glycolic) Acid*

Synthetic polymers are viewed by many researchers as having the most promise as a biomaterial because they can be physically or chemically tailored to induce specific interaction with host cells or proteins. In addition, they can be structurally molded to mimic native biomechanics, they can be tailored to degrade for eventual replacement by host tissue, and they are generally less

expensive to mass produce than natural materials. The most widely used polymers for cellular scaffold materials are poly(lactic) acid (PLA), poly(glycolic) acid (PGA), or a combination of these two polymers (PLGA). PLA, PGA, or PLGA are aliphatic esters that possess excellent biocompatibility³² and can be used as drug delivery materials to deliver biomolecules during tissue regeneration^{33, 34}.

These polymers are also among the few synthetic polymers approved by the US Food and Drug Administration (FDA) for certain human clinical applications. PGA is extremely hydrophilic in nature and, consequently, will lose its mechanical strength within two to four weeks of implantation³⁵. PLA, however, contains one methyl group more than PGA and as a result is more hydrophobic. Degradation rates for PLA scaffolds have been measured up to months and even years^{34, 36}. The degradation rates of these polymers can be tailored by using copolymer blends (PLGA) to give distinct degradation profiles^{31, 34}. However, these polymers undergo acid-catalyzed hydrolysis and bulk erosion, which can cause the polymer to suddenly lose structural integrity before complete cellular incorporation into these ECM constructs. This lack of long-term mechanical stability could inhibit formation of new tissue³⁷.

2.4.2.2 Hydrogels

As an alternative to aliphatic polymers, a class of materials termed hydrogels are being studied that can absorb greater than 30% of their dry weight

in water. These materials are appealing because the polymer properties are controllable and reproducible³⁸ and the large water uptake promotes excellent biocompatibility. 2-hydroxyethylmethacrylate (HEMA) has been widely used in ophthalmology as a contact lens material and more recently has been used as a fibrillar support for nerve regeneration³⁹. Among the most studied hydrogel materials is crosslinked poly(ethylene glycol) (PEG), which has been approved by the FDA for use in certain medical applications⁴⁰. Unfortunately, the high water content of PEG and other hydrogels can cause low cellular and protein adherence, leading to incomplete tissue formation. To gain cellular specificity, researchers have attempted to immobilize growth factors to the surfaces of biomaterials⁴¹. In addition, these materials have been used to encapsulate cells in an attempt to encourage the cells to begin to secrete native ECM molecules^{24, 42}. These strategies only achieve limited success because hydrogel materials are highly crosslinked and do not degrade, thus limiting their effectiveness as a tissue replacement material. Therefore, groups are investigating incorporation of degradable structures such as PLGA into hydrogel materials to produce a degradable structure while still maintaining the high water content of the hydrogel⁴³.

2.4.2.3 Anhydrides

In addition to hydrogels, polymers consisting of anhydride networks have been synthesized for a number of biomedical applications including tissue

engineering and drug delivery⁴⁴. Polyanhydride networks exhibit excellent biocompatibility and contain a large aliphatic component possessing an ester group that undergoes surface erosion via hydrolysis⁴⁵. The deliberate surface erosion is different than the bulk hydrolysis that is undergone by PLA or PGA and can allow biomaterials scaffolds to be made that have very predictable degradation profiles. In addition, the erosion of only the surface of the material allows anhydrides to maintain structural integrity to allow for support of cellular integration. One polyanhydride that has been widely studied and is in clinical trials as a component in the drug delivery device Gliadel™ is poly(methacrylated sebacic anhydride) (MSA). In Gliadel™, drugs such as topotecan are loaded into wafers, and subsequently implanted in brain cancer patients after tumor removal⁴⁶. In the aqueous environment of the body, the wafers undergo slow surface erosion for extended drug delivery at the site of implantation. Degradation of MSA yields methacrylic acid (MAA) and sebacic acid as products which show minimal toxicity in vivo⁴⁷. Polyanhydride networks can also be combined with other polymers to change their degradation and structural characteristics. Jiang and Zhu⁴⁸ showed that anhydride polymers could be polymerized in the presence of PEG to form a crosslinked hydrogel with both hydrophobic and hydrophilic components. The hydrophilic PEG chains increase uptake of water to in turn drive the hydrolysis of the ester bond in the

hydrophobic MSA, and consequently the degradation properties can be tailored by altering the amount of PEG in the polymer.

2.5 Molecular Recognition Using Synthetic Polymer Networks

With the advances in protein chemistry and the increased understanding of protein recognition, researchers are attempting to construct completely synthetic polymeric materials that can specifically bind target molecules. Such materials can have applications ranging from chromatography and solid phase extraction to controlled drug delivery. Many of these polymers are now being created in the presence of the target molecule in order to “memorize” both its shape and chemical functionalities to mimic biological recognition. Synthetic polymers can be advantageous over using biological molecules such as proteins or DNA due to the sheer freedom of molecular design. A wide array of chemical functionalities can be introduced into synthetic systems, and the mechanical properties can be readily tailored.

2.6 Molecular Imprinting

The idea of molecular imprinting was inspired by the theories of Nobel Prize winner Linus Pauling on the formation of antibodies in the immune system^{49, 50}. Pauling theorized that antibodies behaved like denatured proteins, and thus free of hydrogen bonds, their chains were free to move. When in contact with an antigen, chemical functionalities on the antigen would attract

amino acids on the antibody, a mechanism he termed "molecular complementariness"⁵¹. Thus the antibody would then memorize the shape of the antigen⁵² (Figure 2.4). This hypothesis was later disproved, but his idea of a freely moving polymer chain that could form a complimentary mold around a structure inspired the field of molecular imprinting (MIP). In recent years, MIP polymers have come to the forefront of biomedical applications. First used in chromatography columns for the separation of specific analytes, imprinted polymers now have applications ranging from molecular sensors⁵³⁻⁵⁸, solid-phase extraction^{57, 59, 60}, and drug delivery systems⁶¹⁻⁶⁷.

2.6.1 Molecular Imprinting Principles

MIP polymerizations all follow the same general procedure. In a solution of appropriate functional monomers, a template molecule is added, and the solution is mixed. This mixing allows for "self-assembly" of the template with the complimentary monomers to form a pre-polymerization complex. The functional monomer contains specific chemical structures designed to interact with the template either by covalent chemistry⁶⁸⁻⁷⁰, non-covalent chemistry⁷¹⁻⁷⁴, or both⁷⁵.

Once the pre-polymerization complex is formed, the polymerization reaction usually occurs by free radical initiation in the presence of a crosslinking monomer and an appropriate solvent. The template can then be extracted from the formed polymer, producing a porous matrix with specific recognition elements for the template molecule. Thus, MIP creates stereo-specific three-dimensional

binding cavities based on the template molecule of interest^{76, 77} (Figure 2.5). These cavities not only maintain the ordered arrangement of complimentary chemical functionalities but also preserve the overall spatial configuration of the template.

While a few groups are attempting to imprint natural proteins, there are generally two types of molecular imprinting, covalent and non-covalent. The two methods only differ in the initial formation of the pre-polymerization complex. In most cases, non-covalent systems are most favored due to ease in extracting the template molecule and therefore are the most widely studied⁷⁸. Although non-covalent systems are easier to fabricate, the recognition achieved by covalent methods is usually much superior.

2.6.2 Molecular Imprinting in Natural Molecules

Of interesting note are the efforts by certain groups to make completely natural MIP systems by using proteins as the recognition elements to capture small molecular weight molecules^{79, 80}. Slade⁸⁰ lyophilized bovine serum albumin in the presence of *p*-hydroxybenzoic acid. Using this technique, binding activity of *p*-hydroxybenzoic acid could be enhanced by a factor of approximately 3 over that of the non-imprinted protein. In another approach, Luo et al.^{81, 82} placed chicken albumin into contact with an enzyme mimic for glutathione. By crosslinking the albumin with glutaraldehyde in the presence of the mimic, the researchers were able to memorize the conformational binding of glutathione to

the protein. The imprinted protein exhibited an 80-fold increase in enzymatic activity when glutathione was present. The above two protein-imprinting methods not only show that natural MIP systems are possible but also that MIPs have the possibility of mimicking complex protein-molecule binding events to create possible artificial enzyme release systems for the treatment of disease.

2.6.3 Covalent Imprinting in Polymers

Covalent imprinting differs from non-covalent imprinting only in the formation of the template-polymer complex and the subsequent removal of the template. This procedure of imprinting was first developed by Wulff^{83, 84}. In this method, the template is bound covalently to functional monomers normally through the use of a vinyl moiety⁷⁸. The first successful imprinting of this type employed a simple sugar conjugated to a boronic acid derivative. The conjugate was crosslinked using ethylene dimethacrylate. When the ester was cleaved, it was found that the template was bound strongly and selectively.

The success of covalent imprinting lies in chemical linkage that forms the template-monomer complex. This linkage needs to be stable under the reaction conditions, but the bond must be easily broken for the removal of the template. The breaking of this bond must be performed under mild cleavage conditions so that the imprinted network is not disrupted. Unfortunately, relatively few covalent bonds meet these requirements, and as a result, the study of covalent imprinting is not as widespread as its non-covalent counterpart. Monomers that can be

used are boronic acid esters, ketals, disulfide bonds, acetals, and Schiff bases. Examples are given in Figure 2.6. In addition to the limitations of the monomer choice, the re-binding of the template molecule is slower than the recognition achieved in non-covalent imprinting⁷⁸.

2.6.4 Non-Covalent Imprinting in Polymers

In 1981, Mosbach⁸⁵ showed that covalent linkages were not needed in order to successfully imprint a target molecule. In this method, non-covalent interactions occur between chemical functionalities on the template and the functional monomers. The functional monomers and the template are mixed in a proper solution and upon mixing, will “self assemble” to form the complex. Once polymerized, the template then can be removed via simple diffusion, usually in a polar or acidic solvent that can sufficiently overcome the non-covalent interactions between polymer and template. In addition, the rebinding of the template is much more rapid since the formation of a covalent bond is not needed. Not surprisingly, this method is considered to be much simpler than the covalent approach, and therefore most of the research in this area—especially in imprinting biomolecules such as proteins—involves this technique. The scope of this work investigates non-covalent imprinting of proteins; therefore the following sections will be confined to the non-covalent method.

2.6.4.1 *Template and Functional Monomers*

The success of an imprinting system is defined by the ability of the polymer structure to possess a high affinity for a template molecule, and this success is very much dependent upon the template-monomer interaction⁸⁶. The target molecule in MIP reactions, or more aptly named the template, must have a certain number of characteristics amenable to imprinting. Most importantly, the template must have chemical groups that can complex with the functional monomers chosen. Hydrogen bond donating moieties and electrostatic functionalities (carboxyl, amino, hydroxyl, and amide) are some of the most commonly chosen sites on a template molecule. In addition, the template must not have any characteristics that can retard the free-radical polymerization such as the presence of thiol groups that can terminate radical formation. Finally, the template must remain stable under the reaction conditions. For example, if a thermal initiator is chosen, the template should not degrade under the elevated temperatures or, in the case of UV-initiated polymerizations, degrade under UV irradiations. Any change in conformation of the template could lead to incorrectly formed imprinted sites⁸⁷.

Choice of functional monomers is the most important characteristic in targeting a template molecule. Many types of functional monomers have been investigated with a wide array of templates, and the number of functional monomers available continues to grow. Figure 2.7 outlines the rapidly expanding

toolbox of functional monomers for imprinting applications⁸⁸. The choice of monomer can be divided into functionality type: either electrostatic (acidic or basic) or neutral but with hydrogen bond donors. During polymerization, functional monomers are usually used in an excess mole ratio to the template, usually starting at 4:1 and increasing⁸⁸.

The most successful MIP systems (and the most widely studied) are tightly crosslinked polymeric hydrogels that contain acrylic acid or methacrylic acid (MAA) monomers grafted with a PEG derivative⁸⁹. In biological applications, these monomers are most favored because they have anionic acid groups that can non-covalently complex with the template molecule which also allow the template to be removed without harsh conditions⁹⁰. In non-polar solvents, the acid group is protonated and can undergo hydrogen bond donation with electrostatic groups of the template. Conversely, in aqueous biological conditions, the carboxyl group is negatively charged and can target hydrogen bond donors or cationic functionalities. Other monomer functionalities that have been widely investigated include hydrogen bonding such as with acrylamide or 2-hydroxyethyl methacrylate or cationic interactions such as with 2-dimethylpropyl methacrylamide⁸⁷.

The most important factor governing the interaction of either electrostatic or hydrogen bond functionalities is the pK values of both of the components. When in the presence of a strong base, a strong acid will transfer a proton to this

chemical group, and the interaction is almost completely electrostatic. However, when the acid and base are of intermediary strength, the proton is shared between acid and base, and thus hydrogen bonding is dominant. With these factors in mind, the nature of the imprinting and the types of interactions favored should be used to determine the choice of monomers.

2.6.4.2 *Solvents for Non-Covalent Imprinting*

Since solvents are used to dissolve all agents in the MIP reaction, its overall effects on the reaction must also be considered. Foremost, the solvent itself can act as a porogen. The porosity of polymers can be determined by the overall concentration of monomers and crosslinkers in the solution. When polymerization occurs, solvent molecules become incorporated into the structure and create pores. Pores are required to allow the diffusion of the template out of the network and its subsequent diffusion back in during recognition. A thermodynamically good solvent will create well-developed pores within the network and increase the pore surface area⁸⁸. In general, an increase in the solvent concentration can lead to an increase in total pore volume. However, a large amount of solvent can ultimately lead to the formation of micro and nano-spheres rather than large aggregate polymers. The solvent can also act to disperse heat generated by the polymerization—heat which can affect the template-monomer complex.

Finally, the solvent must be chosen with the idea that it will not interfere with the template-monomer complex. If the solvent does indeed have an interaction, it could inhibit formation of imprinted sites. As a result, many imprinting systems shun polar solvents such as water and instead utilize non-polar solvents in order to maximize attraction of the template by the functional monomers^{76, 89, 91}. Chloroform was initially the most widely used solvent, but most commercial chloroforms contain a small amount of ethanol as a stabilizer. This added polarity can interfere with complex formation⁷⁸. Other solvents that have been investigated include dimethyl sulfoxide (DMSO)⁷⁶, toluene⁹¹, and benzene⁷⁸. In an example of imprinting using a nonpolar solvent, Oral and Peppas⁹² fabricated pH sensitive PEG star polymers with MAA fabricated in the organic solvent THF. These polymers exhibited high specificity to glucose over similarly structured fructose, and part of the specificity was attributed to the use of the nonpolar THF as a solvent because it did not interfere with template-monomer complex formation.

Water is an especially poor solvent choice for MIP due to its highly polar nature and the fact that most MIP materials function only in organic solvents. Water is both a hydrogen bond donator and hydrogen acceptor. Thus, many hydrogen bonds that are formed during non-covalent imprinting can be destroyed by the sheer amount of water molecules present. In addition, many crosslinking agents that are soluble in water such as *N,N'*-methylenebisacrylamide (MBA)

have little structural integrity, thus limiting these materials in extraction applications such as high pressure liquid chromatography (HPLC)⁷⁸.

2.6.4.3 Crosslinkers

In addition to the solvent and template monomer interactions, the overall material properties of the structure must be considered, including the amount of crosslinking. The crosslinker not only “freezes” the template-monomer complex upon polymerization to form the pore but also imparts the mechanical stability to the polymer itself. Most successful MIP networks involve hydrogel components such PEG or HEMA that absorb large amounts of water. Upon water uptake, these gels will swell exponentially in volume. In a MIP system, the swelling can cause the template cavities to also swell. If the swelling is large, the distance between functional monomers of the material can become too great and render the recognition of the MIP material useless⁹³. To combat swelling, most imprinted systems will incorporate large ratios of crosslinkers into the backbone. For example, to achieve highly selective MIP materials for D-glucose over the similarly structured D-galactose, Byrne and Peppas⁹⁰ created materials with 66.6% crosslinking. They reasoned that the high crosslinking gives rigidity to the functional cavities to allow recognition, and a search of the literature reveals very little work into systems with 10% or less crosslinking⁹⁴, with crosslinking of 80% not uncommon⁸⁸. Figure 2.8 outlines widely studied crosslinkers in MIP.

The crosslinker must also be sufficiently chosen so that its reactivity is similar to that of the chosen functional monomer(s). This insures random copolymerization and functionalized sites that are spread uniformly throughout the bulk of the polymer. In addition, the mole ratio of functional monomers to crosslinker must be taken into consideration so that the functional cavities are sufficiently spaced to allow formation of individual binding pockets. However, the amount of crosslinking must not be so high as to limit diffusion of the template into the network.

2.7 Obstacles in Large Molecular Weight Template Imprinting

Although MIP technology has been utilized for over 20 years, large molecular weight templates such as proteins or even whole cells have largely not been studied. Proteins themselves are biopolymers that contain both flexible and rigid areas which have diverse dynamic binding functions in nature. Since proteins are composed of linear sequences of amino acids, with each amino acid having a unique residue group with a specific functionality (hydrophilic or hydrophobic; anionic, cationic or neutral; polar or non-polar; etc.), it is these sequences that determine the conformation of the final protein. The direct interactions of these groups with water, with each other, and with other molecules influence the folding of a protein into a stable three-dimensional arrangement⁹⁵.

Cells are inherently more complex than proteins, and the sensitivity of cells to environmental conditions renders many imprinting systems useless for this application. Thus, many groups have attempted to imprint cell surface characteristics such as glycoproteins using carbohydrates or have used cell peptides or antibodies instead of more harsh functional monomers to achieve recognition^{96, 97}. In a noteworthy development, Kofinas and colleagues have recently imprinted baculoviruses using poly(acrylic acid) as the functional monomer, and these polymers show great promise in assay technologies and sensor applications to detect and remove antigenic cells⁹⁸. In addition, Dickert has shown the ability to recognize erythrocytes using a surface imprinted layering technique⁹⁹.

2.7.1 Diffusional Limits in Large Molecular Weight MIPs

One of the main problems faced with imprinting large molecular weight compounds is attributed to the high crosslinking required to achieve recognition. With increased crosslinking, large templates such as proteins can become entrapped in the network after polymerization. If the template molecule cannot be extracted, the network is rendered useless for bulk recognition applications, as template binding only occurs on surface recognition sites¹⁰⁰. In addition, high crosslinking can decrease diffusion by these molecules into the network and lead to longer times needed for recognition. Consequently, most research in protein imprinting has been in producing materials by surface imprinting techniques

because the protein can then be easily removed. Ratner and colleagues have developed a way of depositing proteins on metal surfaces and then coating the material with a simple carbohydrate that non-covalently complexes with amino acid residues of the protein. The carbohydrate is then polymerized in the presence of a crosslinker to create a polymer with specific surface recognition sites for the protein¹⁰¹. However, few other groups have attempted bulk imprinting within gels, although one group has had success imprinting albumin in microgram quantities for sensor applications¹⁰². Another group successfully imprinted both urease and bovine serum albumin (BSA) with polysiloxane but could not universally apply it to myoglobin or hemoglobin¹⁰³.

2.7.2 Limits of Protein Dissolution

The high molecular weights of proteins can be an obstacle in bulk recognition because of the difficulty of protein dissolution in the monomer solution and the low solubility of these structures in non-aqueous solvents. As proteins increase in complexity (i.e. molecular weight), the solubility of these molecules in non-aqueous solvents decreases¹⁰⁴. BSA is an intermediate-sized (~60 kDa), biologically relevant protein that is extremely soluble in water (>100mg/mL). However, in methanol, the solubility drops to less than 0.05 mg/mL, and the addition of other molecules such as monomers or salts will continue to decrease BSA's solvation by non-aqueous solvents^{105, 106}. The low solubility of biological proteins in non-aqueous solvents could be attributed to the

evolutionary affinity of these molecules for the water-rich bloodstream of most animals^{107, 108}. In addition, proteins dissolved in organic solvents exhibit distinctly different biological activity when separated and re-dissolved in aqueous media¹⁰⁴. This change in activity is attributed to a conformational change in the protein due to unfolding and refolding in different media. This conformational change can have profound effects on the biological activity of protein. For instance, BSA dissolved in DMSO exhibited a distinct decrease in binding to bilirubin when placed in aqueous media¹⁰⁹. Therefore, it seems that aqueous solvents are the most relevant reaction solvents for MIP networks in order to imprint the correct conformation for recognition in aqueous media. However, as noted previously, polar solvents such as water can interfere with monomer-template interactions, so this challenge is daunting and can help explain the limited research in using proteins as a template in MIP.

2.8 Applications of MIP Technology

2.8.1 Imprinted Hydrogels as Carriers for Controlled Release

Of recent note in drug delivery systems (DDS) are the efforts by our group and others to use environmentally responsive, MIP hydrogels as carriers for controlled release of therapeutic compounds. Hydrogels have been used as prime carriers for pharmaceutical applications, predominantly as carriers for delivery of drugs, peptides or proteins. They have been used to regulate drug release in reservoir-based, controlled release systems or as carriers in swellable

and swelling-controlled release devices¹¹⁰⁻¹¹². Hydrogels can be rendered sensitive to physiological conditions due to the presence of specific functional groups along their backbone polymer chains. The swelling behavior and associated release kinetics of these gels may be dependent on pH, temperature, ionic strength, or even drug concentration¹¹¹. The technology has evolved to achieve sustained delivery of large molecules such as high molecular weight peptides for long periods of time (e.g., days and months), and certain groups have recently used MIP polymers to give sustained controlled release of small-molecular weight drugs for therapeutic purposes. For example, PEG hydrogels as contact lenses have been composed with imprinted sites for the drug timolol¹¹³. The interaction of the imprinted sites with timolol must be overcome by the uptake of water, which slows the release of this drug into the eye. Thus, MIP contact lenses exhibited longer release times than non-imprinted polymers loaded with the drug^{113, 114}.

2.8.2 Intelligent Gels: Environmentally Responsive DDS

Unfortunately, current drug delivery systems are often limited because they cannot respond directly to the need of a patient. Every person's physiology and pathological conditions vary slightly. Medical conditions also vary through the course of time, and many disease states often possess unpredictable episodes or unnoticeable symptoms that lead to catastrophic physiological effects. Therefore, future DDS need to be able to accurately sense and

determine changes in significant biological markers and then actively respond by releasing a therapeutic agent or a sensible signal. Ideally these systems should also be able to self regulate and effectively be able to switch on and off depending on the therapeutic need. The following portion of this review is dedicated to describing some of the recent developments in actively responding systems.

Tanaka and collaborators¹¹⁴⁻¹¹⁸ have described one recognition system in which polymer gels recognize molecules in a manner very similar to the process in which proteins recognize them. In other words, recognition capabilities are based on a specific molecular conformation, and these gels are able to change in and out of a particular conformation based upon environmental cues such as ionic strength, temperature, or pH. These gels are able to memorize certain configurations based on spatial assemblies of groups of their monomers. Essentially, this group creates a thermo-sensitive polymer and then polymerizes previously end-shielded post-crosslinking monomers in the presence of a template or target molecules (negatively charged molecules that interact with positively charged functional monomers), and the resulting gel is a MIP network with thermo-responsive properties.

When Tanaka et al. compared the recognition aspects of the gel, it was shown that the presence of the template during the additional post-crosslinking step resulted in 3-5 times higher affinity compared to random post-crosslinking.

They were also able to show that the functional monomers with carboxyl groups formed complexes with divalent ions when polymerized, but upon swelling, the affinity for the divalent ions disappeared. However, when the temperature was increased, the gels would shrink, the affinity was recovered, and the original relative positions of the carboxyl groups were recalled--in effect memorizing the original polymer formation. Non-imprinted gels had decreased affinity for divalent ions and trouble forming pairs due to polymer frustrations.

Although these MIP systems show multiple-point absorption, they have yet to recognize molecules other than charged species. However it is interesting to note that the presence of acidic groups is a common feature in drug substances including antibiotics, glucocorticoids, and cholinergic drugs⁶³. Future uses of these systems show great promise in the drug delivery field due to the reversibility of drug release and re-uptake as a function of temperature. They could be applied to pathological conditions which involve local changes in temperature or by triggering the on/off release of drug due to externally applied local hyperthermia.

Perhaps a more specific active recognition/release process is one using a competitive binding system. This system could respond to the individual patient's therapeutic requirements and deliver a specific amount of drug in response to a biological stimulus¹¹⁹. An example of this system is a reversible antigen responsive hydrogel¹²⁰. This gel uses the reversible binding between an antigen

and an antibody as the crosslinking mechanism in semi-interpenetrating networks (semi-IPNs). Miyata et al.¹²⁰ synthesized a semi-IPN which consisted of a polymer containing rabbit antibody (IgG) and goat anti-rabbit as the antigen. Upon placing free antigen, rabbit IgG, into a solution with the IPN the hydrogel swelled (Figure 2.9). This is due to the competition between free and polymer-immobilized antigen. The group was also able to show that the hydrogel swelling was reversible by removing the free antigen and that this relationship was based on free antigen concentration. In order to demonstrate the relevance this system has in a drug delivery system, drug was entrapped in the network and shown to release proportional to stepwise changes in antigen concentration. While not an MIP system, this network shows once again the hydrogel systems could be tailored to release a drug in response to an external stimulus.

The competitive binding method outlined above can be extended to creating networks that include non-imprinted drugs which are released when the template molecule appears in the surrounding medium. For this application, the MIP network must possess a weak affinity for a therapeutic drug and a strong affinity for the template molecule. When in the presence of imprint molecule, the network binds this molecule, which consequently leads to the release of drug. Such an MIP system has been shown to release hydrocortisone upon recognition of testosterone⁶³. Other MIP competitive binding systems include the use of

anesthetic drugs, methylxanthines and/or other sterols to trigger the responsive release of drug⁶³.

There are several physiological and pathological conditions that release particular analytes as direct indicators of the progression of the disease state. Therefore, a need exists to develop systems that are environmentally responsive hydrogels for given analytes. These analyte sensitive systems could be molecularly recognitive for biologicals produced at certain intervals and be able to release therapeutic agents in response. One such system is a calcium-responsive bioerodible drug delivery system which was devised by Goldbart and Kost¹²¹. This system is a starch-cellulose matrix that contains α -amylase, which is a biological protein regulated by calcium. As calcium enters the hydrogel system, bound α -amylase binds with this ion and is cleaved to become active. This active calcium can then be utilized by the body, and these gels could eventually be used to treat calcium dependent diseases such as osteoporosis.

In future technologies, imprinted gels or chains possessing certain macromolecular architecture with binding abilities could be used as the sensing elements within analyte sensitive controlled release systems. The design and implementation of imprinted recognition release systems would be challenging, but certainly one can envision imprinted gel films loaded with therapeutics. It could be reasoned that binding of target molecules to active sites or specific chemical groups could change the overall ionic character or hydrophilicity or

hydrophobicity and in turn cause the swelling of a polymer gel for release of a drug. Kataoka and coworkers^{122, 123} have shown this effect using a hydrogel that contains a borate-glucose complex. These gels exhibit a sharp transition in swelling degree with respect to glucose concentration. As glucose binds, the network becomes more hydrophilic due to the formation of a charged template-binding group complex. Thus, as the authors speculate, this type of polymer gel can be used as a chemical valve to regulate drug release in response to glucose concentration for use as a DDS in the treatment of diabetes.

2.8.3 MIP Hydrogels as Sensing/Actuating Elements in DDS

Although research groups have now demonstrated the ability to fabricate analyte sensitive polymers, there is a strong need to combine this sensing element with a transducing element in order to develop miniature diagnostic devices capable of rapidly detecting disease states and releasing therapeutic agents. These microdevices could be implantable, therefore increasing the ability to sense initial disease states and thus improving therapeutic efficacy, hereby reducing patient costs.

In recent years, fabrication techniques have been utilized to construct MEMS/NEMS, microarrays, microfluidic devices, micro total analysis systems (a.k.a. lab-on-a-chip), and other micro-/nanodevices. MEMS integrate mechanical and electronic elements on a common substrate to create devices for various applications. Microarrays have been established as the preferred

method for carrying out genetic analysis on a massive scale¹²⁴. Dubbed DNA arrays, DNA chips, or GeneChips, these devices have revolutionized the way researchers analyze gene expression in cells and tissue. Other researchers have focused on developing microfluidic devices, which are required for all microsystems requiring fluid transport¹²⁵. Total microanalysis systems integrate microvalves, micropumps, micro-separations, microsensors, and other components to create miniature analysis system, also known as lab-on-a-chip¹²⁶. These are extremely powerful devices that, as their name states, are capable of replacing entire conventional analytical labs with a microchip.

A fundamental component of the above systems and other micro-/nanodevices is sensors. A sensor measures a specific entity in the surrounding environment using a sensing element and then via a transducer(s), provides an output relating what was measured. Common transducers utilized for sensors include quartz crystal microbalances (QCM)¹²⁷, field effect transistors (FETs)¹²⁸, and microcantilevers¹²⁹. For biosensor applications, the sensor element is designed to interact with a specific biologically significant target molecule or condition, and the measurement can be made via a direct or an indirect method.

Many groups have recently begun utilizing environmentally responsive hydrogels in microscale applications as sensing and actuating components¹³⁰. Beebe and collaborators have micropatterned pH-sensitive hydrogels inside microfluidic channels to create micro-valves that could sense

environmental conditions and rapidly actuate in response¹³¹. Similarly, Madou and coworkers utilized a blend of a hydrogel and a redox polymer to create an “artificial muscle” that could act as an electro-actuated microvalve for possible applications in controlled drug delivery. Hayden et al. formed MIP hydrogels directly onto QCMs in order to create a size-independent analyte detector. This mass sensitive system was able to distinguish specific viruses and enzymes and could potentially be used in future DDS systems which release drugs based on a mass deflection in a cantilever⁹⁹. Additionally, researchers have developed microchips facilitating the controlled delivery of many therapeutics over a substantial period of time¹³².

In previous works, processes were developed for integrating environmentally responsive hydrogels into micro-scale applications^{76, 133-136}. In initial work, pH-sensitive hydrogels were photolithographically patterned onto silicon microcantilevers to create an ultrasensitive pH microsensor. The photolithographic process also allowed for multiple applications of different polymers on different cantilevers on the same chip. When compared with other micro-scale pH sensing techniques such as ion-sensitive field-effect transistors or potentiometric metal oxide electrodes, the sensitivity of this pH microsensor was at least two orders of magnitude greater. This ultrasensitive microsensor platform could contribute to the creation of innovative microdevices, such as an implantable chip that could monitor a physiological condition with ultrasensitivity,

as a key component of a therapeutic micro-device, and future research is focusing on bringing this idea to reality.

With success of the above techniques, focusing is now turning to creating MIP sensors that can recognize an analyte and in turn cause the release of a therapeutic compound. MIP polymer networks are advantageous in such systems because they can be tailored to bind any molecule with controlled selectivity and affinity. Preliminary results qualitatively and quantitatively demonstrate that these recognitive macromolecular networks are specific for small molecules, such as D-glucose¹³⁶ or larger proteins¹³⁷, and these networks can be effectively micropatterned in fine dimensions. These results are encouraging for the further development of functionalized biosensors and diagnostic devices and are applicable to other biologically significant molecules and biomimetic polymer networks, in which hydrogen bonding, hydrophobic, or ionic contributions will direct recognition.

2.9 Figures

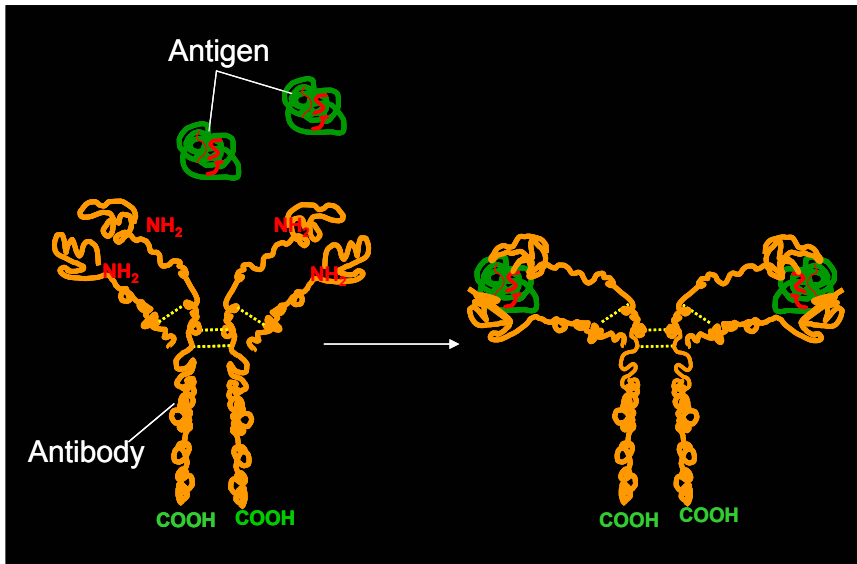


Figure 2.1: Antibody-Antigen recognition.

Antibodies are “Y” structures that recognize antigens via a very specific arrangement of amino acids.

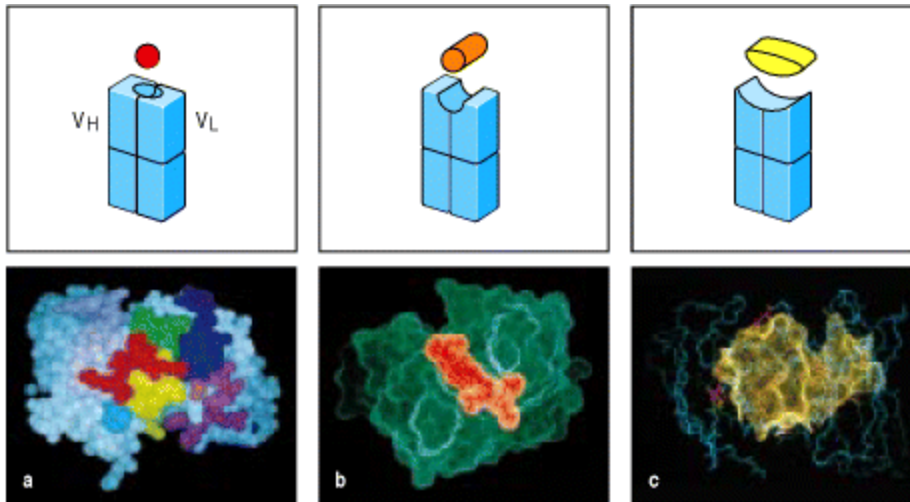


Figure 2.2: Antigens can bind in pockets or grooves, or on extended surfaces in the binding sites of antibodies.

The panels in the top row show schematic representations of the different types of binding site in the variable region of an antibody: *left*, pocket; *center*, groove; *right*, extended surface. Below are examples of each type. **Panel a:** the interaction of a small peptide antigen (colored regions) with pocketed antigen-binding site. **Panel b:** a peptide from the human immunodeficiency virus binds along a groove formed between the heavy- and light-chains. **Panel c:** complex between hen egg-white lysozyme and an antibody fragment, HyHel5. Image reproduced from Janeway et. al¹³.

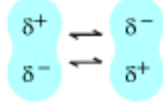
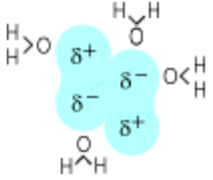
Noncovalent forces	Origin	
Electrostatic forces	Attraction between opposite charges	$\text{—NH}_3^+ \quad ^-\text{OOC—}$
Hydrogen bonds	Hydrogen shared between electronegative atoms (N,O)	$\begin{array}{c} >\text{N} & \text{—} & \text{H} & \cdots & \text{O} & = & \text{C} < \\ \delta^- & & \delta^+ & & \delta^- & & \end{array}$
Van der Waals forces	Fluctuations in electron clouds around molecules oppositely polarize neighboring atoms	
Hydrophobic forces	Hydrophobic groups interact unfavorably with water and tend to pack together to exclude water molecules. The attraction also involves van der Waals forces	

Figure 2.3: Non-covalent forces between antibodies and antigens.
 Reproduced from *Immunobiology* by C.A. Janeway et al¹³.

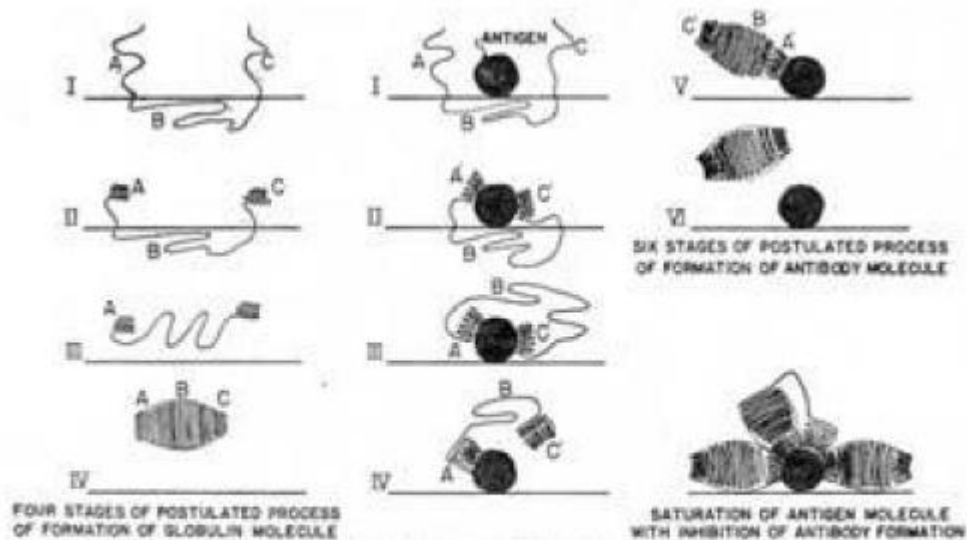


Fig. 1.—Diagrams representing four stages in the process of formation of a molecule of normal serum globulin (left side of figure) and six stages in the process of formation of an antibody molecule as the result of interaction of the globulin polypeptide chain with an antigen molecule. There is also shown (lower right) an antigen molecule surrounded by attached antibody molecules or parts of molecules and thus inhibited from further antibody formation.

Figure 2.4: Pauling's Original Drawings on Antibody Formation.

Pauling hypothesized that that free antibody chains could surround an antigen and “memorize” its shape, thus allowing the immune system to render the antigen inactive.

MIP Methodology

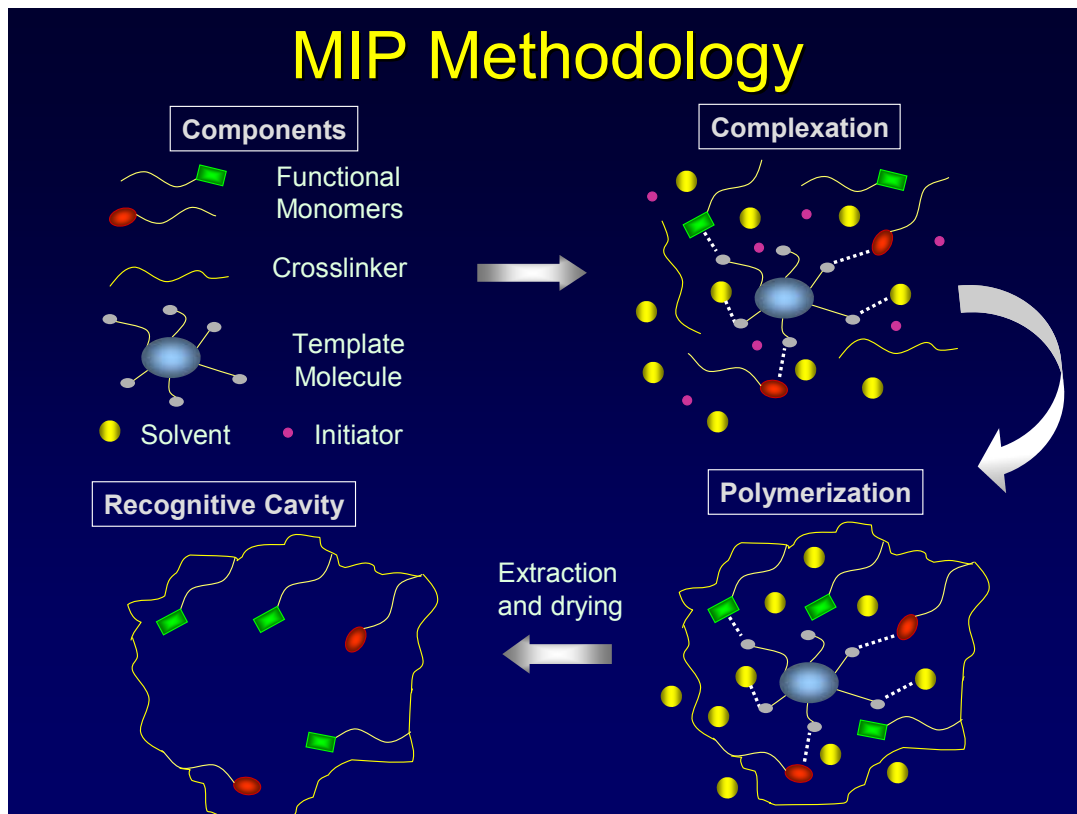
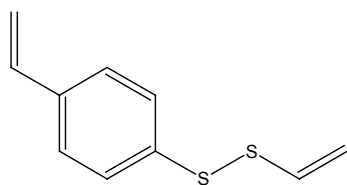
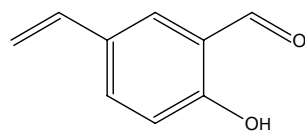


Figure 2.5: Molecular Imprinting Methodology.

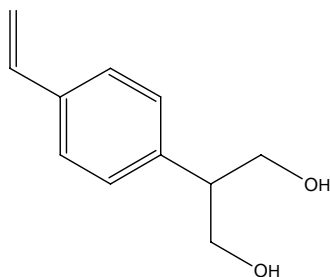
(*Components*) Functional monomers are placed in solution with an initiator and crosslinker. (*Complexation*) A complex forms between the functional monomers and the template. (*Polymerization*) The solution is then polymerized via free-radical polymerization. (*Recognitive Cavity*) The template can then be extracted to create a polymer with imprinted recognitive cavities.



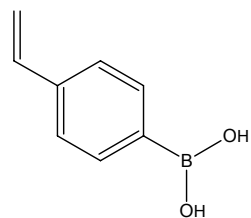
1-vinyl-4-(vinylthio)benzene



2-hydroxy-5-vinylbenzaldehyde



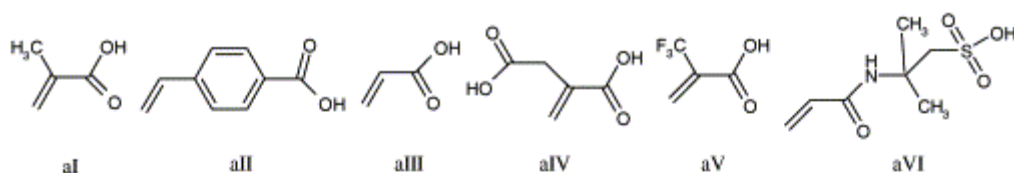
2-(4-vinylphenyl)propane-1,3-diol



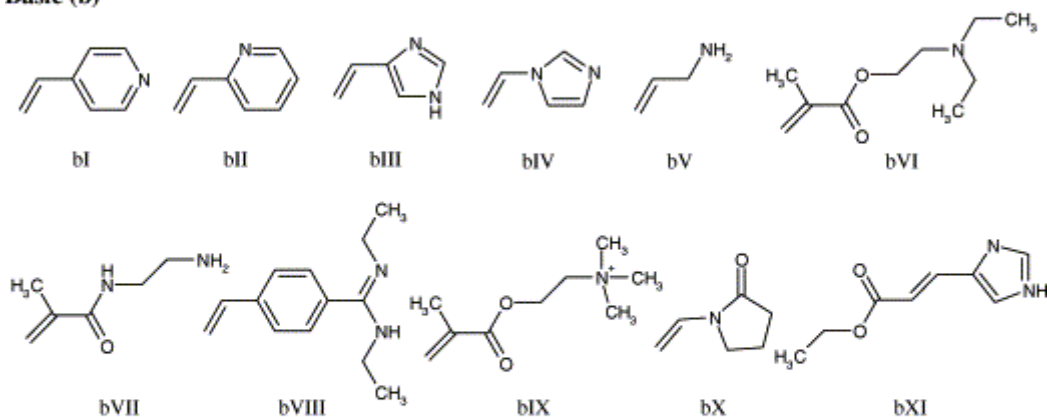
(4-vinylphenyl)methanediol

Figure 2.6: Functional Monomers in Covalent MIP

Acidic (a)



Basic (b)



Neutral (n)

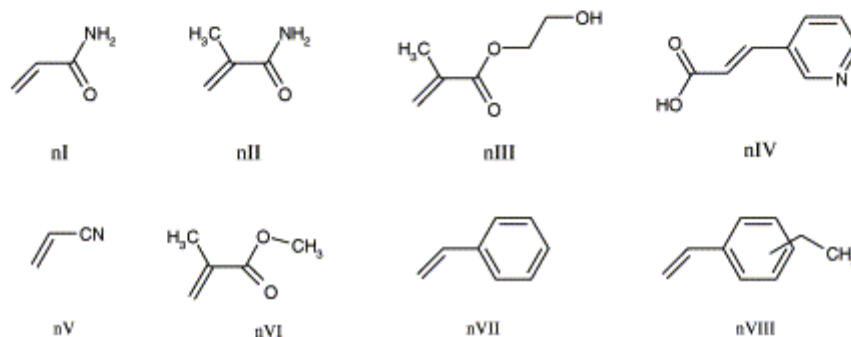


Figure 2.7: Functional Monomers in Non-Covalent MIP

The above figure outlines possible monomer choices arranged by functionality type. **Acidic;** **aI:** methacrylic acid (MAA); **aII:** *p*-vinylbenzoic acid; **aIII:** acrylic acid (AA); **aIV:** itaconic acid; **aV:** 2-(trifluoromethyl)-acrylic acid; **aVI:** acrylamido-(2-methyl)-propane sulfonic acid; **Basic;** **bI:** 4-vinylpyridine; **bII:** 2-vinylpyridine; **bIII:** 4-(5)-vinylimidazole; **bIV:** 1-vinylimidazole; **bV:** allylamine; **bVI:** *N,N*-diethyl aminoethyl methacrylamide; **bVII:** *N*-(2-aminethyl)-methacrylamide; **bVIII:** *N,N*-diethyl-4-styrylamidine; **bIX:** *N,N,N*-trimethyl aminoethylmethacrylate; **bX:** *N*-vinylpyrrolidone; **bXI:** urocanic ethyl ester. **Neutral;** **nI:** acrylamide; **nII:** methacrylamide; **nIII:** 2-hydroxyethyl methacrylate; **nIV:** trans-3-(3-pyridyl)-acrylic acid; **nV:** acrylonitrile; **nVI:** methyl methacrylate; **nVII:** styrene; **nVIII:** ethylstyrene⁸⁸.

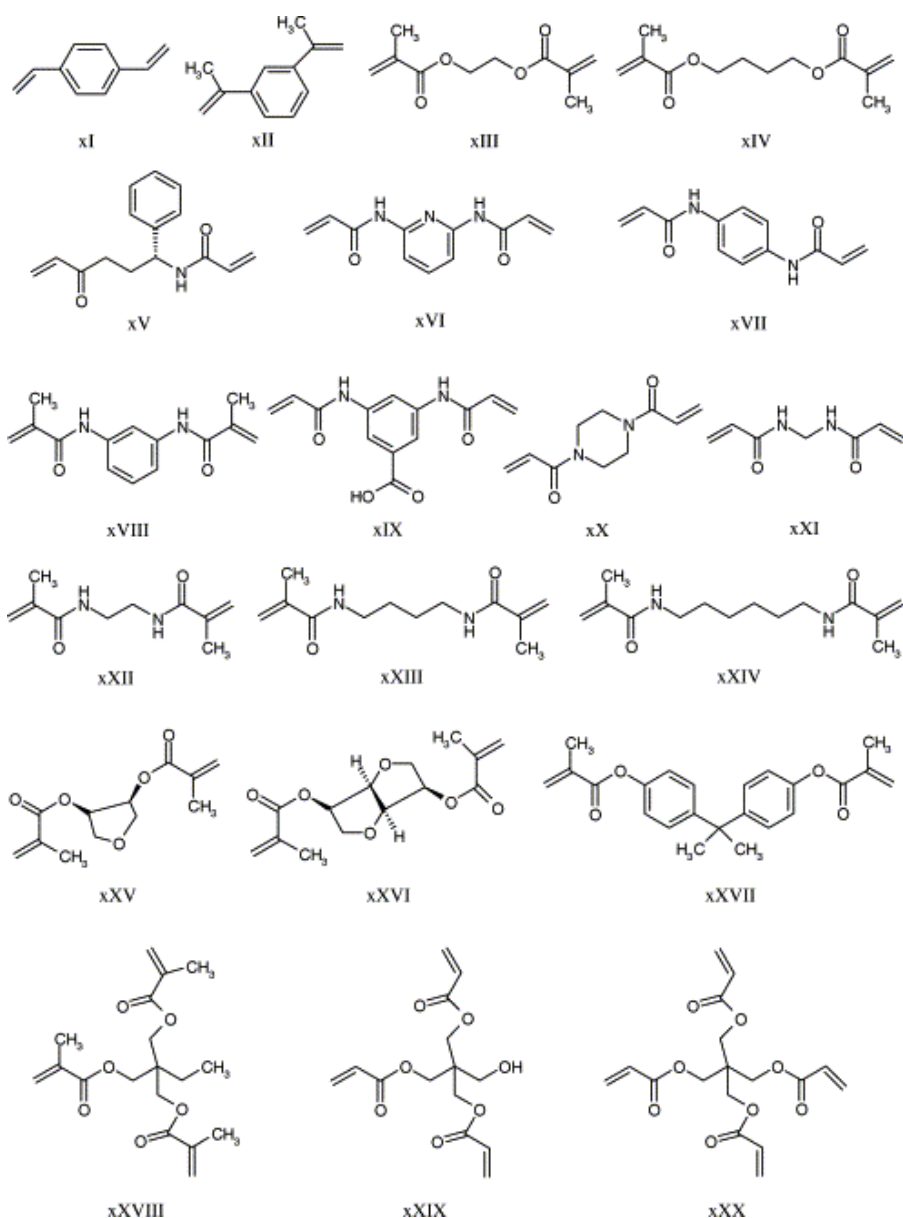


Figure 2.8: Crosslinkers Used in MIP

Widely studied crosslinkers in MIP **xI**: *p*-divinylbenzene; **xII**: 1,3-diisopropenyl benzene; **xIII**: ethylene glycol dimethacrylate; **xIV**: tetramethylene dimethacrylate; **xV**: *N,O*-bisacryloyl-L-phenylalaninol; **xVI**: 2,6-bisacryloylamidopyridine; **xVII**: 1,4-phenylene diacrylamide; **xVIII**: *N,N'*-1,3-phenylenebis(2-methyl-2-propenamide); **xIX**: 3,5-bisacrylamido benzoic acid; **XX**: 1,4-diacryloyl piperazine; **XXI**: *N,N'*-methylene bisacrylamide; **XXII**: *N,N'*-ethylene bismethacrylamide; **XXIII**: *N,N'*-tetramethylene bismethacrylamide; **XXIV**: *N,N'*-hexamethylene bismethacrylamide; **XXV**: anhydroerythritol dimethacrylate; **XXVI**: 1,4,3,6-dianhydro- β -sorbitol-2,5-dimethacrylate; **XXVII**: isopropylenebis(1,4-phenylene) dimethacrylate; **XXVIII**: trimethylpropane trimethacrylate; **XXIX**: pentaerythritol triacrylate; **XXX**: pentaerythritol tetraacrylate.

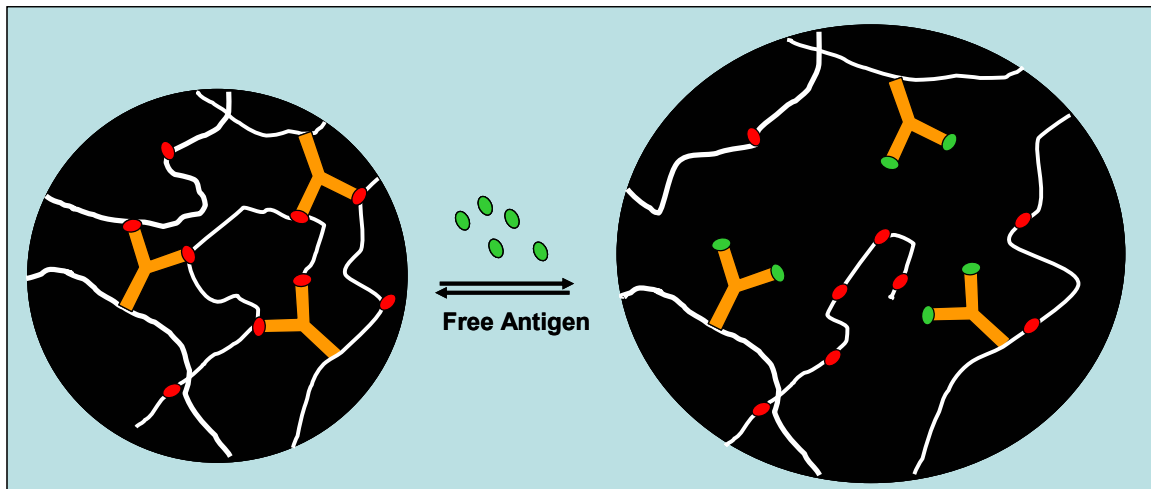


Figure 2.9: Reversible Antigen/Antibody Responsive Polymers.

In the presence of a higher affinity antigen, bound antibodies will release immobilized antigens and bind free antigens, thus causing swelling of the system.

2.10 References Cited

1. Chen, B. N.; Piletsky, S.; Turner, A. P. F., Molecular Recognition: Design of "Keys". *Comb. Chem. High Throughput Screen.* **2002**, 5, (6), 409-427.
2. Tulinsky, A., Molecular Interactions of Thrombin. *Semin. Thromb. Hemost.* **1996**, 22, (2), 117-124.
3. Cudic, P.; Behenna, D. C.; Kranz, J. K.; Kruger, R. G.; Wand, A. J.; Veklich, Y. I.; Weisel, J. W.; McCafferty, D. G., Functional Analysis of the Lipoglycopeptide Antibiotic Ramoplanin. *Chem. Biol.* **2002**, 9, (8), 897-906.
4. Britschgi, M.; von Greyerz, S.; Burkhart, C.; Pichler, W. J., Molecular Aspects of Drug Recognition by Specific T Cells. *Current Drug Targets* **2003**, 4, (1), 1-11.
5. Jimenez, R.; Salazar, G.; Baldrige, K. K.; Romesberg, F. E., Flexibility and Molecular Recognition in the Immune System. *Proc. Natl. Acad. Sci. U. S. A.* **2003**, 100, (1), 92-97.
6. Sundberg, E. J.; Mariuzza, R. A., Molecular Recognition in Anti Body-Antigen Complexes. *Protein Modules and Protein-Protein Interactions* **2003**, 61, 119-160.
7. Gitlin, G.; Bayer, E. A.; Wilchek, M., Studies on the Biotin-Binding Site of Avidin - Tryptophan Residues Involved in the Active-Site. *Biochem. J.* **1988**, 250, (1), 291-294.

8. Andersson, L.; Lunden, R., The Composition of Human Plasma. In Blomback, B.; Hanson, L., Eds. John Wiley and Sons: Bath, Great Britain, 1979; pp 17-21.
9. Green, N. M., Avidin. In *Adv. Protein Chem.*, Anfinsen, C. B., Ed. Academic Press: New York, 1975; Vol. 29.
10. Pugliese, L.; Coda, A.; Malcovati, M.; Bolognesi, M., 3-Dimensional Structure of the Tetragonal Crystal Form of Egg-White Avidin in Its Functional Complex with Biotin at 2.7-Angstrom Resolution. *J. Mol. Biol.* **1993**, 231, (3), 698-710.
11. Gitlin, G.; Bayer, E. A.; Wilchek, M., Studies on the Biotin-Binding Site of Avidin - Lysine Residues Involved in the Active-Site. *Biochem. J.* **1987**, 242, (3), 923-926.
12. Glick, B. R.; Pasternak, J. J., Microbial Production of Theurapeutic Agents. In *Molecular Biotechnology: Principles and Applications of Recombinant DNA*, ASM Press: Washington D.C., 1998; pp 235-237.
13. Janeway, C. A.; Travers, P.; Walport, M.; Shlomchik, M. J., *Immunobiology: The Immune System in Health and Disease*. Garland Publishing: New York, 2001.
14. Golub, E. S.; Green, D. R., *Immunology: A Synthesis*. Sinauer Assoc.: Sunderland, MA, 1991.

15. Rachkov, A.; Minoura, N., Towards Molecularly Imprinted Polymers Selective to Peptides and Proteins. The Epitope Approach. *Biochimica et Biophysica Acta (BBA) - Protein Structure and Molecular Enzymology* **2001**, 1544, (1-2), 255.
16. Haupt, K.; Mosbach, K., Plastic Antibodies: Developments and Applications. *Trends. Biotechnol.* **1998**, 16, (11), 468-475.
17. Vlatakis, G.; Andersson, L. I.; Muller, R.; Mosbach, K., Drug Assay Using Antibody Mimics Made by Molecular Imprinting. *Nature* **1993**, 361, (6413), 645.
18. Reid, L. M.; Zern, M. A., *Extracellular Matrix Chemistry and Biology*. Marcel Dekker: New York, 1993.
19. Schoen, F. J.; Mitchell, R. N., Tissues, the Extracellular Matrix, and Cell-Biomaterial Interactions. In *Biomaterials Science: An Introduction to Materials in Medicine*, 2 ed.; Ratner, B. D.; Hoffmann, A. S.; Schoen, F. J.; Lemons, J. E., Eds. Elsevier, Inc.: San Diego, 2004; pp 260-281.
20. DeBakey, M. S., F., Battle Injuries of the Arteries. *Am. J. Surg.* **1946**, 123, 534.
21. Voorhees, A. B. J., A.; Blakemore, A.H., The Use of Tubes Constructed from "Vinyon" N Cloth in Bridging Arterial Defects. *Ann. Surg.* **1952**, 135, 332.
22. Padera, R. F.; Schoen, F. J., Cardiovascular Medical Devices. In *Biomaterials Science: An Introduction to Materials in Medicine*, 2 ed.; Ratner, B.

D.; Hoffmann, A. S.; Schoen, F. J.; Lemons, J. E., Eds. Elsevier, Inc.: San Diego, 2004; pp 470-493.

23. Shin, H.; Jo, S.; Mikos, A. G., Biomimetic Materials for Tissue Engineering. *Biomaterials* **2003**, 24, (24), 4353-4364.

24. Burdick, J. A.; Anseth, K. S., Photoencapsulation of Osteoblasts in Injectable RGD-Modified PEG Hydrogels for Bone Tissue Engineering. *Biomaterials* **2002**, 23, (22), 4315-4323.

25. Hern, D. L.; Hubbell, J. A., Incorporation of Adhesion Peptides into Nonadhesive Hydrogels Useful for Tissue Resurfacing. *J. Biomed. Mater. Res.* **1998**, 39, (2), 266-276.

26. Mann, B. K.; Tsai, A. T.; Scott-Burden, T.; West, J. L., Modification of Surfaces with Cell Adhesion Peptides Alters Extracellular Matrix Deposition. *Biomaterials* **1999**, 20, (23-24), 2281-2286.

27. Nguyen, K. T.; West, J. L., Photopolymerizable Hydrogels for Tissue Engineering Applications. *Biomaterials* **2002**, 23, (22), 4307-4314.

28. Lee, C. H.; Singla, A.; Lee, Y., Biomedical Applications of Collagen. *Int. J. Pharm.* **2001**, 221, (1-2), 1-22.

29. Frenkel, S. R.; Toolan, B.; Menche, D.; Pitman, M. I.; Pachence, J. M., Chondrocyte Transplantation Using a Collagen Bilayer Matrix for Cartilage Repair. *J. Bone Joint Surg. Br.* **1997**, 79B, (5), 831-836.

30. Kobashi, T.; Matsuda, T., Fabrication of Compliant Hybrid Grafts Supported with Elastomeric Meshes. *Cell Transplant.* **1999**, 8, (5), 477-488.
31. Ma, P. X., Scaffolds for Tissue Fabrication. *Materials Today* **2004**, 7, (5), 30-40.
32. Li, S. M., Hydrolytic Degradation Characteristics of Aliphatic Polyesters Derived from Lactic and Glycolic Acids. *J. Biomed. Mater. Res.* **1999**, 48, (3), 342-353.
33. Whang, K.; Goldstick, T. K.; Healy, K. E., A Biodegradable Polymer Scaffold for Delivery of Osteotropic Factors. *Biomaterials* **2000**, 21, (24), 2545-2551.
34. Brannon-Peppas, L.; Vert, M., Polylactic and Polyglycolic Acids as Drug Delivery Carriers. In *Handbook of Pharmaceutical Controlled Release Technology*, Wise, D.; Brannon-Peppas, L.; Klibanov, A. M.; Langer, R.; Mikos, A. G.; Peppas, N. A.; Trantolo, D. J.; Yaszemski, M. J.; Wnek, G. E., Eds. 2000; pp 99-130.
35. Reed, A. M.; Gilding, D. K., Biodegradable Polymers for Use in Surgery -- Poly(Glycolic)/Poly(lactic Acid) Homo and Copolymers: 2. In vitro Degradation. *Polymer* **1981**, 22, (4), 494-498.
36. Pitt, C. G.; Gratzl, M. M.; Kimmel, G. L.; Surles, J.; Schindler, A., Aliphatic Polyesters.2. The Degradation of Poly(dl-Lactide), Poly(Epsilon-Caprolactone), and Their Copolymers *in vivo*. *Biomaterials* **1981**, 2, (4), 215-220.

37. Moran, J. M. B., L.J., Fabrication and Characterization of PLA/PGA Composites for Cartilage Tissue Engineering. *Tissue Eng.* **1998**, 4, S498.
38. Peppas, N. A., Devices Based on Intelligent Biopolymers for Oral Protein Delivery. *Int. J. Pharm.* **2004**, 277, (1-2), 11-17.
39. Flynn, L.; Dalton, P. D.; Shoichet, M. S., Fiber Templating of Poly(2-Hydroxyethyl Methacrylate) for Neural Tissue Engineering. *Biomaterials* **2003**, 24, (23), 4265-4272.
40. Drury, J. L.; Mooney, D. J., Hydrogels for Tissue Engineering: Scaffold Design Variables and Applications. *Biomaterials* **2003**, 24, (24), 4337-4351.
41. Mann, B. K.; Schmedlen, R. H.; West, J. L., Tethered-TGF-[Beta] Increases Extracellular Matrix Production of Vascular Smooth Muscle Cells. *Biomaterials* **2001**, 22, (5), 439-444.
42. Elisseeff, J.; Anseth, K.; Sims, D.; McIntosh, W.; Randolph, M.; Langer, R., Transdermal Photopolymerization for Minimally Invasive Implantation. *Proc. Natl. Acad. Sci. U. S. A.* **1999**, 96, (6), 3104-3107.
43. Hubbell, J. A. P., C.K.; Sawhney, A.S.; Amarpreet, S.; Desai, N.P.; Neil, P.; Hill-West, J.L., *Photopolymerizable Biodegradable Hydrogels as Tissue Contacting Materials and Controlled-Release Carriers*. 2001.

44. Burkoth, A. K.; Anseth, K. S., A Review of Photocrosslinked Polyanhydrides: In Situ Forming Degradable Networks. *Biomaterials* **2000**, 21, (23), 2395-2404.
45. Davis, K. A.; Burdick, J. A.; Anseth, K. S., Photoinitiated Crosslinked Degradable Copolymer Networks for Tissue Engineering Applications. *Biomaterials* **2003**, 24, (14), 2485-2495.
46. Brem, H.; Gabikian, P., Biodegradable Polymer Implants to Treat Brain Tumors. *J. Controlled Release* **2001**, 74, (1-3), 63-67.
47. Anseth, K. S.; Shastri, V. R.; Langer, R., Photopolymerizable Degradable Polyanhydrides with Osteocompatibility. *Nature Biotech.* **1999**, 17, 156-159.
48. Jiang, H. L.; Zhu, K. J., Preparation, Characterization, and Degradation Characteristics of Poly(Anhydrides) Containing Poly(Ethylene Glycol). *Polym. Int.* **1999**, 48, 47-52.
49. Ansell, R. J.; Ramstrom, O.; Mosbach, K., Towards Artificial Antibodies Prepared by Molecular Imprinting. *Clin. Chem.* **1996**, 42, (9), 1506-1512.
50. Mosbach, K.; Ramstrom, O., The Emerging Technique of Molecular Imprinting and Its Future Impact on Biotechnology. *Bio/Technology* **1996**, 14, (2), 163-170.
51. Cambrosio, A.; Jacobi, D.; Keating, P., Arguing with Images: Pauling's Theory of Antibody Formation. *Representations* **2005**, 89, (1), 94-130.

52. Pauling, L., A Theory of the Structure and Process of Formation of Antibodies. *J. Am. Chem. Soc.* **1940**, 62, 2645-2655.
53. Zhou, Y. X.; Yu, B.; Levon, K., Potentiometric Sensor for Dipicolinic Acid. *Biosens Bioelectron* **2005**, 20, (9), 1851-1855.
54. Zhang, Z. H.; Li, H.; Liao, H. P.; Nie, L. H.; Yao, S. Z., Influence of Cross-Linkers' Amount on the Performance of the Piezoelectric Sensor Modified with Molecularly Imprinted Polymers. *Sensors And Actuators, B: Chemical* **2005**, 105, (2), 176-182.
55. Lin, T. Y.; Hu, C. H.; Chou, T. C., Determination of Albumin Concentration by MIP-QCM Sensor. *Biosens Bioelectron* **2004**, 20, (1), 75-81.
56. Liu, T. B.; Burger, C.; Chu, B., Nanofabrication in Polymer Matrices. *Progress In Polymer Science* **2003**, 28, (1), 5-26.
57. Ansell, R. J.; Kriz, D.; Mosbach, K., Molecularly Imprinted Polymers for Bioanalysis: Chromatography, Binding Assays and Biomimetic Sensors. *Current Opinion in Biotechnology* **1996**, 7, (1), 89-94.
58. Adhikari, B.; Majumdar, S., Polymers in Sensor Applications. *Progress in Polymer Science* **2004**, 29, (7), 699-766.
59. Ulbricht, M., Membrane Separations Using Molecularly Imprinted Polymers. *Journal Of Chromatography B* **2004**, 804, (1), 113-115.

60. Yoshikawa, M., Molecularly Imprinted Polymeric Membranes. *Bioseparation* **2000**, 10, (6), 277-286.
61. Ciardelli, G.; Cioni, B.; Cristallini, C.; Barbani, N.; Silvestri, D.; Giusti, P., Acrylic Polymeric Nanospheres for the Release and Recognition of Molecules of Clinical Interest. *Biosens Bioelectron* **2004**, 20, (6), 1083-1090.
62. Bures, P.; Huang, Y. B.; Oral, E.; Peppas, N. A., Surface Modifications and Molecular Imprinting of Polymers in Medical and Pharmaceutical Applications. *J. Controlled Release* **2001**, 72, (1-3), 25-33.
63. Alvarez-Lorenzo, C.; Concheiro, A., Molecularly Imprinted Polymers for Drug Delivery. *J. Chromatogr. B Analyt. Technol. Biomed. Life Sci.* **2004**, 804, (1), 231-245.
64. Gallardo, A.; Eguiburu, J. L.; Berridi, M. J. F.; San Roman, J., Preparation and *in vitro* Release Studies of Ibuprofen-Loaded Films and Microspheres Made from Graft Copolymers of Poly(L-Lactic Acid) on Acrylic Backbones. *J. Controlled Release* **1998**, 55, (2-3), 171-179.
65. Oral, E.; Peppas, N. A., Responsive and Recognitive Hydrogels Using Star Polymers. *J. Biomed. Mater. Res. A* **2004**, 68A, (3), 439-447.
66. Hilt, J. Z., Nanotechnology and Biomimetic Methods in Therapeutics: Molecular Scale Control with Some Help from Nature. *Adv. Drug Deliv. Rev.* **2004**, 56, (11), 1533-1536.

67. Hilt, J. Z.; Byrne, M. E., Configurational Biomimesis in Drug Delivery: Molecular Imprinting of Biologically Significant Molecules. *Adv. Drug Deliv. Rev.* **2004**, 56, (11), 1599-1620.
68. Hwang, C.-C.; Lee, W.-C., Chromatographic Characteristics of Cholesterol-Imprinted Polymers Prepared by Covalent and Non-Covalent Imprinting Methods. *J. Chromatogr. A* **2002**, 962, (1-2), 69.
69. Takeda, K.; Kobayashi, T., Bisphenol A Imprinted Polymer Adsorbents with Selective Recognition and Binding Characteristics. *Science and Technology of Advanced Materials* **2005**, 6, (2), 165.
70. Hedin-Dahlstrom, J.; Shoravi, S.; Wikman, S.; Nicholls, I. A., Stereoselective Reduction of Menthone by Molecularly Imprinted Polymers. *Tetrahedron: Asymmetry* **2004**, 15, (15), 2431.
71. Sellergren, B., Noncovalent Molecular Imprinting: Antibody-Like Molecular Recognition in Polymeric Network Materials. *Trac-Trends In Analytical Chemistry* **1997**, 16, (6), 310-320.
72. Wulff, G. u. n.; Knorr, K., Stoichiometric Noncovalent Interaction in Molecular Imprinting. *Bioseparation* **2000**, 10, (6), 257-276.
73. Mosbach, K., Molecular Imprinting. *Trends Biochem. Sci.* **1994**, 19, (1), 9-14.

74. Mosbach, K., Toward the Next Generation of Molecular Imprinting with Emphasis on the Formation, by Direct Molding, of Compounds with Biological Activity (Biomimetics). *Anal. Chim. Acta* **2001**, 435, (1), 3-8.
75. Whitcombe, M.; Rodriguez, M.; Villar P, Vulfson EN, A New Method for the Introduction of Recognition Site Functionality into Polymers Prepared by Molecular Imprinting: Synthesis and Characterization of Polymeric Receptors for Cholesterol. *J. Am. Chem. Soc.* **1995**, 117, 7105-7111.
76. Byrne, M. E.; Park, K.; Peppas, N. A., Molecular Imprinting within Hydrogels. *Advanced Drug Delivery Reviews* **2002**, 54, (1), 149-161.
77. Wizeman, W., Kofinas P, Molecularly Imprinted Polymer Hydrogels Displaying Isomerically Resolved Glucose Binding. *Biomaterials* **2001**, 22, 1485-1495.
78. Komiyama, M.; Toshifumi, T.; Mukawa, T.; Asanuma, H., *Molecular Imprinting: From Fundamentals to Application*. Wiley-VCH: Morlenbach, Germany, 2003.
79. Mishra, P.; Griebenow, K.; Klibanov, A. M., Structural Basis for the Molecular Memory of Imprinted Proteins in Anhydrous Media. *Biotechnol. Bioeng.* **1996**, 52, (5), 609-614.
80. Slade, C. J., Molecular (or Bio-) Imprinting of Bovine Serum Albumin. *J. Mol. Catal., B Enzym.* **2000**, 9, (1-3), 97-105.

81. Liu, J.; Luo, G.; Gao, S.; Zhang, K.; Chen, X.; Shen, J., Generation of a Glutathione Peroxidase-Like Mimic Using Bioimprinting and Chemical Mutation. *Chem. Commun.* **1999**, 5, (2), 199.
82. Motherwell, W. B.; Bingham, M. J.; Six, Y., Recent Progress in the Design and Synthesis of Artificial Enzymes. *Tetrahedron* **2001**, 57, (22), 4663.
83. Wulff, G.; Grobeeinsler, R.; Vesper, W.; Sarhan, A., Enzyme-Analogue Built Polymers.5. Specificity Distribution of Chiral Cavities Prepared in Synthetic-Polymers. *Makromolekulare Chemie-Macromolecular Chemistry and Physics* **1977**, 178, (10), 2817-2825.
84. Wulff, G.; Vesper, W.; Grobeeinsler, R.; Sarhan, A., Enzyme-Analogue Built Polymers.4. Synthesis of Polymers Containing Chiral Cavities and Their Use for Resolution of Racemates. *Makromolekulare Chemie-Macromolecular Chemistry and Physics* **1977**, 178, (10), 2799-2816.
85. Arshady, R.; Mosbach, K., Synthesis of Substrate-Selective Polymers by Host-Guest Polymerization. *Macromolecular Chemistry and Physics-Makromolekulare Chemie* **1981**, 182, (2), 687-692.
86. Bures, P.; Huang, Y.; Oral, E.; Peppas, N. A., Surface Modifications and Molecular Imprinting of Polymers in Medical and Pharmaceutical Applications. *Journal of Controlled Release* **2001**, 72, (1-3), 25-33.
87. Davies, M. P.; De Biasi, V.; Perrett, D., Approaches to the Rational Design of Molecularly Imprinted Polymers. *Anal. Chim. Acta* **2004**, 504, (1), 7-14.

88. Cormack, P. A. G.; Elorza, A. Z., Molecularly Imprinted Polymers: Synthesis and Characterisation. *Journal of Chromatography B* **2004**, 804, (1), 173.
89. Oral, E.; Peppas, N. A., Molecularly Imprinted Hydrogels with Polyfunctional Methacrylates. In *Molecularly Imprinted Polymer Science and Technology*, Brain, K. R.; Alexander, C. J., Eds. STS Publishing: Cardiff, 2000; Vol. 111.
90. Byrne, M. E.; Peppas, N. A. Biomimetic Materials for Recognition of Biomolecules: Recognitive Networks for Drug Delivery and Bionanotechnology. Purdue University, West Lafayette, IN, 2003.
91. Cormack, P. A. G.; Elorza, A. Z., Molecularly Imprinted Polymers: Synthesis and Characterisation. *Journal of Chromatography B* **2004**, 804, (1), 173-182.
92. Oral, E.; Peppas, N. A., Responsive and Recognitive Hydrogels Using Star Polymers. *Journal Biomedical Materials Research Part A* **2004**, 68A, (3), 439-477.
93. Parmpi, P.; Kofinas, P., Biomimetic Glucose Recognition Using Molecularly Imprinted Polymer Hydrogels. *Biomaterials* **2004**, 25, (10), 1969-1973.

94. Lu, Y.; Li, C. X.; Liu, X. H.; Huang, W. Q., Molecular Recognition through the Exact Placement of Functional Groups on Non-Covalent Molecularly Imprinted Polymers. *J. Chromatogr. A* **2002**, 950, (1-2), 89-97.
95. Bao, G., Mechanics of Biomolecules. *Journal of the Mechanics and Physics of Solids* **2002**, 50, (11), 2237-2274.
96. Miyata, T.; Uragami, T.; Nakamae, K., Biomolecule-Sensitive Hydrogels. *Adv. Drug Deliv. Rev.* **2002**, 54, (1), 79-98.
97. Keegan, M. E.; Whittum-Hudson, J. A.; Mark Saltzman, W., Biomimetic Design in Microparticulate Vaccines. *Biomaterials* **2003**, 24, (24), 4435-4443.
98. Bolisay, L. D. V.; March, J. F.; Bentley, W. E.; Kofinas, P. In *Separation of Baculoviruses Using Molecularly Imprinted Polymer Gels*, Materials Research Society, San Fransisco, 2004; Materials Research Society: San Fransisco, 2004; pp G3.1.1-G3.1.5.
99. Dickert, F. L.; Lieberzeit, P.; Miarecka, S. G.; Mann, K. J.; Hayden, O.; Palfinger, C., Synthetic Receptors for Chemical Sensors--Subnano- and Micrometre Patterning by Imprinting Techniques. *Biosensors and Bioelectronics* **2004**, 20, (6), 1040.
100. Lai, J. P.; Lu, X. Y.; Lu, C. Y.; Ju, H. F.; He, X. W., Preparation and Evaluation of Molecularly Imprinted Polymeric Microspheres by Aqueous Suspension Polymerization for Use as a High-Performance Liquid Chromatography Stationary Phase. *Anal. Chim. Acta* **2001**, 442, (1), 105-111.

101. Shi, H.; Tsai, W. B.; Garrison, M. D.; Ferrari, S.; Ratner, B. D., Template-Imprinted Nanostructured Surfaces for Protein Recognition. *Nature* **1999**, 398, (6728), 593-597.
102. Lin, T.-Y.; Hu, C.-H.; Chou, T.-C., Determination of Albumin Concentration by MIP-QCM Sensor. *Biosensors and Bioelectronics* **2004**, 20, (1), 75-81.
103. Venton, D. L.; Gudipati, E., Influence of Protein on Polysiloxane Polymer Formation: Evidence for Induction of Complementary Protein-Polymer Interactions. *Biochimica et Biophysica Acta (BBA) - Protein Structure and Molecular Enzymology* **1995**, 1250, (2), 126.
104. Bromberg, L. E.; Klibanov, A. M., Transport of Proteins Dissolved in Organic-Solvents across Biomimetic Membranes. *Proc. Natl. Acad. Sci. U. S. A.* **1995**, 92, (5), 1262-1266.
105. Vaidya, A. A.; Lele, B. S.; Kulkarni, M. G.; Mashelkar, R. A., Thermoprecipitation of Lysozyme from Egg White Using Copolymers of N-Isopropylacrylamide and Acidic Monomers. *J. Biotechnol.* **2001**, 87, (2), 95-107.
106. Sternberg, M.; Hershberger, D., Separation of Proteins with Polyacrylic Acids. *Biochimica et Biophysica Acta (BBA) - Protein Structure* **1974**, 342, (1), 195-206.
107. Ragab, D. M.; Babiker, E. E.; Eltinay, A. H., Fractionation, Solubility and Functional Properties of Cowpea (*Vigna Unguiculata*) Proteins as Affected by pH and/or Salt Concentration. *Food Chem.* **2004**, 84, (2), 207-212.

108. Droge, J. H. M.; Janssen, L. H. M.; Wilting, J., A Comparative-Study of Some Physicochemical Properties of Human-Serum Albumin Samples from Different Sources.1. Some Physicochemical Properties of Isoionic Human-Serum Albumin Solutions. *Biochem. Pharmacol.* **1982**, 31, (23), 3775-3779.
109. Vogel, V.; Thomas, W. E.; Craig, D. W.; Krammer, A.; Baneyx, G., Structural Insights into the Mechanical Regulation of Molecular Recognition Sites. *Trends. Biotechnol.* **2001**, 19, (10), 416-+.
110. Peppas, N. A.; Bures, P.; Leobandung, W.; Ichikawa, H., Hydrogels in Pharmaceutical Formulations. *Eur. J. Pharm. Biopharm.* **2000**, 50, (1), 27-46.
111. Peppas, N. A.; Khare, A. R., Preparation, Structure and Diffusional Behavior of Hydrogels in Controlled-Release. *Adv. Drug Deliv. Rev.* **1993**, 11, (1-2), 1-35.
112. Peppas, N. A.; Colombo, P., Analysis of Drug Release Behavior from Swellable Polymer Carriers Using the Dimensionality Index. *J. Controlled Release* **1997**, 45, (1), 35-40.
113. Alvarez-Lorenzo, C. H., H.; Gomez-Amoza, J.L.; Martinez-Pacheco, R.; Souto, C.; Concheiro, A., Soft Contact Lenses Capable of Sustained Delivery of Timolol. *J. Pharm. Sci.* **2002**, 91, (10), 2182.
114. Alvarez-Lorenzo, C.; Guney, O.; Oya, T.; Sakai, Y.; Kobayashi, M.; Enoki, T.; Takeoka, Y.; Ishibashi, T.; Kuroda, K.; Tanaka, K.; Wang, G. Q.; Grosberg, A. Y.; Masamune, S.; Tanaka, T., Reversible Adsorption of Calcium Ions by

Imprinted Temperature Sensitive Gels. *J. Chem. Phys.* **2001**, 114, (6), 2812-2816.

115. Enoki, T.; Tanaka, K.; Watanabe, T.; Oya, T.; Sakiyama, T.; Takeoka, Y.; Ito, K.; Wang, G. Q.; Annaka, M.; Hara, K.; Du, R.; Chuang, J.; Wasserman, K.; Grosberg, A. Y.; Masamune, S.; Tanaka, T., Frustrations in Polymer Conformation in Gels and Their Minimization through Molecular Imprinting. *Phys. Rev. Lett.* **2000**, 85, (23), 5000-5003.

116. Alvarez-Lorenzo, C.; Guney, O.; Oya, T.; Sakai, Y.; Kobayashi, M.; Enoki, T.; Takeoka, Y.; Ishibashi, T.; Kuroda, K.; Tanaka, K.; Wang, G.; Grosberg, A.; Masamune, S.; Tanaka, T., Polymer Gels That Memorize Elements of Molecular Conformation. *Macromolecules* **2000**, 33, (23), 8693-8697.

117. Alvarez-Lorenzo, C.; Hiratani, H.; Tanaka, K.; Stancil, K.; Grosberg, A.; Tanaka, T., Simultaneous Multiple-Point Adsorption of Aluminum Ions and Charged Molecules a Polyampholyte Thermosensitive Gel: Controlling Frustrations in a Heteropolymer Gel. *Langmuir* **2001**, 17, (12), 3616-3622.

118. Hiratani, H.; Alvarez-Lorenzo, C.; Chuang, J.; Guney, O.; Grosberg, A.; Tanaka, T., Effect of Reversible Cross-Linker, N,N '-Bis(Acryloyl)Cystamine, on Calcium Ion Adsorption by Imprinted Gels. *Langmuir* **2001**, 17, (14), 4431-4436.

119. Salins, L. L. E.; Deo, S. K.; Daunert, S., Phosphate Binding Protein as the Biorecognition Element in a Biosensor for Phosphate. *Sens. Actuators, B* **2004**, 97, (1), 81-89.

120. Miyata, T.; Asami, N.; Uragami, T., A Reversibly Antigen-Responsive Hydrogel. *Nature* **1999**, 399, (6738), 766.
121. Goldbart, R.; Kost, J., Calcium Responsive Bioerodible Drug Delivery System. *Pharm. Res.* **1999**, 16, (9), 1483-1486.
122. Kataoka, K.; Miyazaki, H.; Bunya, M.; Okano, T.; Sakurai, Y., On-Off Regulation of Insulin-Release by Totally Synthetic Polymer Gels Responding to External Glucose Concentration. *Abstr. Pap. Am. Chem. Soc.* **1999**, 217, U564-U564.
123. Uchimura, E.; Otsuka, H.; Okano, T.; Sakurai, Y.; Kataoka, K., Totally Synthetic Polymer with Lectin-Like Function: Induction of Killer Cells by the Copolymer of 3-Acrylamidophenylboronic Acid with N,N-Dimethylacrylamide. *Biotechnol. Bioeng.* **2001**, 72, (3), 307-314.
124. Gershon, D., Microarray Technology - an Array of Opportunities. *Nature* **2002**, 416, (6883), 885-886.
125. Thorsen, T.; Maerkl, S.; Quake, S., Microfluidic Large-Scale Integration. *Science* **2002**, 298, (5593), 580-584.
126. Reyes, D.; Iossifidis, D.; Auroux, P.; Manz, A., Micro Total Analysis Systems. 1. Introduction, Theory, and Technology. *Anal. Chem.* **2002**, 74, (12), 2623-2636.

127. O'Sullivan, C. K.; Guilbault, G. G., Commercial Quartz Crystal Microbalances - Theory and Applications. *Biosens. and Bioelec.* **1999**, 14, (8-9), 663.
128. Schoning, M.; Poghossian, A., Recent Advances in Biologically Sensitive Field-Effect Transistors (BioFETs). *Analyst* **2002**, 127, (9), 1137-1151.
129. Sepaniak, M.; Datskos, P.; Lavrik, N.; Tipple, C., Microcantilever Transducers: A New Approach to Sensor Technology. *Anal. Chem.* **2002**, 74, (21), 568A-575A.
130. Byrne, M. E.; Henthorn, D. B.; Huang, Y.; Peppas, N. A., Micropatterning Biomimetic Materials for Bioadhesion and Drug Delivery. In *Biomimetic Materials and Design: Biointerfacial Strategies, Tissue Engineering and Targeted Drug Delivery*, Diller, A. K.; Lowman, A., Eds. Dekker: New York, 2002; pp 443-470.
131. Beebe, D.; Moore, J.; Bauer, J.; Yu, Q.; Liu, R.; Devadoss, C.; Jo, B., Functional Hydrogel Structures for Autonomous Flow Control inside Microfluidic Channels. *Nature* **2000**, 404, (6778), 588-+.
132. Santini, J.; Cima, M.; Langer, R., A Controlled-Release Microchip. *Nature* **1999**, 397, (6717), 335-338.
133. Bashir, R.; Hilt, J. Z.; Elibol, O.; Gupta, A.; Peppas, N. A., Micromechanical Cantilever as an Ultrasensitive pH Microsensor. *Appl. Phys. Lett.* **2002**, 81, (16), 3091-3093.

134. Hilt, J. Z.; Gupta, A. K.; Bashir, R.; Peppas, N. A., Ultrasensitive BioMEMS Sensors Based on Microcantilevers Patterned with Environmentally Responsive Hydrogels. *Biomed. Microdevices* **2003**, 5, (3), 177-184.
135. Ward, J. H.; Bashir, R.; Peppas, N. A., Micropatterning of Biomedical Polymer Surfaces by Novel UV Polymerization Techniques. *J. Biomed. Mater. Res.* **2001**, 56, (3), 351-360.
136. Byrne, M.; Oral, E.; Hilt, J.; Peppas, N., Networks for Recognition of Biomolecules: Molecular Imprinting and Micropatterning Poly(Ethylene Glycol)-Containing Films. *Polym. Advan. Technol.* **2002**, 13, (10-12), 798-816.
137. Bergmann, N.; Peppas, N. A., Protein-Imprinted Microparticles for Tissue Engineering Application. *Trans. Soc. Biomat.* **2003**, 29, 457.

Chapter 3: Objectives

The application of polymeric materials to biosensors and biomaterials is an exciting research area. The major property of many of material successes lies in their ability to recognize and bind a specific target molecule. In this work, we investigated biocompatible acrylamide-based polymer systems that utilized non-covalent interactions. The recognition of these networks to a template protein in aqueous solutions was determined using various methods, and the material properties of the gels were studied.

The properties of polymer networks as recognition-based materials were determined by:

- (i) preparation of molecularly imprinted acrylamide, methacrylic acid and 2-(dimethylaminoethyl) methacrylate polymers and copolymers fabricated utilizing non-covalent interactions between template protein lysozyme and functional monomers; and
- (ii) examination of the equilibrium capacity of these polymers to recognize the template molecule and selectivity in uptake of the network for the template and structurally similar compounds.

Fundamental properties of these recognition-based networks were investigated by:

- (i) scanning electron microscopy to determine differences between imprinted polymers and controls;
- (ii) differential scanning calorimetry and Fourier Transform Infrared Spectroscopy to determine if template presence during polymerization affected the overall composition and molecular weight between crosslinks of polymers.

Recognitive networks were developed by:

- (i) preparation and characterization of imprinted polymers with increasing amounts of functional monomers to determine the effect of functional site density on imprinted properties;
- (ii) determination of the effect of type and quantity of cross-linking agent and functional groups on swelling of network properties.

Finally, recognitive polymer properties that would allow for their use in different types of biosensor and modulated delivery devices were investigated by:

- (i) determination of the effect of monomer type on lysozyme loading and determination release as part of a drug delivery system;
- (ii) the effect of buffer ionic strength on template release.

Chapter 4: Fabrication of Acrylamide-Based MIP Polymers

4.1 Introduction

As stated previously, special requirements need to be considered when using large molecular weight proteins as the template. In order to preserve biological activity, proteins must be dissolved in water, a solvent that can interfere with the template-monomer complex formation. In addition, since water uptake is desired for protein diffusion into the network, hydrogel components are favored. Finally, the network needs to be stable when in contact with water and exhibit good biocompatibility within the body. In order to meet these requirements, an acrylamide-based hydrogel system was chosen and investigated for imprinting the template protein lysozyme.

4.1.1 Acrylamide-Based Hydrogels

Polyacrylamide hydrogels and derivatives have been used for many years in gel-electrophoresis applications for the separation of large molecular weight proteins. The polymer networks are relatively inert with little non-specific serum protein adhesion¹, and the polymerization mechanisms of these gels are widely understood². As a result, gels properties can be easily manipulated to produce networks with a wide range of desired properties like specific porosity or pore size or even specific mechanical strengths. Polyacrylamide gels also exhibit excellent biocompatibility in vivo³, and the networks can be formed over a wide

range of temperature conditions and pH ranges. For these reasons, polyacrylamide gels are promising materials to investigate as for MIP of serum proteins.

4.1.1.1 Polyacrylamide Gel Polymerization

Polyacrylamide gels are formed through the copolymerization of acrylamide monomer (Aam) with the bifunctional crosslinker N,N'-methylenebisacrylamide (MBA). This polymerization is initiated by a free radical generator and propagates through the vinyl bonds of the monomer and crosslinking agent, creating a three-dimensional network of linear polyacrylamide chains randomly connected by chemical crosslinking. The key variables for this polymerization are the monomer concentration and the crosslinker concentration—the acrylamide concentration dictates the average length, and thus molecular weight, of the linear polymer chains, while the crosslinker concentration dictates the extent of crosslinking. These two variables are important in determining such gel physical characteristics as pore size, elasticity, density, and mechanical strength.

Acrylamide gel polymerization is initiated with the peroxide ammonium persulfate (APS) to generate free radicals and is catalyzed by the quaternary amine N,N,N',N'-tetramethylethylenediamine (TEMED). Since the gel polymerization occurs via a free radical mechanism, the presence of oxygen (a well-known free radical scavenger) will inhibit the polymerization; thus, the gel mixtures must be degassed prior to use in order to remove any dissolved

oxygen. The ideal temperature range for these polymerizations is 25-30°C, with the majority of the polymerization occurring in a few minutes. These gels must still be allowed to react for at several hours, however, to ensure complete polymerization before being utilized.

The effective pore size of the acrylamide gel network is affected by both the total concentration of acrylamide and cross-linker monomer as well as the concentration of the cross-linker to monomer alone. Thus, two parameters have been denoted (%T and %C) to characterize gel composition. %T is defined as the acrylamide monomer plus cross-linking monomer expressed as a % (w/v). %C is defined as the weight percentage of total monomer which is the cross-linking monomer. Variation of %C and %T enables the creation of polyacrylamide gels with a range of pore sizes. For instance, the effective gel pore size can be systematically increased by reducing %T at fixed %C, to a certain extent; dilute gels (<2.5%T) are mechanically unstable. This characteristic limits the maximum effective pore size to approximately 80 nm, which is useful for separating molecules (via electrophoresis or size exclusion chromatography) with a molecular mass up to 10^6 Daltons. Conversely, gel polymerizations at high values of %T (>30%T) yield very small effective pores capable of resolving molecules with a molecular mass as low as 2000 Daltons. Thus, these two parameters must be optimized for a particular protein sample to allow for its sufficient diffusion into and out of the crosslinked MIP gel network.

As the %C is increased at a fixed %T, the effective pore size decreases until reaching a minimum value (which is dependent upon the particular value of %T). Continued increase of the %C value then increases the effective gel pore size, presumably due to the formation of bead-like structures within the gel rather than the predicted three-dimensional matrix. Stable gels with very high pore sizes (up to 250 nm) can be synthesized in this manner; however, at values higher than 30%C, the resulting gels can become translucent, hydrophobic, and mechanically unstable.

4.1.2 Lysozyme as a Template Protein

In 1922, Peter Fleming noticed that tear fluid and certain other body secretions exhibited a unique antibacterial property and could break down certain saprophytic cocci. He was able to isolate the lytic enzyme responsible for this occurrence, which he promptly named lysozyme. Lysozyme is a 14.5 kDa protein that is present in human serum, tears, seminal fluid and breast milk (Figure 4.4). Lysozyme is produced by the neutrophils of the immune system as a defense against bacterial infection. In many forms of cancer, including both acute and chronic myelomonocytic leukemia and chronic myelocytic leukemia, a rise in serum lysozyme levels is one of the first indicators of disease⁴. In addition, increased lysozyme activity in the serum are present in tuberculosis^{5, 6}, Crohn's disease⁷, acute bacterial infections⁸, sarcoidosis⁹, and ulcerative colitis⁷.

Elevated lysozyme levels in urine can occur during severe renal failure¹⁰, renal transplant rejection¹¹, urinary tract infections¹², and nephritis¹⁰.

Although lysozyme is not an ECM protein, it is present in the bloodstream in small amounts and therefore is a good model protein to use for the investigation of imprinting of Aam polymers. This protein is also much less expensive than many other proteins (especially ECM proteins) and thus can be used to formulate proper MIP formulations without cost constraints.

Lysozyme catalyses the depolymerization of mucopolysaccharides that are found in the cell walls of gram-positive bacteria and, upon action, reduces these mucoids into simpler saccharides by releasing the simple sugar hexosamine via hydrolysis. Lysozyme hydrolyzes the β -(1-4)-glucosidic linkages between N-acetylmuramic acid and N-acetyl-D-glucosamine residues present in the cell wall (Figure 4.1).

4.1.3 MIP in Acrylamide-Based Hydrogels

Lysozyme is composed of 129 amino acids, and each amino acid carries a side chain which at a biological pH is either charged, polar, or neutral. Lysozyme contains carries five amino acids which have ionizable side chains. At neutral pH, glutamic acid and aspartic acid are deprotonated and negatively charged (Figure 4.2), while lysine, histidine, and arginine are ionized and positively charged (Figure 4.3). Lysozyme has an isoelectric point of ~ 10.4 ; thus, at a biological pH of 7.4, lysozyme carries an overall net positive charge. According

to Figure 4.4, positively and negatively charged amino acids make up approximately 14% and 8%, respectively, of the overall amino acid composition. In addition, lysozyme carries other amino acids that can undergo hydrogen bonding with functional monomers.

Thus, by targeting charged and hydrogen bond-donating amino acids with corresponding functional monomers, we attempted to use MIP to structurally recognize chicken egg-white lysozyme. Previously, researchers have exploited just this interaction when purifying lysozyme from chicken egg whites using acidic polymers^{13, 14}. In addition, Ou et al.¹⁵ have been able to synthesize lysozyme imprinted polymers by also exploiting the attraction between acidic monomers and basic amino acid residues.

Along with Aam functional monomer, the charge functional monomers methacrylic acid (MAA) and 2-(dimethylamino)ethyl methacrylate (DMAEMA) were utilized to exploit oppositely charged amino acids present in lysozyme. MAA, which has a pK_a value of 4.5, is largely negatively charged at the neutral pH (7.2-7.4) used in this study. DMAEMA, with a pK_a value of 8.2, has a tertiary amine functional group and is positively charged at biological pH. DMAEMA can target a negatively-charged glutamic acid group (Figure 4.5), while MAA can target positively-charge amino acids like lysine (Figure 4.6) to give a MIP network that chemically interact with the lysozyme template.

4.2 Materials and Methods

4.2.1 Fabrication of Lysozyme MIP Polymers

In a typical experiment utilizing three functional monomers and MBA as a crosslinker, MAA (Sigma, St. Louis) and DMAEMA (Sigma) were added to an amber glass bottle. Next Tris buffer was added, and the pH of the solution was adjusted to ~7.0 with 5.0N NaOH. A solution of chicken egg-white lysozyme (Sigma, L6876) was then added and gently stirred. Aam and MBA were added and allowed to dissolve into the solution under gentle agitation for 20 min.

The solution was then allowed to complex for an additional 20 min. The bottle was then covered with parafilm and placed in a nitrogen atmosphere. A needle was introduced through the parafilm and nitrogen was bubbled through the solution for a period of 30 minutes to remove oxygen. To this solution, the free radical initiator ammonium persulfate (0.6 wt% monomers) was added along with the catalyst TEMED (0.8 wt% monomers). The control polymer was made with exactly the same composition, except lysozyme was not added. Functional monomer feed compositions of this type were maintained at 50:1 moles of monomer/mole of corresponding total charged amino acid. For example, since lysozyme contains 10 negatively charged amino acids, DMAEMA was mixed at a 50:1 mol/mol ratio of negatively charged amino acids as calculated from the starting weight of lysozyme. Tris buffer (0.02M, pH 7.4) was added to give a monomer concentration of 5 wt% of the total solution weight, while MBA was

added at 10 wt% of the monomers. Structures of monomers, crosslinkers, TEMED, and APS are given in Figure 4.7.

The reaction proceeded at ambient conditions for 30 min and then the resulting gel was crushed and sieved through a 150 micron sieve. Particles were then placed in 50 mL conical tubes and placed on a rotating mixer and resuspended within multiple wash steps (24 hour duration; 3 Tris buffer washes; 2 Tris Buffer containing 0.5M NaCl; then 4 washes in Tris Buffer) to remove template and excess monomer. To validate the washing procedure, samples from the final wash were analyzed for remaining template and monomer via UV-Vis spectroscopy. Control polymers were subjected to equivalent washing conditions as imprinted polymers. The resulting particles were then filtered and dried in air at ambient conditions and placed in a vacuum oven ($T=26\text{ }^{\circ}\text{C}$, 28 mm Hg vacuum) until a constant weight was obtained (less than 0.1 wt% difference). Particles were then sieved to obtain particles of size 75-90 μm .

4.2.2 Equilibrium and Dynamic Recognition Studies

To determine if lysozyme was successfully imprinted into our matrices, 30 mg of microparticles of a specific formulation in 50 mL conical tubes and 10 mL of Tris buffer (0.020 M, pH 7.4) was added and then placed on a rotating mixer at 25 rpm. Polymers were allowed to swell and equilibrate for 20 min. Then, 10 mL of a 0.3 mg/mL solution of lysozyme in Tris buffer was added to the particles to

give a final lysozyme concentration of 0.15 mg/mL and a final particle concentration of 1.5 mg/mL. At varying timepoints, supernatant was removed and analyzed for lysozyme concentration using UV-Vis spectroscopy at 285 nm. For equilibrium studies, a final sample was removed after 24 h.

4.2.3 Specific Recognition Studies

To establish the specificity of our imprinted network, similarly sized molecular weight proteins cytochrome c (MW ~12.6 kDa), human lysozyme (MW ~14.5 kDa), or soybean trypsin inhibitor (MW ~15 kDa) were added according to the method previously described. Briefly, 30 mg of particles were placed in 50 mL conical tubes and 10 mL of Tris buffer (0.020 M, pH 7.4) was added and then placed on a rotating mixer at 25 rpm. Polymers were allowed to equilibrate in the buffer for 20 min. Then, 10 mL of 0.3 mg/mL solution of soybean trypsin inhibitor human lysozyme or cytochrome c in Tris buffer was added to the particles. At 10 min, supernatant was removed and analyzed for protein concentration using UV-Vis spectroscopy at 285 nm.

4.2.4 Presence of Ionic Strength on Recognition Properties

Because the presence of ions can interfere with an imprinted material by competing for recognition with polymer functional groups, differing salt concentrations were investigated to determine the effects on recognition. NaCl was dissolved in Tris buffer (0.020 M, pH 7.4) at differing concentrations. Then, 15 mg of particles were placed in 15 mL conical tubes, and 5 mL of the salt

solution was added and gently agitated. After 20 min, 5 mL of 0.3 mg/mL solution of lysozyme in Tris buffer was added to the particles, where the concentration of salt in the solution was the same as in the microparticle solution. At 10 min, supernatant was removed and analyzed for lysozyme concentration using UV-Vis spectroscopy at 285 nm.

4.2.5 Effects of pH on Recognition Properties

Because a change in pH can change the overall charge of both the polymer components and the amino acids of a protein, recognition of lysozyme in imprinted gels was investigated at a pH of 3.0. Tris buffer was adjusted to pH of 3.0 using HCl. Then, 15 mg of particles were placed in 15 mL conical tubes, and 5 mL of the low pH buffer was added and gently agitated. After 20 min, 5 mL of 0.3 mg/mL solution of lysozyme in low pH Tris buffer was added to the particles. At 10 min, supernatant was removed and analyzed for lysozyme concentration using UV-Vis spectroscopy at 285 nm.

4.3 Results and Discussion

To assess the success of an imprinted polymer, several factors are important. The maximum amount of protein that can be recognized at equilibrium is important in identifying the difference between imprinted and non-imprinted polymers in binding of the template molecule. The capacity can also be used to calculate the selectivity, a measure of the specific recognition of our template over similar proteins.

4.3.1 Equilibrium Recognition Studies

The overall goals of this work were (i) to design systems that were compatible with aqueous solutions and were able to recognize a hydrophilic macromolecule; and (ii) to produce a MIP network that was capable of recognition but not limited by diffusion. To attain these goals, variation in the ratio of functional monomers was investigated.

The amount of equilibrium protein recognition, P_{rec} (units of mg-protein / g-polymer), in the polymers was calculated by a simple mass balance:

$$P_{rec} = \frac{V(C_{initial} - C_{equilibrium})}{M_p}$$

where $C_{initial}$ is the starting protein concentration, $C_{equilibrium}$ the final concentration after of protein in supernatant after protein loading, V the volume of protein solution, and M_p the mass of polymer microparticles used. The percentage of recognition of MIP to control was then calculated.

The equilibrium recognition results are given in Figure 4.8 and Table 4.1. P(MAA-DMAEMA-Aam)MIP polymers exhibited the greatest equilibrium recognition over controls. This polymer contains positive, negative, and hydrogen bonding functional monomers that can non-covalently interact with lysozyme. This balance of complexation is very similar to the recognition that happens in nature; therefore it is not surprising that the three functional monomer

formulation of P(MAA-DMAEMA-Aam) contained the greatest recognition over controls.

4.3.2 Dynamic Recognition Studies

The percentage of protein that was recognized by the P(MAA-DMAEMA-Aam) polymer samples over time was calculated by the following simple mass balance:

$$\%P_{rec} = \left(\frac{C_{st}V_{st}}{C_{si}V_{si}} \right) 100\%$$

Here, C_{si} is the initial concentration of protein in the solution in mg/mL, V_{si} is the initial volume of solution in mL, C_{st} is the concentration of protein at time t , and V_{st} is the volume of solution at time t .

Recognition studies of P(MAA-DMAEMA-Aam) formulations revealed a higher level of template recognition compared to non-imprinted control microparticles, with this recognition following an exponential isotherm. After 1 min, the MIP polymer had absorbed 71% of the lysozyme present in solution and, after 10 min, had bound 96% of the template. Indeed, at the early time points MIP gels exhibited significantly more recognition (>20%) over controls for the first ten minutes, with >30% after 1 h. These results are promising toward our end goal of an imprinted system that can quickly recognize and bind free-blood proteins either in biomedical applications such as assays or as a tissue engineering scaffold that can rapidly bind free ECM proteins or growth factors

from the bloodstream. We believe the non-specific recognition of the lysozyme to the control polymer is due to the presence of functional groups that are randomly polymerized throughout the polymer and can attract and bind free template over time.

4.3.3 Specific Recognition of MIP Polymers

When MIP particles were placed into solution with similar molecules, the recognition to the proteins was greatly reduced (Figure 4.10). Human lysozyme is the same approximate molecular weight as our chicken lysozyme template, but it contains 20 different amino acid residues. Therefore, its composition and structure are slightly different than our template. The recognition to this protein was 20% less than the recognition to our template protein. In addition, cytochrome c, which is a smaller molecule (12.5 kDa) than lysozyme, also was recognized significantly less, while the recognition to soybean trypsin inhibitor was less than 3% for the P(MAA-DMAEMA-Aam)MIP microparticles. These results give convincing proof of the specificity of our technique to the lysozyme template. In addition, control polymers yielded less than 5% recognition to either pepsin or trypsin inhibitor but showed a high recognition affinity toward human lysozyme (~70% at 30 min).

This result could be contributed to the differences in the total net charge that each protein carries. Lysozyme carries a net positive charge of +7 at neutral pH. This positive charge can lead to a greater affinity for complexation with the

negatively charged MAA functional monomer, and it is this complexation that could be driving not only the specific recognition of lysozyme to MIP polymers but also the recognition of lysozyme to non-imprinted controls. In the same way, soybean trypsin inhibitor carries a net negative charge of -6 at neutral pH which could lead to electrostatic repulsion with the negatively charged carboxylic acid group of the methacrylic acid, resulting in low recognition. In addition, the specificity to our lysozyme between phenotypes lends credence to the idea of a specific MIP polymer. These results indicate that the imprinting technique is not based upon size but is based upon a specific polymer-template complex that involves a balance of positive and negative charges and hydrogen bonding.

4.3.4 Ionic and pH Effects upon Recognition

Because ionic strength can affect the recognition of template molecules to imprinted controls, the addition of NaCl during template recognition was investigated. Increasing salt concentration did indeed decrease the recognition of template to both MIP and controls (Figure 4.11). Interestingly, the addition of salt led to a more significant decrease in recognition of template in the MIP polymers compared to the control polymers. We believe that the higher concentration of functional monomers contained in the imprinted pockets attracts the salt ions and leads to a effective concentration increase of Na^+ and Cl^- ions inside these pockets, further inhibiting recognition of the lysozyme template.

In addition, a change in pH can change the charge of both amino acids present on the lysozyme template as well as the charge of functional monomers of the network. At a low pH, MAA is protonated and carries no charge. Since we believe that the recognition of the overall positively charged lysozyme is driven mainly by complexation with the negatively charged carboxyl of MAA at neutral pH, a decrease in pH is likely to have a significant impact on recognition. Indeed, at low pH, recognition of lysozyme template was greatly reduced (Figure 4.12). This also supports the theory of a MIP polymer network with recognition driven by electrostatic interactions.

4.4 Conclusions

MIP gels with specific recognition for lysozyme template were fabricated. P(MAA-DMAEMA-Aam) terpolymer formulations exhibited >200% increase in recognition to lysozyme template over controls. In addition, this polymer formulation exhibited specific recognition to the template protein over similarly sized macromolecules. In addition, the changes in recognition based upon both the presence of ions in solution and a change in pH support out theory of a recognitive polymer containing sites with electrostatic functionalities for the lysozyme molecule.

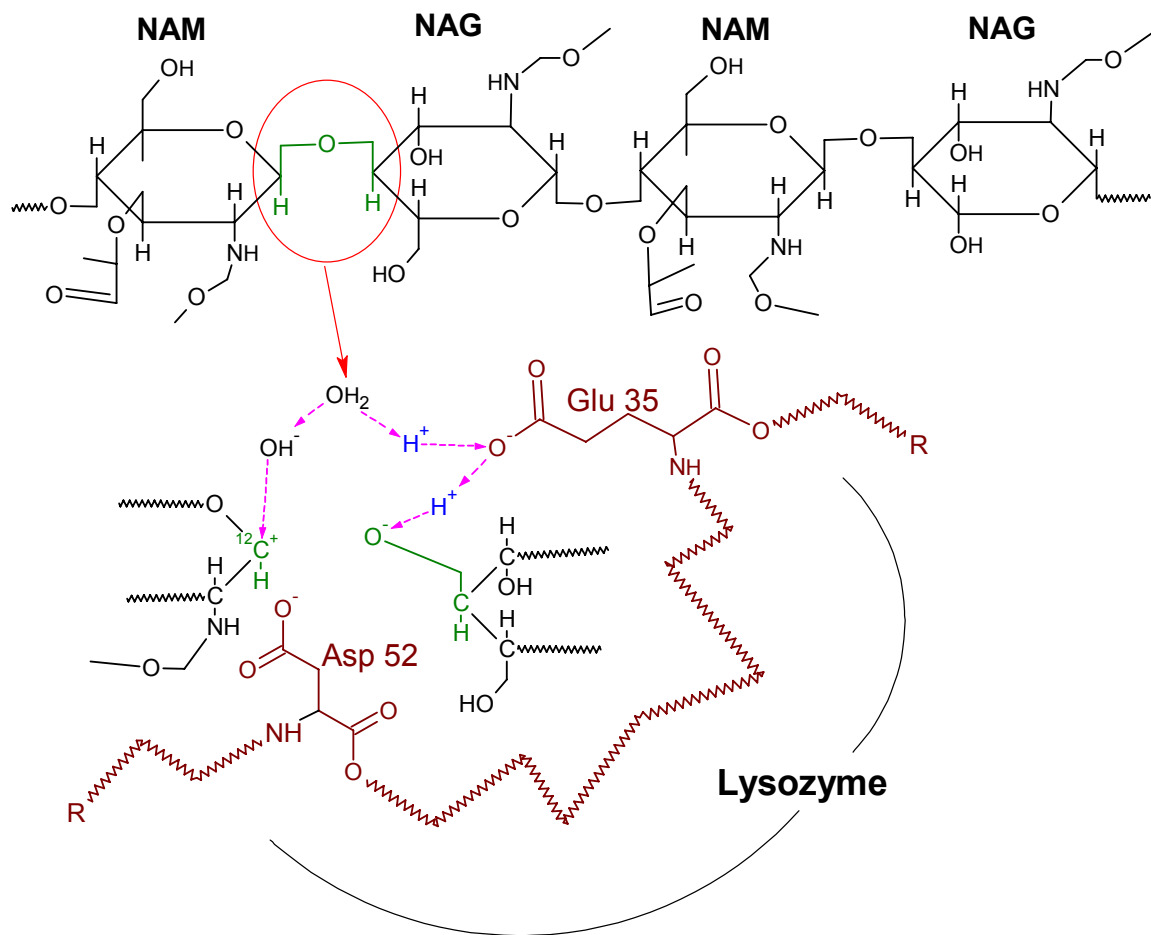
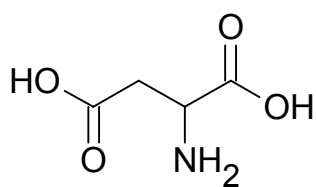
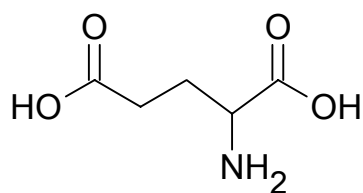


Figure 4.1: Mechanism of Lysozyme Cleavage

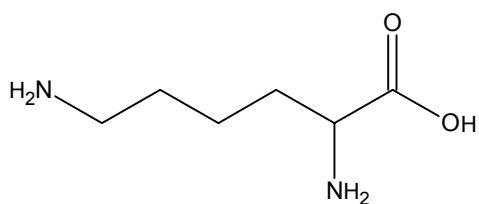


Aspartic
Acid (Asp)

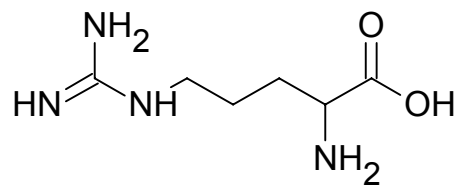


Glutamic
Acid (Glu)

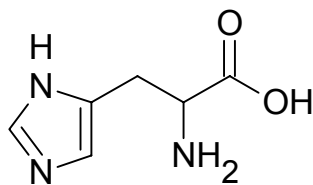
Figure 4.2: Negatively Charged Amino Acids



Lysine (Lys)

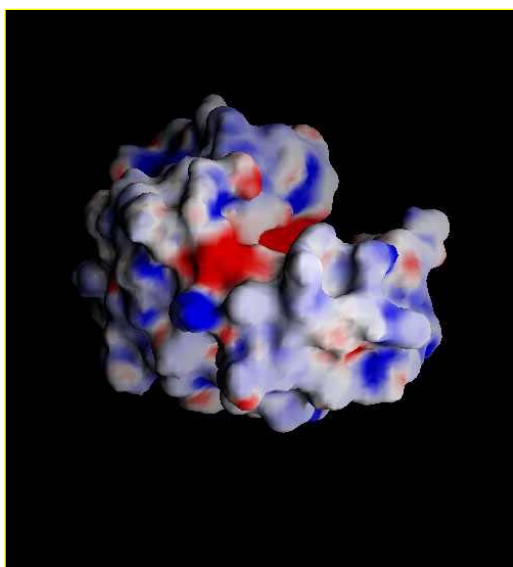


Arginine (Arg)



Histidine (His)

Figure 4.3: Positively-Charged Amino Acids



	Amino Acid	# in Lysozyme		Total Percent
Nonpolar	Ala (A)	12	9.30%	39.53%
	Val (V)	6	4.65%	
	Leu (L)	8	6.20%	
	Ile (I)	6	4.65%	
	Pro (P)	2	1.55%	
	Met (M)	2	1.55%	
	Phe (F)	3	2.33%	
	Gly (G)	12	9.30%	
Polar, Uncharged	Trp (W)	6	4.65%	38.76%
	Ser (S)	10	7.75%	
	Thr (T)	7	5.43%	
	Tyr (Y)	3	2.33%	
	Cys (C)	8	6.20%	
	Asn (N)	13	10.08%	
	Gln (Q)	3	2.33%	
Neg. Charged	Asp (D)	8	6.20%	7.75%
	Glu (E)	2	1.55%	
Pos. Charged	Lys (K)	6	4.65%	13.95%
	Arg (R)	11	8.53%	
	His (H)	1	0.78%	
	Total Residues	129		

Figure 4.4: Lysozyme Surface Charge and Amino Acid Composition

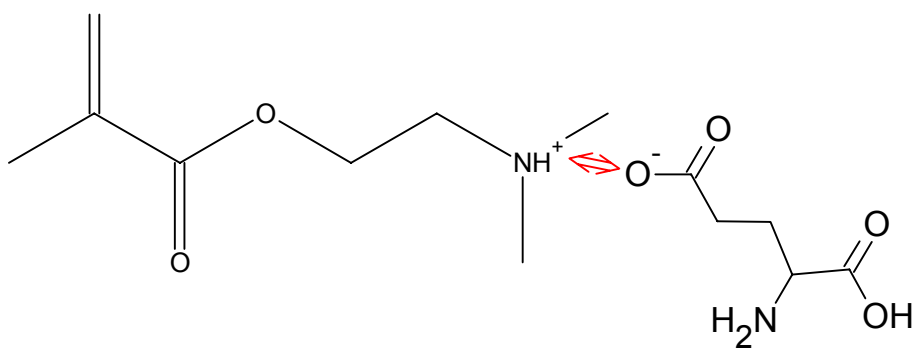
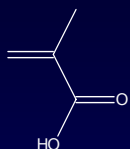


Figure 4.5: Expected DMAEMA Non-covalent Association with Glutamic Acid



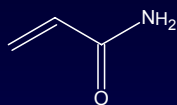
Figure 4.6: Expected MAA Non-Covalent Association with Lysine

System Components



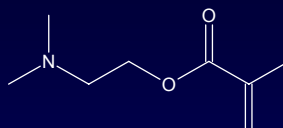
Methacrylic Acid (MAA)

Functional Monomer



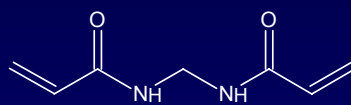
Acrylamide (AAm)

Functional Monomer



2-Dimethylaminoethyl Methacrylate (DMAEMA)

Functional Monomer

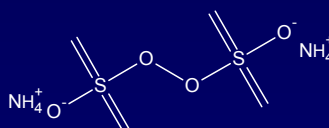


N,N'-Methylenebisacrylamide (MBA)

Crosslinking agent



N,N,N',N'-Tetramethylethylenediamine (TEMED)



Ammonium Persulfate

Initiator

Figure 4.7: Components of MIP Polymer System for Lysozyme

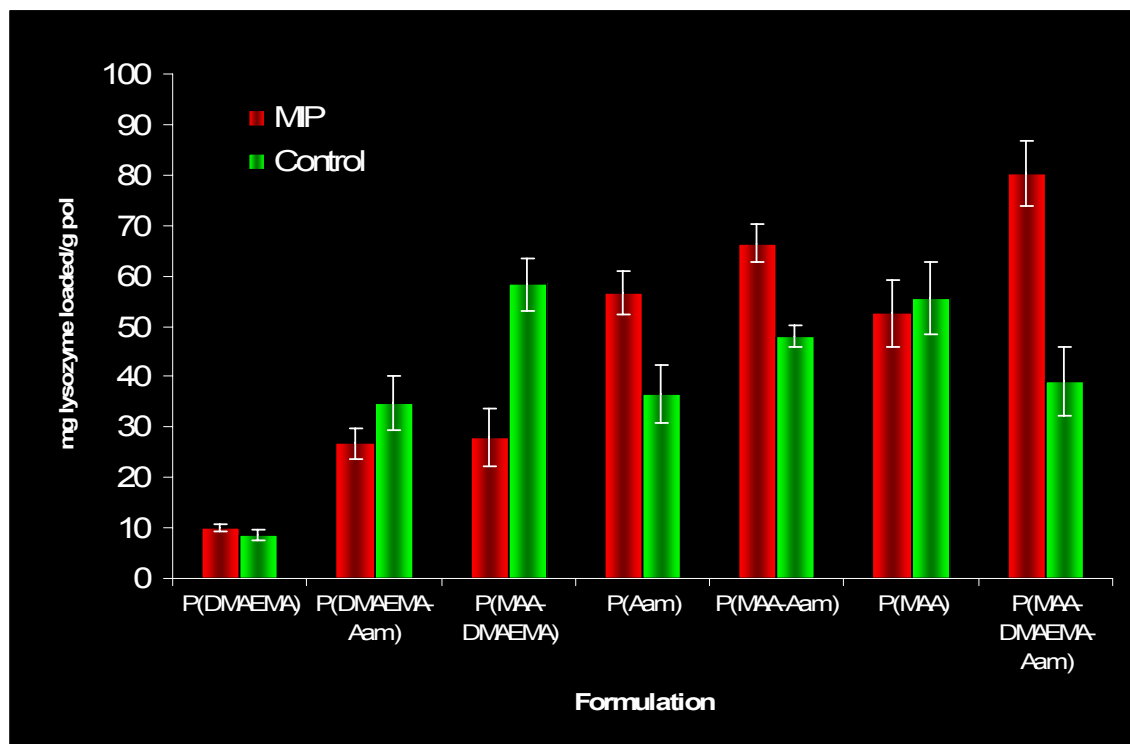


Figure 4.8: Equilibrium Recognition Across Polymer Formulations.
P(MAA-DMAEMA-Aam) gels exhibited the greatest recognition over controls.

ID	Moles DMAEMA	Moles MAA	Moles Aam	Recognition % (g lysozyme in MIP/ g lysozyme in controls)
P(DMAEMA)	0.1234	0.0987	0.1123	115.98%
P(DMAEMA-Aam)	0.215	0.253	0.317	77.00%
P(MAA-DMAEMA)	0.3564	0.2689	0.2544	47.72%
P(Aam)	0.5643	0.59	0.693	154.17%
P(MAA-Aam)	0.743	0.5897	0.7158	138.55%
P(MAA)	0.6897	0.7123	0.7894	94.75%
P(MAA-DMAEMA-Aam)	0.7564	0.8765	0.6884	206.16%

Table 4.1: Functional Monomer Composition in MIP and Control Formulations and Equilibrium Recognition over Controls.

The P(MAA-DMAEMA-Aam)MIP polymers exhibited the greatest recognition to lysozyme template over controls.

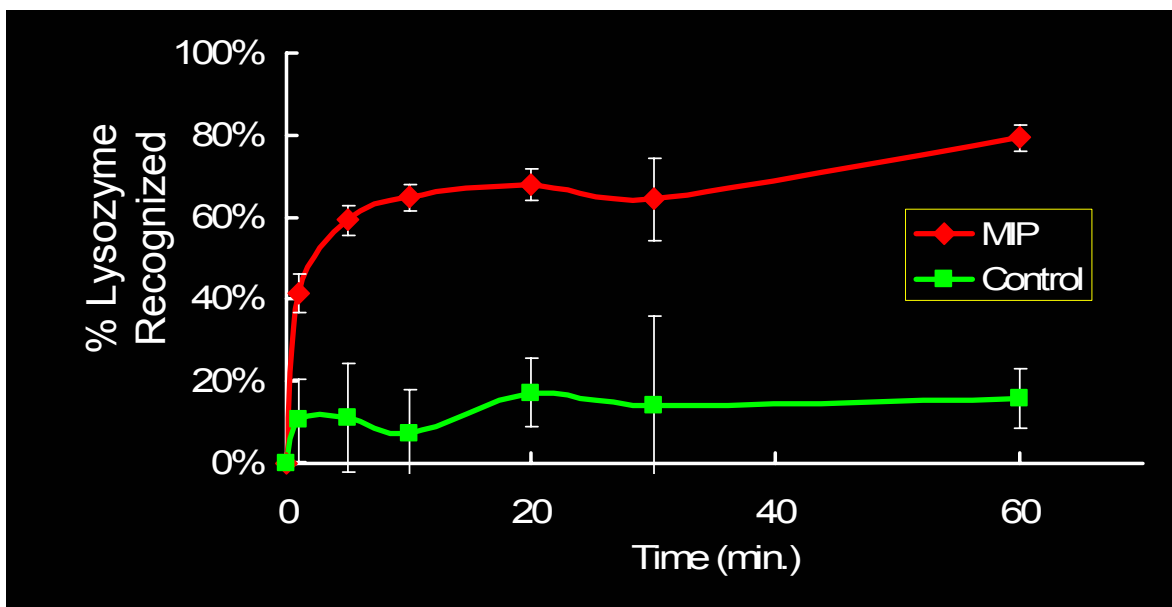


Figure 4.9: Dynamic Recognition in P(MAA-DMAEMA-Aam) polymers over time.
MIP polymers exhibited a greater increase in recognition over control gels.

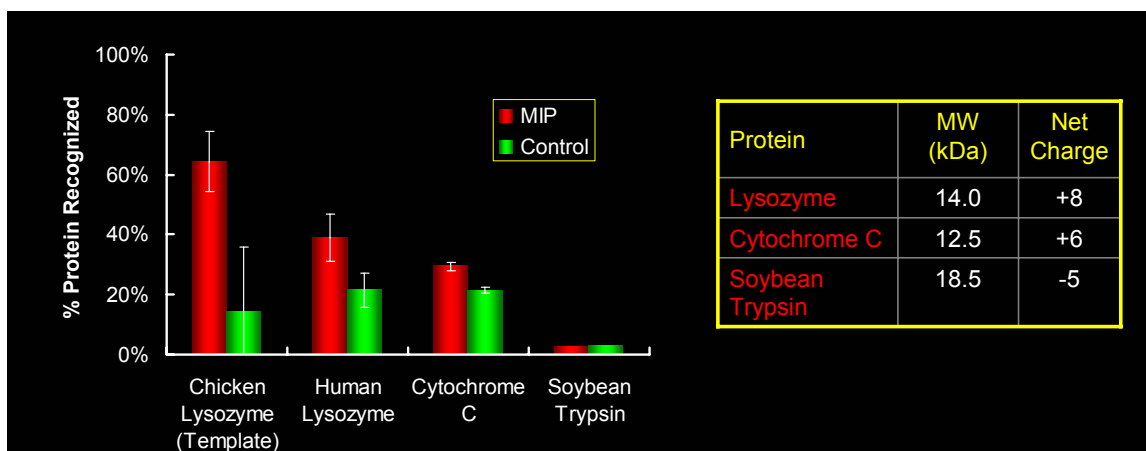


Figure 4.10: Specific Recognition of P(MAA-DMAEMA-Aam)MIP Polymer

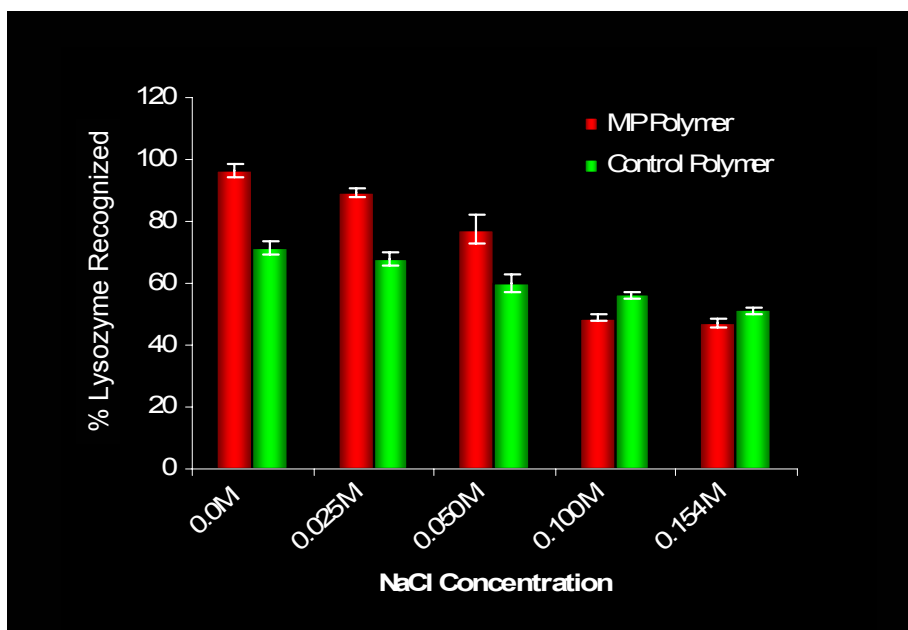


Figure 4.11: Effects of Ionic Concentration upon P(MAA-DMAEMA-Aam)MIP polymers.

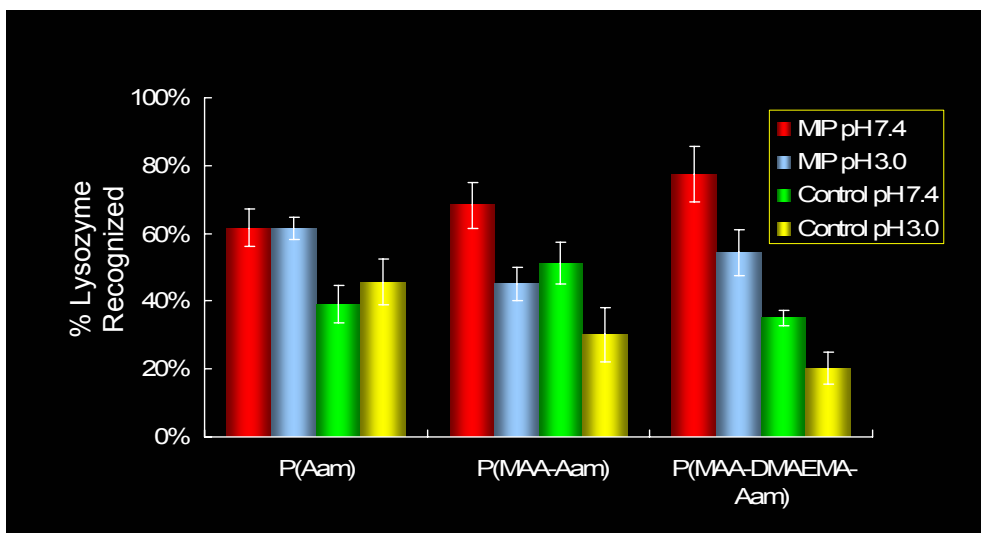


Figure 4.12: Effect of pH Upon Recognition

4.5 References Cited

1. Tong, D.; Hetenyi, C.; Bikadi, Z.; Gao, J. P.; Hjerten, S., Some Studies of the Chromatographic Properties of Gels ('Artificial Antibodies/Receptors') for Selective Adsorption of Proteins. *Chromatographia* **2001**, 54, (1-2), 7-14.
2. Dunn, M. J., *Gel Electrophoresis: Proteins*. Alden Press Ltd.: Oxford, UK, 1993.
3. Saraydin, D.; Unver-Saraydin, S.; Karadag, E.; Koptagel, E.; Guven, O., In Vivo Biocompatibility of Radiation Crosslinked Acrylamide Copolymers. *Nucl. Instrum. Methods Phys. Res., Sect. B* **2004**, 217, (2), 281.
4. Kaiserling, E.; Horny, H. P.; Geerts, M. L.; Schmid, U., Skin Involvement in Myelogenous Leukemia - Morphologic and Immunophenotypic Heterogeneity of Skin Infiltrates. *Mod. Pathol.* **1994**, 7, (7), 771-779.
5. Rakovskaya, R. V.; Popova, I. I.; Beniaminov, V. O., Content of Lysozyme in the Blood-Serum of Patients with Pulmonary Tuberculosis and Chronic Unspecific Pulmonary-Diseases. *Vrach. Delo.* **1985**, (6), 41-42.
6. Jain, V. K.; Jamil, Z.; Shukla, O. P., Serum Lysozyme in Pulmonary Tuberculosis. *Indian. J. Chest. Dis. Allied. Sci.* **1978**, 20, (4), 168-172.
7. Omorain, C.; Smethurst, P.; Levi, A. J.; Peters, T. J., Biochemical-Analysis of Enzymic Markers of Inflammation in Rectal Biopsies from Patients with

Ulcerative-Colitis and Crohns-Disease. *J. Clin. Pathol.* **1983**, 36, (11), 1312-1316.

8. Sherwood, R. L.; Lippert, W. E.; Goldstein, E., Effect of 0.64 ppm Ozone on Alveolar Macrophage Lysozyme Levels in Rats with Chronic Pulmonary Bacterial-Infection. *Environ. Res.* **1986**, 41, (2), 378-387.

9. Cummiskey, J. M.; Melinn, M.; Mclaughlin, H., Lysozyme Levels in Sarcoidosis. *Ir. J. Med. Sci.* **1978**, 147, (3), 108-111.

10. Niwa, T.; Katsuzaki, T.; Yazawa, T.; Tatemichi, N.; Emoto, Y.; Miyazaki, T.; Maeda, K., Urinary Trehalase Activity in Chronic Glomerulonephritis. *Nephron* **1993**, 63, (4), 423-428.

11. Jung, K.; Diego, J.; Strobelt, V.; Scholz, D.; Schreiber, G., Diagnostic-Significance of Some Urinary Enzymes for Detecting Acute Rejection Crises in Renal-Transplant Recipients - Alanine Aminopeptidase, Alkaline-Phosphatase, Gamma-Glutamyl-Transferase, N-Acetyl-Beta-D-Glucosaminidase, and Lysozyme. *Clin. Chem.* **1986**, 32, (10), 1807-1811.

12. Dick, W.; Theilmann, L., Urinary Levels of Lysozyme in Children with Acute or Chronic Recurrent Urinary-Tract Infection. *Pediatr. Padiol.* **1980**, 15, (4), 345-350.

13. Vaidya, A. A.; Lele, B. S.; Kulkarni, M. G.; Mashelkar, R. A., Thermoprecipitation of Lysozyme from Egg White Using Copolymers of N-Isopropylacrylamide and Acidic Monomers. *J. Biotechnol.* **2001**, 87, (2), 95-107.

14. Sternberg, M.; Hershberger, D., Separation of Proteins with Polyacrylic Acids. *Biochimica et Biophysica Acta (BBA) - Protein Structure* **1974**, 342, (1), 195-206.
15. Ou, S. H.; Wu, M. C.; Chou, T. C.; Liu, C. C., Polyacrylamide Gels with Electrostatic Functional Groups for the Molecular Imprinting of Lysozyme. *Anal. Chim. Acta* **2004**, 504, (1), 163.

Chapter 5: Materials Characterization of Acrylamide-Based MIP Polymers

5.1 Introduction

Because the molecular imprinting process has not been widely applied to proteins, there are few studies characterizing the material properties of these polymer systems. Thus, the overall macroscopic properties of protein imprinted gels were examined for the first time using scanning electron microscopy (SEM) in order to determine morphological differences between the MIP polymers and the controls. In addition, Fourier Transform Infrared Spectroscopy (FTIR) was performed to determine if the presence of template affected the overall gel composition, while differential scanning calorimetry (DSC) was used to determine the molecular weight between crosslinks of MIP polymers and controls.

5.1.1 Scanning Electron Microscopy of Polymers

The electron beam of a scanning electron microscope (SEM) comes from the field emission gun located on the pinnacle of the instrument¹. The resulting electron stream is attracted, and thus accelerated, by the anode using a high voltage (200V – 30kV). This stream then passes through the anode into the condenser column, which condenses these electrons into a single beam. This beam then passes through an objective lens, which focuses it into a fine point and directs it towards the sample stage. The beam then passes through the scan coils, which use a varying voltage supply to create a magnetic field to deflect the electron beam in a controlled manner in order to scan the surface of

the sample. The electron beam then strikes the surface of the sample and interacts with its atoms, emitting secondary electrons, primary backscattered electrons, Auger electrons, and characteristic X-rays. The secondary electrons give the surface features of the sample. The primary backscattered electrons provide not only surface features but also an average atomic number of the each scanned section of the sample. The general setup of a SEM is given in Figure 5.1.

Both the surface and bulk structures of polyacrylamide gels have been well-characterized by SEM microcrographs²⁻⁸. In addition, SEM is a widely used tool for imaging surface morphologies of polymer systems, and this technique has been used extensively to image the characteristics of gels containing entrapped proteins, drugs, and other molecules⁸⁻¹¹. Li and colleagues¹² noted marked surface differences between control collagen films and collagen films loaded with hemoglobin. Park and colleagues also observed a greater porosity in a PLGA film that was polymerized in the presence of sodium bicarbonate¹³. These highly porous gels had a greater release of tissue-type plasminogen activator than polymers formed in the absence of sodium bicarbonate. SEM has also been used to observe resulting morphology changes upon polymer exposure to different environmental conditions. Using SEM, Zhang and colleagues could measure the porosity changes in pH-sensitive methyl cellulose membranes after membranes had been exposed to an increase in pH¹⁴.

To date, SEM has not been widely used to visualize MIP systems involving small molecules as templates. The features of these gels (pore size distribution, porosity, etc) are usually not as distinctive as those structures formed during polymerization in the presence of macromolecules. Therefore, differences in the formed structures generally cannot be viewed with this technique. Thus, SEM is not usually considered a useful tool for imaging macroscopic differences in imprinted gels versus controls with small molecules as the templates. Despite this fact, a few groups have witnessed a slight morphology change between MIP polymers and controls¹⁵⁻²⁰. Recently, Byrne and Peppas, utilizing a cryo-SEM method, observed a higher macroporosity in glucose imprinted PEG hydrogels when compared to control gels^{18, 19}. In addition, Ulbricht and Malaisamy also observed macroscopic differences between Rhodamine-B imprinted polysulfone membranes and controls¹⁶. The MIP gels exhibited a courser surface texture and a higher porosity as the amount of template present during polymerization increased. Finally, Nichols and Rosengren²¹ have observed macroscopic changes in protein surface imprinted polymers containing MAA.

5.1.2 FTIR Analysis of Polymer Networks

FTIR is a common tool for the study of polymer samples due to the ease and simplicity of analysis. FTIR involves rapid data collection and is applicable to both solid and liquid polymer samples. In addition, the instrumentation is inexpensive and robust. Because of these attributes, FTIR is the most useful spectroscopic technique for the identification of chemical compounds and,

specifically, those compounds present in polymers. In these studies, FTIR was utilized to determine the composition of the MIP polymers and controls. In addition, the resulting FTIR spectra was used to determine if the template had any overall chemical compositional differences as indicated by a peak shifts in the spectrum between the MIP gels and the controls.

Atoms in polymers are held together by covalent bonds that vibrate by thermal energy. These molecular vibrations have characteristic quantized vibrational energy levels that can absorb incoming infrared (IR) radiation with energies corresponding exactly with these vibrational energy level transitions. In order for molecular bonds to absorb this IR radiation, the corresponding vibrational change must cause a net change in the dipole moment of the bond. The two common classes of vibrations that result from IR absorption are stretching and bending, with the four types of bending being scissoring, rocking, wagging, and twisting. Thus, the bonds of functional groups such as carbonyl, hydroxyl, and amine groups absorb infrared radiation at characteristic energies and thus characteristic frequencies. These frequencies usually occur in the 3600 cm^{-1} and 1200 cm^{-1} wavenumber range of the IR spectrum, thus known as the group frequency region. The range from 1200 cm^{-1} and 600 cm^{-1} is known as the fingerprint region of the IR spectrum because small changes in the structure of the molecule can significantly impact the location and shape of the absorption peaks in this region. Thus, analyzing polymer samples using FTIR can provide powerful insight into the overall chemical composition of a particular sample.

During the operation of an FTIR instrument, an infrared source emits infrared radiation in the middle IR region (3500 cm^{-1} to 650 cm^{-1}) that travels to the instrument's optical system, a Michelson interferometer, which is comprised of a fixed-position mirror, a moving mirror, and a beam splitter. The IR radiation from the source passes through the beamsplitter, where half of it is reflected towards the fixed-position mirror and the other half is reflected towards the moving mirror. The returning beams from both mirrors are recombined at the beamsplitter, and half of this light is then emitted to the sample compartment (the other half is lost as it travels back to the source). This light then excites the molecular bonds into higher vibrational states through energy absorption, and the remainder of this light is transmitted to the detector, which records the interferogram, a time domain representation of the light interference pattern induced by the interferometer. The interferogram consists of the sum of the sine waves measured for each individual frequency of the instrument range. This interferogram provides a representation of signal as a function of mirror placement. The computer software then performs the Fourier transform, which converts the interferogram into a spectrum of the data in the frequency domain. A single scan over the entire wavenumber range takes only seconds, so many scans can be performed to reduce the signal to noise ratio, which scales with \sqrt{N} (where N represents the number of scans), and thus improve the accuracy of this technique.

FTIR is a powerful tool for determining the overall composition of polymer samples. In MIP, FTIR has been used to determine the nature of the template-monomer complex for small molecular weight drugs and for determining the change in composition of polymers that are templated^{17, 22}. In fabricated uracil template MIP polymers, Kobayashi et. al¹⁷ have shown no shift in spectra between MIP gels and controls. These results were similar those obtained by Fuji and collaborators who imprinted amino acids onto Nylon-6²³. Data obtained also indicated no change in the FTIR spectra between imprinted polymers and controls.

5.1.3 DSC Analysis of Polymers

Polymer molecules possess thermal energy that allows them to oscillate in the space immediately surrounding them. These vibrations create a free volume in the bulk polymer that scales with increasing temperature and is correlated to the coefficient of thermal expansion for that specific polymer. As its temperature increases, the free volume of the polymer reaches a critical value, at which point the polymer molecules have sufficient free volume to allow them to change their positions relative to one another through bond rotations and vibrations. The temperature where this free volume reaches its critical value corresponds to the glass transition temperature of the polymer, T_g . Below this temperature, the polymers are rigid and brittle, but they can undergo plastic deformation once the temperature exceeds T_g . This transition between a polymer's glassy and rubbery

state is not a sharp transition but rather often occurs over a wide temperature range (20-30°C), the center of which is taken represent the T_g value.

The glass transition temperature is not an absolute value for a given polymer, as it depends on certain characteristics of the polymer in question. For instance, the T_g of a polymer depends on its molecular weight, with low molecular weight polymers having a higher T_g value since they possess a higher free volume as a result of more chain ends per unit volume. In addition, crosslinking in polymers can have a dramatic effect on T_g of a given polymer; in essence, crosslinking reduces the effective free volume of the polymers because the individual polymer chains are tied closer together by the crosslinker. It has been shown that the addition of 5 wt% crosslinker to a poly(2-hydroxyethyl methacrylate) hydrogel system effectively increased the T_g of that polymer by nearly 70°C²⁴.

The main technique utilized to determine a polymer's T_g is DSC. In this technique, a polymer sample is placed in a sample pan and placed in a furnace along with a reference pan (a sample pan with no material loaded in it). The temperature of these pans is then increased linearly according to the program designated by the user. The DSC then monitors the difference in energy needed to heat the sample pan compared to the amount of energy needed to heat the reference pan for the same temperature changes. The DSC instrument then provides a plot of this differential heat flow as a function of sample temperature.

Thus, the DSC will record both endothermic transitions (glass transition, melting) and exothermic transitions (crystallization) of polymers.

5.2 Materials and Methods

5.2.1 Polymer Preparation for SEM

Polymer films were prepared as outlined previously in Chapter 4. Disks of diameter 7.5 cm were cut using an aluminum cork borer. To remove the lysozyme template and unreacted monomer, the disks were washed in triplicate in a Tris buffer solution (0.02M, pH 7.4) containing 0.5 M NaCl and then washed twice in Tris buffer (0.02 M, pH 7.4) containing no salt. The disks were then removed from solution and cut into fourths with a scalpel. During the cutting, the blade was held at an approximate 45° angle to ensure the creation of a sloping edge. In addition, a portion of the top layer of the polymer samples was sectioned off if possible (certain hydrated gel samples lacked the rigidity for the removal of the surface layer). If the surface layer could not be sectioned, only the cut edge was imaged. Both of the aforementioned techniques were employed to ensure that the bulk of the polymer was imaged instead of the smooth surface layer that had contacted the glass slides.

To prepare the polymers for SEM imaging, a cryofreezing method was used. An aluminum stub was placed into a glass Petri dish and covered with liquid nitrogen. When the liquid evaporated below the top of the stub, the polymer was placed onto the stub, and the gel was held in place to freeze. Because carbon tape will not stick to frozen aluminum, the frozen polymer was

then transferred to a room temperature stub containing carbon tape and gently patted down. Immediately, the polymer was sputter-coated with a thin layer of gold. This technique was employed in order to “freeze” the pores of the polymer as they exist in their hydrated state. Polymer samples were subsequently imaged using a SEM (LEO 1530, Carl Zeiss, Germany) at 10kV with a working distance of 6mm.

5.2.2 Polymer Preparation for FTIR

Polymer samples were fabricated as outlined in SEM studies and washed free of lysozyme template. These samples were dried in a vacuum oven until no mass change was detected, and then dry gels were ground into particles of 75-150 μm . To obtain FTIR spectra, polymer samples were then dispersed in KBr pellets at a concentration of 2-3 mg of polymer in 150 mg of KBr. FTIR spectra (Infinity Gold Series Spectrometer, Mattson, Wisconsin) were then obtained using 128 scans with a resolution of 1 cm^{-1} .

5.2.3 Polymer Preparation for DSC

Polymer samples were fabricated as outlined in SEM studies and washed free of lysozyme template. These samples were dried in a vacuum oven until no mass change was detected, and then dry gels were ground into particles of 75-150 μm . DSC (Perkin-Elmer 7 DSC, PerkinElmer, Boston) scans were begun at 50°C and increased to at least 250°C at a rate of $10^{\circ}\text{C}/\text{min}$ (the exception was P(DMAEMA), whose scan started at -30°C due to the reportedly low T_g value of this polymer).

5.3 Results and Discussion

5.3.1 SEM Analysis of MIP Polymer Networks

Because lysozyme is a macromolecule with an effective hydrodynamic radius of 1.9 nm, it was hypothesized that a distinct change in the macroscopic properties could be viewed in MIP polymers. Indeed, when the MIP polymers were compared with their respective controls, a considerable difference in the porosity and the overall morphology was observed across all formulations. MIP polymers also displayed randomly oriented “ribbons” in their bulk, termed striations.

Upon observations at ~320X magnification, P(Aam)MIP and P(Aam)C polymers showed only a slight surface difference, with the P(Aam)MIP gel exhibiting higher surface roughness (Figure 5.2). As magnification increased to ~955X and ~8700X, the differences in morphology became apparent. The P(Aam)MIP disk contained a greater amount of pores and disorganized striations. These features, however, were absent in the P(Aam)C polymer morphology. P(Aam)MIP gel's pores ranged in size from 0.25-1.0 μ m, and the distance between striations was ~1.0 μ m.

At low magnification (~330X), the P(MAA)MIP displayed a greater surface roughness over the P(MAA)C gels. As magnification increased to 947X, a marked macroporosity was observed in P(MAA)MIP as compared to the control (Figure 5.3). The P(MAA)C disk contained no pores and appeared to be more

dense than the P(MAA)MIP polymer. The average pore size was on the order of 10 μ m, so large that the presence of striations was not detected.

For the P(MAA-Aam) copolymer gels, a morphological difference was also observed (Figure 5.4). Upon observation of the edge features of the gels at ~330X magnification, the edge of the P(MAA-Aam)MIP gel appeared to have a larger pores and a more uneven surface texture than P(MAA-Aam)C. High magnification of the bulk of the gels (~8700X) showed P(MAA-Aam)MIP gels, with pores ranging from 0.25-0.50 μ m. In addition, these gels exhibited disorganized striations with 0.25 μ m between them. P(MAA)C gels appeared smooth with no pores. Finally, observation of the terpolymer P(MAA-DMAEMA-Aam) gels reveals a distinct morphological difference between MIP polymer and control gels, with P(MAA-DMAEMA-Aam)MIP disks exhibiting striations and pores of 0.5 – 1.0 μ m (Figure 5.5). Distance between striations was ~1.0 μ m. P(MAA-DMAEMA-Aam)C gels appeared smooth with no striations.

When MIP polymers were compared, a considerable difference was noted in both the porosity and striation organization across formulations (Figure 5.6). P(MAA-Aam)MIP gel contained the smallest pore sizes at 0.25 μ m, and P(MAA)MIP polymer contained the largest pores at 10 μ m. The presence of the larger pores in the P(MAA)MIP polymers could be contributed to the ionic repulsion between carboxylic acid groups in MAA functional monomer. In the same respect, the small pore size in P(MAA-Aam) could be attributed to

hydrogen bonding between amine groups and carboxyl groups of the Aam and MAA monomers.

In addition, P(Aam)MIP and P(MAA-DMAEMA-Aam)MIP had roughly the same pore size, but the striation organization was markedly different. P(MAA-DMAEMA-Aam)MIP striations were more laterally organized while the other formulations showed disordered striations. It is believed that the differences in morphologies can be attributed to the change in chemical functionalities present in the different formulations. These functional monomers will interact with the template lysozyme in markedly different ways and will contribute to a difference in the bulk structure across polymer types.

Although the use of proteins and other biological macromolecules in imprinting methodologies has been scarce, many researchers have attempted to fabricate macroporous polyacrylamide gels using a technique termed “templating”^{25, 26}. In this technique, polyacrylamide gels are polymerized in the presence of another polymer (PEG, hydroxymethylcellulose, polyvinylpyrrolidone, etc...) or an externally applied electric field to form macroscopic pores in the bulk of the gel. These polymer systems have been widely applied to SDS-PAGE gel electrophoresis to separate very large molecular weight (<100 kDa) macromolecules in solution. Guinta and colleagues^{27, 28} polymerized Aam in the presence of an externally applied electric field, resulting in polymers with an ordered ribbon-like structure as compared with the control under confocal microscopy (Figure 5.7). While the distance between ribbons is greater and they exhibit parallel order, the

polymer striations formed in this gel exhibit similarities to the MIP gels polymerized in the presence of lysozyme.

In addition, Righetti and collaborators have seen similar morphology changes when acrylamide gels are polymerized in the presence of the hydrophilic polymer PEG²⁹. In such gels, the addition of the polymer created small pores with randomly ordered dense chains. The dense chains maintain a similar morphology to the randomly oriented striations observed in our MIP gels. Of special note are the results that they observed when their reactions are run in the presence of PEG at 20 kDa, which is approximately the same molecular weight as lysozyme. The comparable pore sizes of 0.25-0.5 μm that were observed in these gels greatly resembled the pores obtained in P(MAA-Aam)MIP polymers.

Charlione⁶ has combined the two templating methods outlined above to produce macroporous gels. In this study, Aam was polymerized in the presence of PEG and under the influence of an electric field. This study noted that as the PEG size increased, the striations became more ordered with parallel arrangement. In addition, the resulting pores also increased as the MW of the PEG increased. They observed pores 1 μm that appear similar to pores formed in P(MAA-DMAEMA-Aam)MIP and P(Aam)MIP.

From the results above, Righetti has developed a theory that is termed “dense chain formation” to explain the macroporous networks with striations when gels are polymerized in the presence of macromolecules such as PEG

(Figure 5.8). Since PEG can bind up to 1.5 water molecules per oxygen molecule on its chain, the number of water molecules bound will increase with increasing PEG molecular weight. It is believed the hydrophilicity of the polymer sequesters water to the PEG surface and affects the growing polymer chain formation. The high water concentration forms hydrogen bonds with amine functional groups on the Aam monomer. The resulting interactions between the amine groups and the water/PEG complex form dense, fibrillar bundles around the PEG template. The crosslinker then locks the bundles in place around the macromolecule. The resulting gel then contains macropores with dense surrounding chains. These chains resembled the striations found in the MIP gels in this work.

Similar to the above theory, we believe that the change in morphology of the MIP gels over the control polymers can be attributed to the presence of the charged, hydrophilic protein lysozyme. The presence of lysozyme interacts with chemical groups on the monomers via electrostatic attraction and/or hydrogen bonding. As the chains form, the crosslinker freezes the orientation of the chemical groups that have non-covalently interacted with the protein. If this theory is correct, the functional groups of the monomers orient themselves toward the protein, increasing tacticity while leaving the aliphatic backbone oriented away from the template surface. The increase in tacticity then leads to formation of the dense polymer striations, while the presence of protein during polymerization contributes to pore formation.

5.3.2 Determination of Chemical Composition Using FTIR

Figure 5.9 shows the FTIR spectrum of P(MAA)C polymer. This spectrum shows a strong absorption peak at 1556 cm^{-1} that corresponds to the asymmetric stretching of the C=O bond of a bound carboxylic acid group, meaning one whose hydroxyl group has undergone a reaction to remove the hydrogen. The presence of this peak is most likely due to a condensation reaction with the functional monomers in which two carboxyl groups react to dimerize and form the anhydride, thus releasing a water molecule. This reaction most likely occurs during the polymerization as the exothermic nature of the reaction heats up the mixture, a condition that would promote this anhydride formation from the methacrylic acid groups. The peak at 1421 cm^{-1} corresponds to the symmetric stretching of the C=O bond of the bound carboxylic acid group. The peak at 1649 cm^{-1} represents the C=O stretching of the free carboxylic acid groups, meaning those with the hydroxyl group still intact. The intensity of this peak is much lower than that of the bound carboxylic acid peak, indicating that majority of the methacrylic acid monomers have reacted to form an anhydride during polymerization³⁰. The other notable peak is the broad peak at $\sim 3400\text{ cm}^{-1}$, which corresponds to the O-H stretch of the free carboxylic acid groups.

Figure 5.10 shows the FTIR spectrum of P(Aam)C polymer. This spectrum shows a strong absorption peak at 1673 cm^{-1} corresponding to the stretching of the C=O bond. The peak also contains a shoulder peak at 1615 cm^{-1} , which represents the N-H bending of the amine group. Other notable peaks

are the sharp peak found at 1118 cm^{-1} corresponding to the C-N stretch and the broad peak at $\sim 3400\text{ cm}^{-1}$ representing the N-H stretching of the amine group.

Figure 5.11 shows the FTIR spectrum of P(DMAEMA)C polymer. This spectrum shows an absorption peak at 1728 cm^{-1} corresponding to the C=O stretching of the carbonyl functionality. The other notable peak is at 1147 cm^{-1} that represents the C-N stretch of the tertiary amine.

Figure 5.12 shows the FTIR spectrum of P(MAA-Aam)C copolymer. By comparing this spectrum with those of the P(MAA)C and P(Aam)C homopolymers, the presence of both monomer types in the copolymer can be confirmed. In this spectrum, the strong absorption peak at 1556 cm^{-1} representing the C=O stretch of the bound carboxyl group indicates the presence of MAA. The peak 1673 cm^{-1} (C=O stretch) and its shoulder peak at 1615 cm^{-1} (N-H bending) indicate the presence of Aam in the copolymer.

Figure 5.13 shows the FTIR spectrum of P(MAA-Aam-DMAEMA)C copolymer. By comparing this spectrum with those of three homopolymers, peaks from each homopolymer can be discerned. The strong absorption peak at 1673 cm^{-1} (C=O stretch) and its shoulder peak at 1615 cm^{-1} (N-H bending) confirms the presence of Aam in the copolymer. The absorption peak at 1556 cm^{-1} (C=O stretch from bound carboxylic acid groups) indicates that the copolymer contains MAA. The peaks at 1728 cm^{-1} (C=O) and 1147 cm^{-1} (C-N stretch) indicate the presence of DMAEMA in the copolymer.

5.3.3 Chemical Composition of MIP Polymers Compared to Controls

In addition to the above studies, FTIR was employed to ascertain if the MIP and control polymers displayed any chemical differences. Using this method, differences in the bonding environments of the polymers would result in peak shifts and changes in peak shape and intensity, especially in the fingerprint region of the IR spectrum. In MIP reactions, the template molecule should not have any effect upon the overall composition of the polymer and should be similar, if not the same, in composition to the control. Figure 5.14 shows a comparison of the FTIR spectrum of the P(MAA)MIP and P(MAA)C polymers. The locations, shapes, and relative intensities of the peaks are identical not only in the fingerprint region but also over the entire spectrum range, indicating that these polymers are chemically identical. Figure 5.15 makes the same comparison for P(Aam)MIP versus its control and again demonstrates matching chemical bonding environments for these polymers. These two results support the theory that template molecules do not change the chemical nature of the polymer but instead only act to direct the macroscopic properties as outlined previously in SEM studies in Section 5.3.1.

5.3.4 DSC Determination of MIP Polymer Properties

The T_g values were determined by using the tangent lines at the onset and end of the transition using the half C_p method, giving a T_g value that corresponds to the middle of this energy transition. The T_g values from the DSC scans for the MIP and control polymers are summarized in Table 5.1.

This T_g value for the crosslinked polymer can be used to determine an effective number-average molecular weight between crosslinks \overline{M}_c using the following empirical relationship³¹:

$$\overline{M}_c = \frac{3.9 \times 10^4}{(T_g - T_{g0})}$$

In this equation, T_g represents that of the crosslinked polymer, while T_{g0} is the glass transition temperature of an uncrosslinked polymer of the same composition.

In this study, the T_{g0} values of the respective homopolymers are 19°C, 165°C, and 228°C for P(DMAEMA), P(Aam), and P(MAA), respectively³². For the copolymers, the T_{g0} values were calculated according to the Fox equation for random copolymers:

$$\frac{1}{T_g} = \frac{w_1}{T_{g1}} + \frac{w_2}{T_{g2}}$$

In this equation, w_1 and w_2 are the weight fractions of the homopolymers, and T_{g1} and T_{g2} are their respective glass transition temperatures (in K). This equation can readily be extended to a random copolymer with three monomer types by adding a third term to the right side of the equation.

The \overline{M}_c values from the DSC results are summarized in Table 5.2. For comparison, the theoretical molecular weight between crosslinks, $\overline{M}_{c,th}$, can be calculated using the following equation:

$$\overline{M}_{c,th} = \frac{M_r}{2X}$$

In this equation, M_r is the molecular weight of the repeating unit, and X is the molar crosslinking ratio (defined as moles crosslinker/moles total monomer). For the copolymers, the effective M_r was determined by a weight average of the individual monomer types as follows:

$$M_r = w_1 * M_{r1} + w_2 * M_{r2}$$

This equation was readily expanded to a copolymer of three monomer types by adding a third term to the right side of the equation. The $\overline{M}_{c,th}$ values for these polymers are also summarized in Table 5.2.

The DSC scans of these polymers show an endothermic step that equates to the glass transition temperature (Figure 5.16, Figure 5.17). The T_g value is taken to be the middle of this step, as calculated by utilizing the tangential lines before and after the step by the DSC software. As evidenced from the T_g results summarized in Table 5.1, the glass transition temperatures for the MIP and control polymers are similar in value for both the MIP and control polymers. The standard deviation for these T_g values among scans was as high as $\pm 3^\circ\text{C}$. Considering this result, no significant differences appear between the T_g values for the MIP and control polymers. Thus, for \overline{M}_c calculations, the average T_g value was used.

Upon comparing these T_g values to the T_{g0} values for the uncrosslinked polymer, it becomes obvious how significantly the crosslinking of these polymers raises their effective T_g values. This augmentation of the T_g values is reasonable, however, when considering the \overline{M}_c values calculated from these

results. The data in Table 5.2 shows that the \overline{M}_c values from the DSC results are similar to those of the theoretical value determined from the degree of crosslinking. Of note, a glass transition temperature was not observed for the crosslinked P(MAA), but this result is not surprising when considering the degree of crosslinking. If one assumes a comparable \overline{M}_c value to the $\overline{M}_{c,th}$ value, the observed T_g should be approximately 284°C, which is approaching the thermal degradation range of this polymer³³. The heat flow on the DSC scan for this polymer starts an endothermic swing at around 275°C, which is most likely the initiation of its glass transition; however, before this is completed, the polymer undergoes a strong exothermic process beginning around 300°C, signaling the beginning of the thermal degradation of this polymer (Figure 5.18). Thus, this polymer actually begins to decompose before fully undergoing its glass transition.

Of interest, these polymers only demonstrate a T_g upon the first DSC scan. At first glance, this result is unusual for typical polymer samples. The reason for this result stems from the high temperatures needed to see the T_g in the first DSC scan; all of these polymers contain functional, and hence reactive, side chain groups that can undergo intra- and intermolecular reactions that are thermally catalyzed. Thermal analysis of P(MAA) shows that these polymers can undergo a condensation reaction across the hydroxyl group of the carboxyl functionality at temperatures as low as 150°C³³. This reaction can form an anhydride ring if the two reacting carboxyl groups are within the same polymer chain or a link between two polymer chains if the reacting carboxyl groups are on

adjacent chains. In essence, this reaction not only changes the chemical composition of these polymers, which can change the T_g value, but also augments the degree of crosslinking, which can raise the T_g value significantly. Similar reactions can occur across the amide group of P(DMAEMA)³⁴ and the carboxyl group of P(Aam)³⁵ as well as between the different functional groups in the copolymers. Thus, a T_g value is not observed upon repeating the same temperature scans, most likely because the reactions of the functional groups increases the T_g above the temperature scan range. Upon raising the upper limit of the second temperature scans, the degradation temperature of these polymers is reached; thus, these polymers undergo thermal decomposition before exhibiting a T_g on the second scan.

5.4 Conclusions

The observations of the macroscopic properties using SEM revealed marked differences in the overall morphology between MIP polymers and their controls. The presence of a charged, hydrophilic protein has profound effects on the polymerization, inducing formation of a porous structure with macroscopic order. It is believed that the presence of a template containing groups that will electrostatically interact with the monomers during polymerization influences the overall formation of the gels. This supports our theory of the formation of a chemically and spatially oriented polymer for our template protein lysozyme. Considering these initial intriguing results, this phenomenon warrants further attention, and it would be advantageous if the polymers can be imaged in their

hydrated state using an environmental SEM in order to better determine the differences in morphology between the MIP and control gels.

In addition to SEM, FTIR spectroscopy was used to confirm the presence of the respective monomer types in the two copolymers by comparing the spectra with those of the homopolymers. FTIR was also utilized to demonstrate that the MIP and control polymers in this study are chemically identical. However, although FTIR is accurate about the frequencies and relative intensities of the chemical bonds present in a sample, it is nonetheless difficult to obtain precise quantitative measurements using this technique.

Finally, DSC results show comparable T_g values for the MIP and control polymers for each polymer type. The average molecular weight between crosslinks calculated from these T_g results are of the same order as the theoretical value calculated from the degree of crosslinking, indicating that these T_g values are reasonable. A glass transition was only observed on the first DSC scan for these polymers, most likely due to the high temperatures of the first scan initiating intra- and intermolecular reactions of the functional side groups.

The results outlined in these studies support our theory of the formation of a MIP recognitive network for the protein lysozyme. The presence of lysozyme creates a macroporous network but does not influence either the composition or crosslinking of the network. Future studies should focus on characterizing the exact nature of the protein interaction with the network and determining the exact composition of the resulting gels.

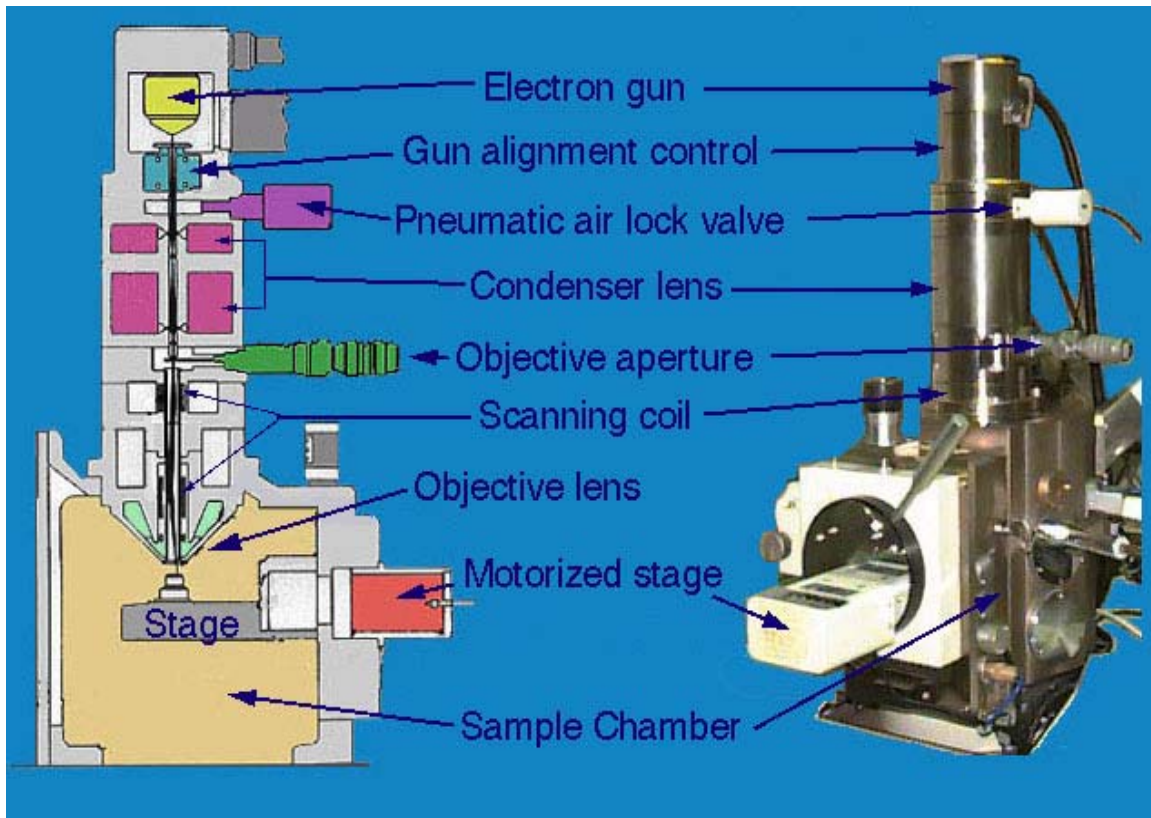


Figure 5.1: Schematic of Scanning Electron Microscope

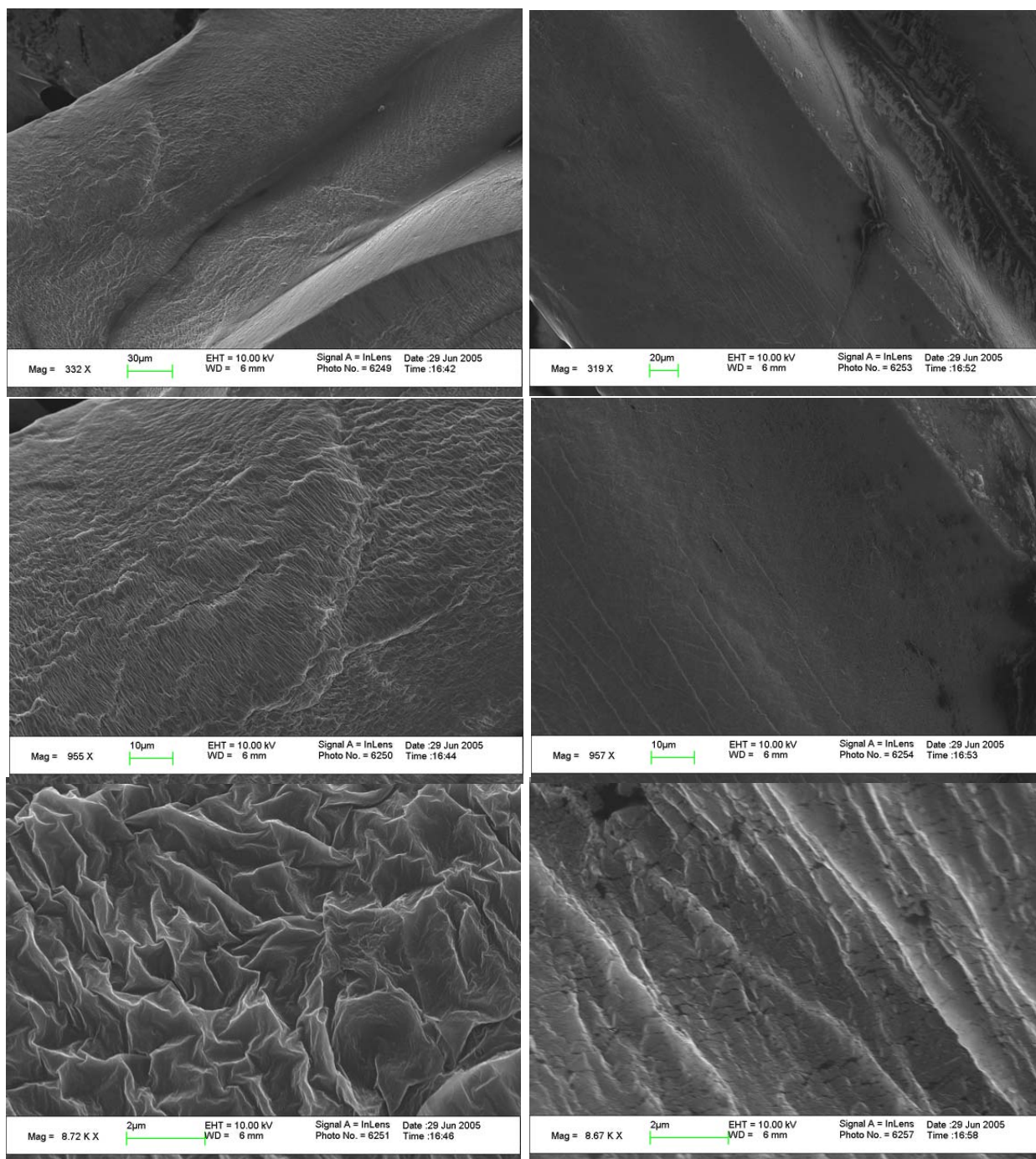


Figure 5.2: P(Aam)MIP (Left) and P(Aam)C (Right) gels at increasing magnifications. Observation of the gels reveals a distinct morphological difference between MIP polymer and control gels, with P(Aam)MIP disks exhibiting striations and pores of 0.25 – 1.0 µm. Distance between striations was ~1.0 µm. P(Aam)C gels appeared smooth with no striations.

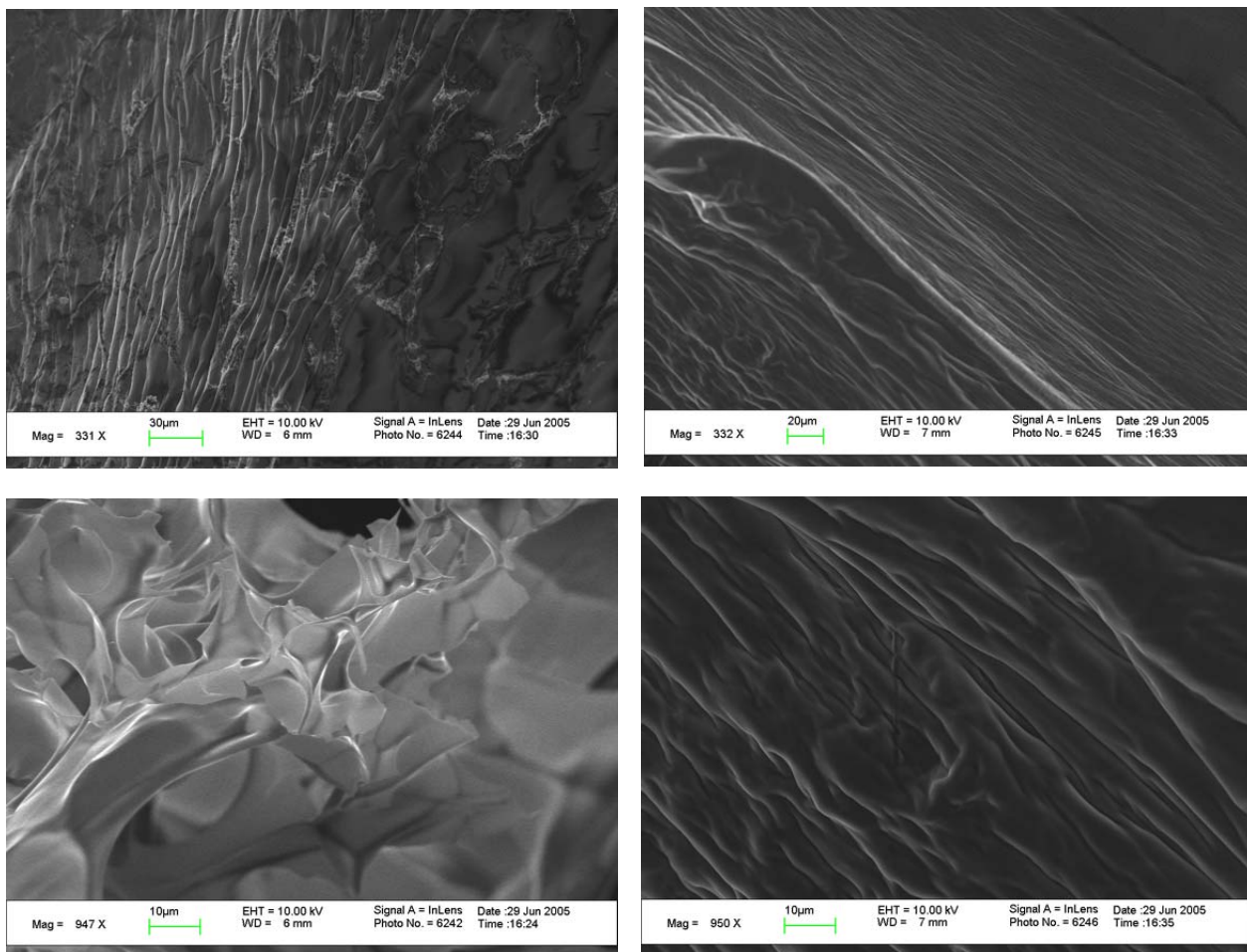


Figure 5.3 P(MAA)MIP (Left) and P(MAA)C (Right) gels at increasing magnifications. Observation of the gels reveals a distinct morphological difference between MIP polymer and control gels, with P(MAA)MIP disks exhibiting pores of 5-10 μm . Striations observed in other formulations were absent in this one. P(MAA)C gels appeared smooth with no pores.

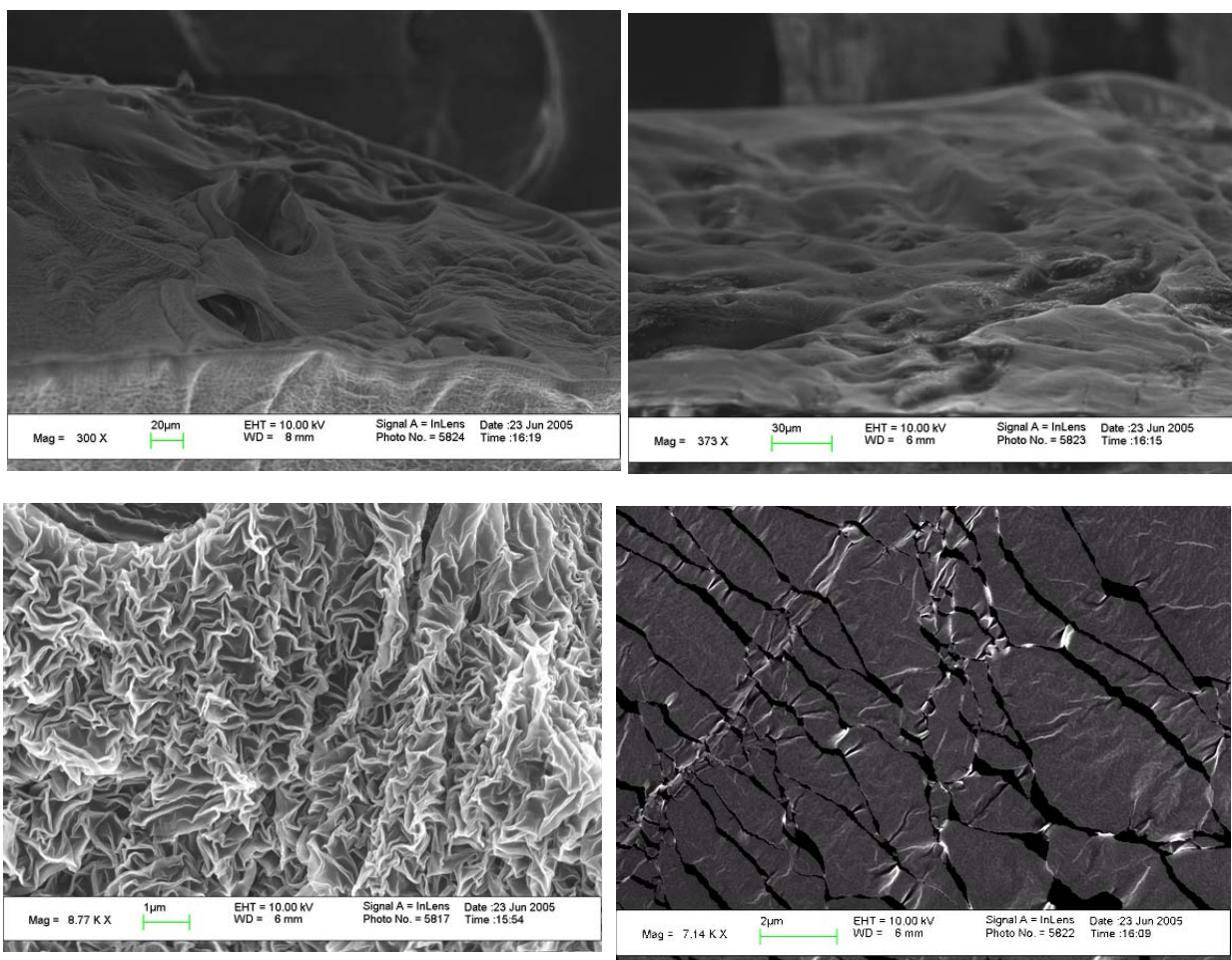


Figure 5.4: P(MAA-Aam)MIP (Left) and P(MAA-Aam)C (Right) gels at increasing magnifications.

Top two images show the edge feature of P(MAA-Aam) gels. The edge of the P(MAA-Aam)MIP gel appeared to have a larger pores and a more uneven surface texture. The bottom two photos show the bulk of the gels at high magnification. Observation of the gels reveals a distinct morphological difference between MIP polymer and control gels, with P(MAA)MIP disks exhibiting pores of 0.25-0.50 μm and the polymer striations. Distance between striations measured 0.25 μm . P(MAA)C gels appeared smooth with no pores.

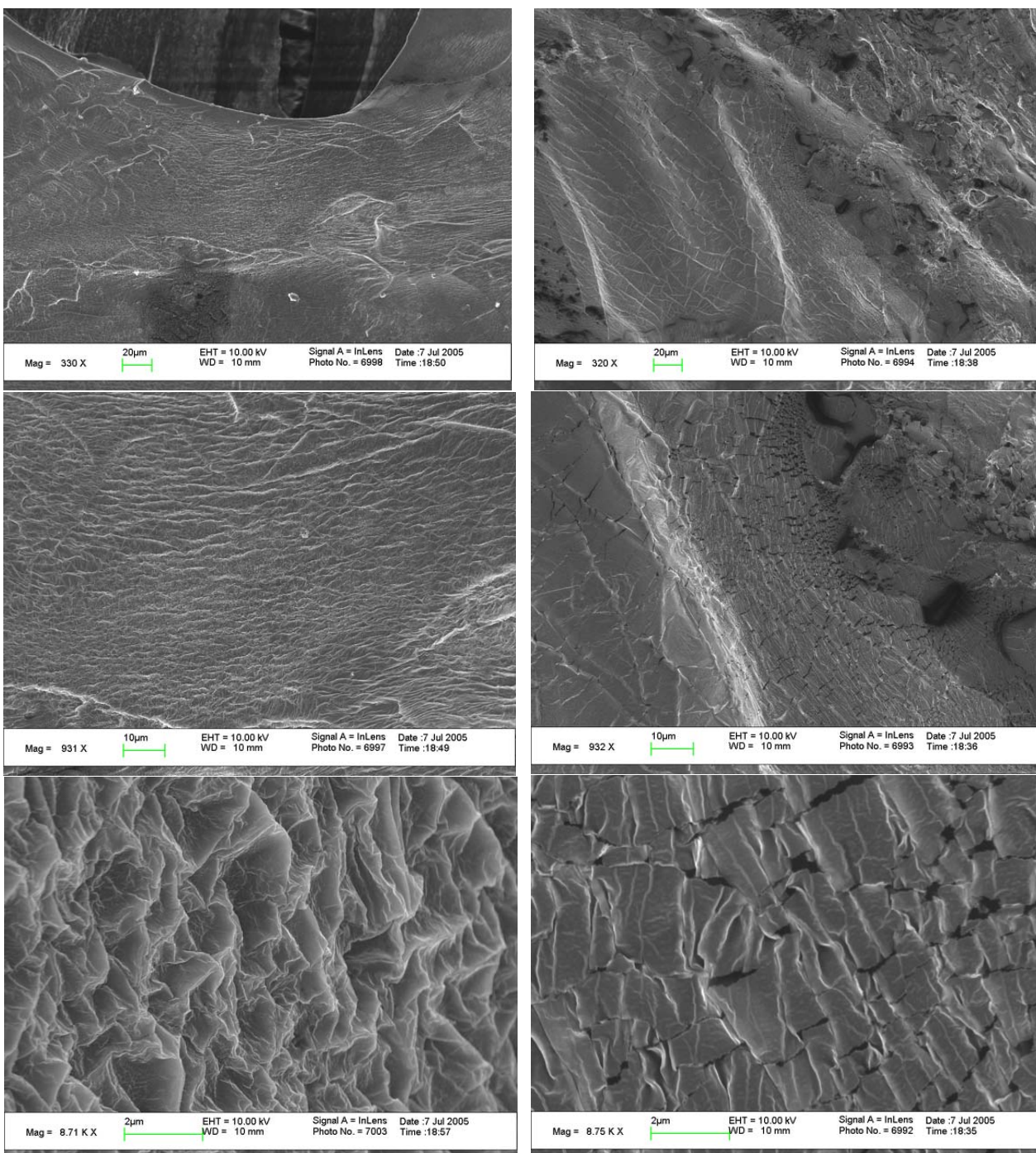


Figure 5.5: P(MAA-DMAEMA-Aam)MIP (Left) and P(MAA-DMAEMA-Aam)C (Right) gels at increasing magnifications.

Observation of the gels reveals a distinct morphological difference between MIP polymer and control gels, with P(MAA-DMAEMA-Aam)MIP disks exhibiting striations and pores of 0.5 – 1.0 μm. Distance between striations was ~1.0 μm. P(MAA-DMAEMA-Aam)C gels appeared smooth with no striations.

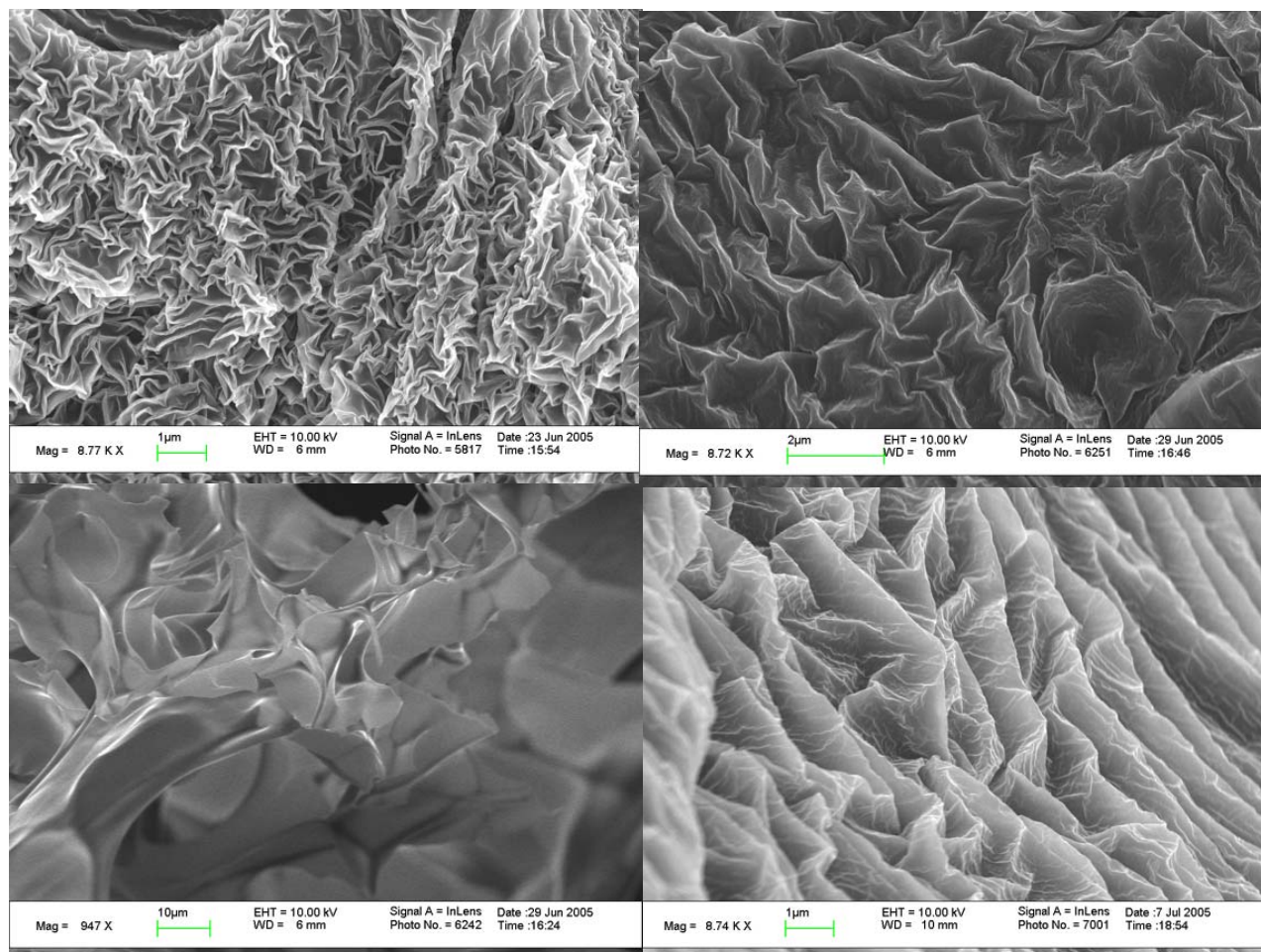


Figure 5.6: Differences in the Bulk Morphology of MIP gels.

Top Left: P(MAA-Aam)MIP; *Top Right:* P(Aam)MIP; *Lower Left:* P(MAA)MIP; *Lower Right:* P(MAA-DMAEMA-Aam)MIP. Upon macroscopic comparison of the four different MIP formulations, a distinct morphological difference was observed. P(MAA-Aam)MIP exhibited the smallest pore size at 0.25 μm , while P(MAA)MIP disks exhibited the largest pore size at 10 μm . P(MAA)MIP gels did not exhibit the striations that other gels exhibited, and striation distance and organization differed across the other three formulations. P(MAA-Aam)MIP polymers had the smallest distance between striations at 0.25 μm .

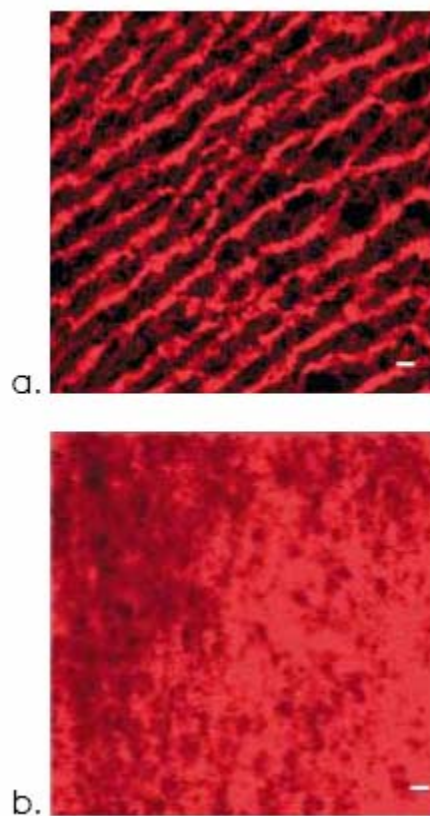


Figure 5.7: Flourescent Image of P(Aam) gel Polymerized under Electric Field

Confocal laser scanning microscopy images of a hydrogel polymerized while under the influence of an externally applied electric field (a.) Polymer contained oriented striations that resembled the striations of imprinted gels. Control gels (b.) exhibited no striations. Bar represents 10 μm . Reproduced from the work of Guinta and colleagues^{27, 28}.

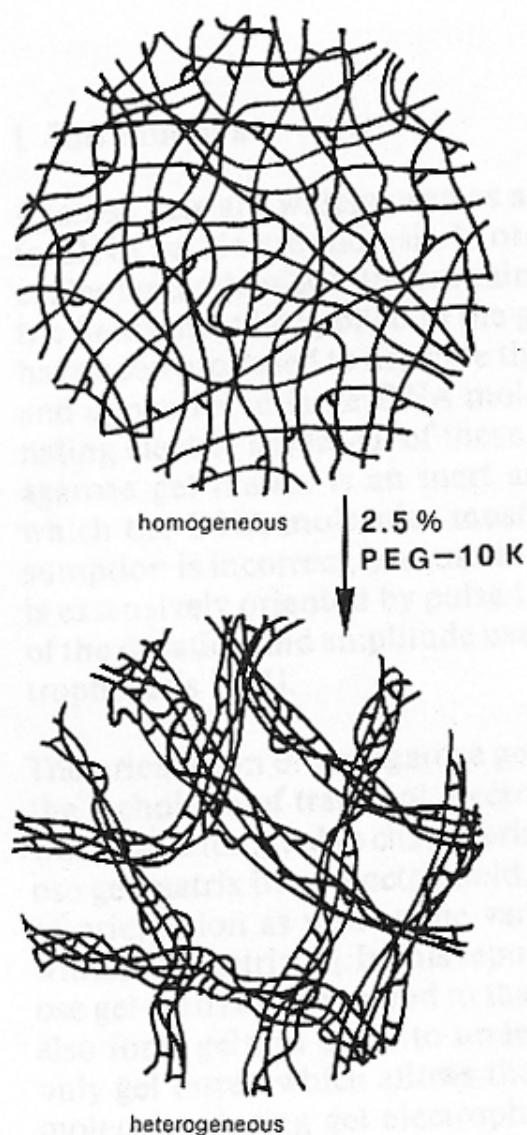


Figure 5.8: Theory of Dense Chain Formation

The top figure represents the structure of a control gel where the fibers form a random mesh network. However, when gels are polymerized in the presence a hydrophilic template such as PEG, the individual fibers bundle due to directed arrangement around the template, and a porous network is formed. Thus, the average porosity of the gel is greatly increased, and polymer striations are formed. Reproduced from the work of Righetti²⁹.

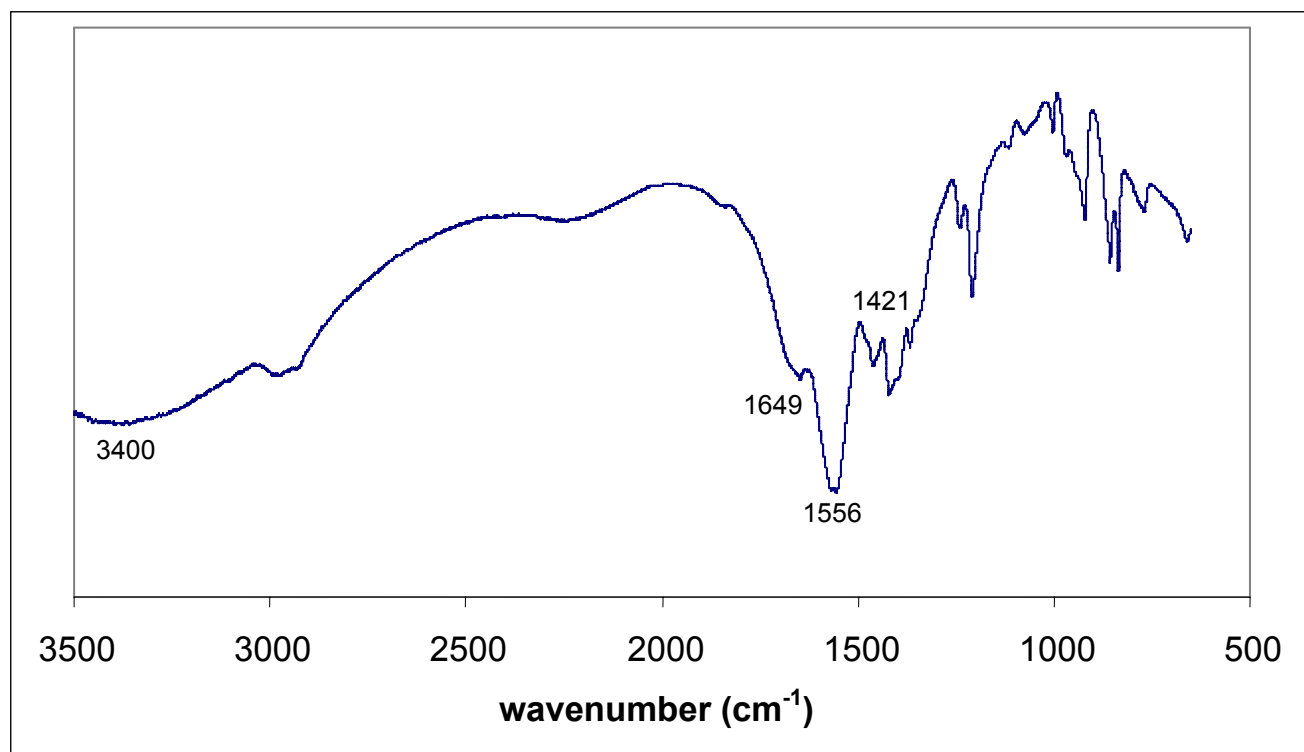


Figure 5.9: FTIR spectrum of P(MAA)C polymer

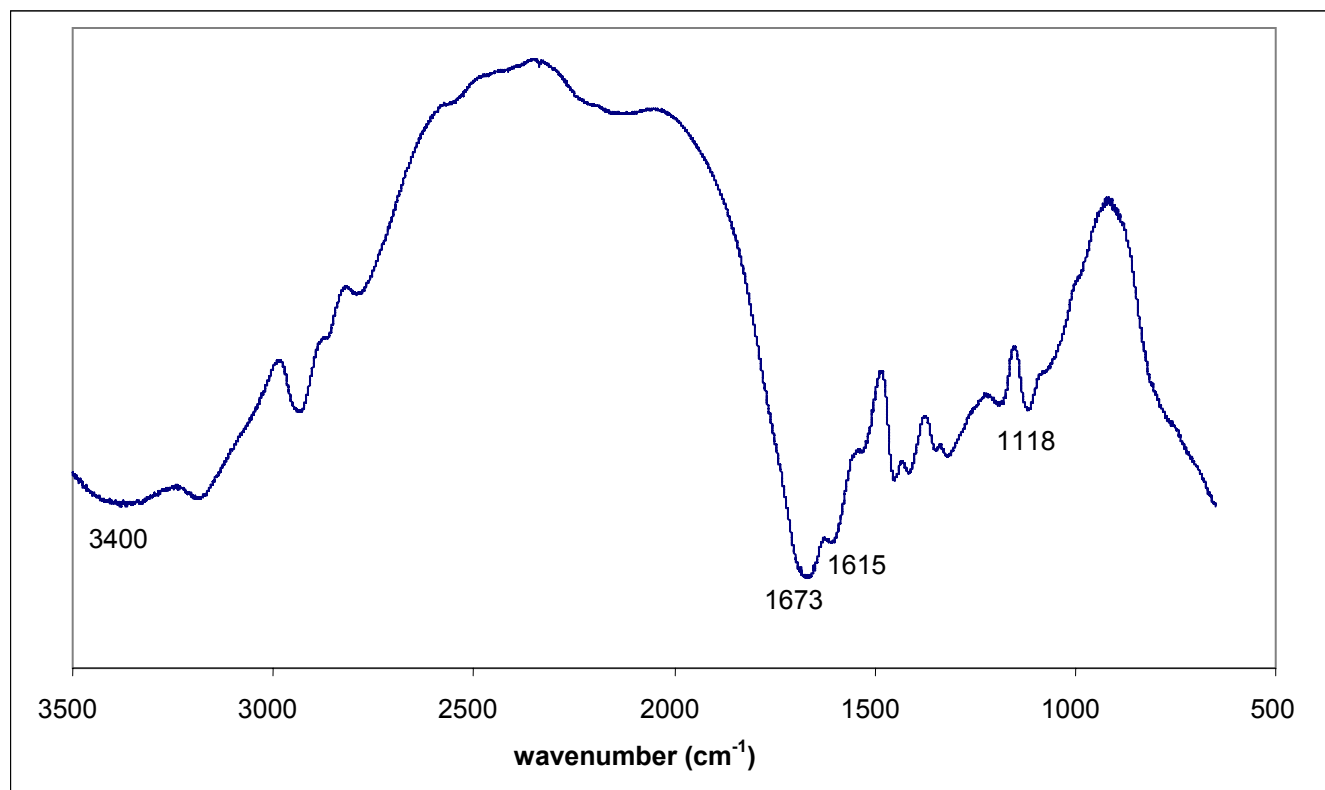


Figure 5.10: FTIR spectrum of P(Aam)C polymer

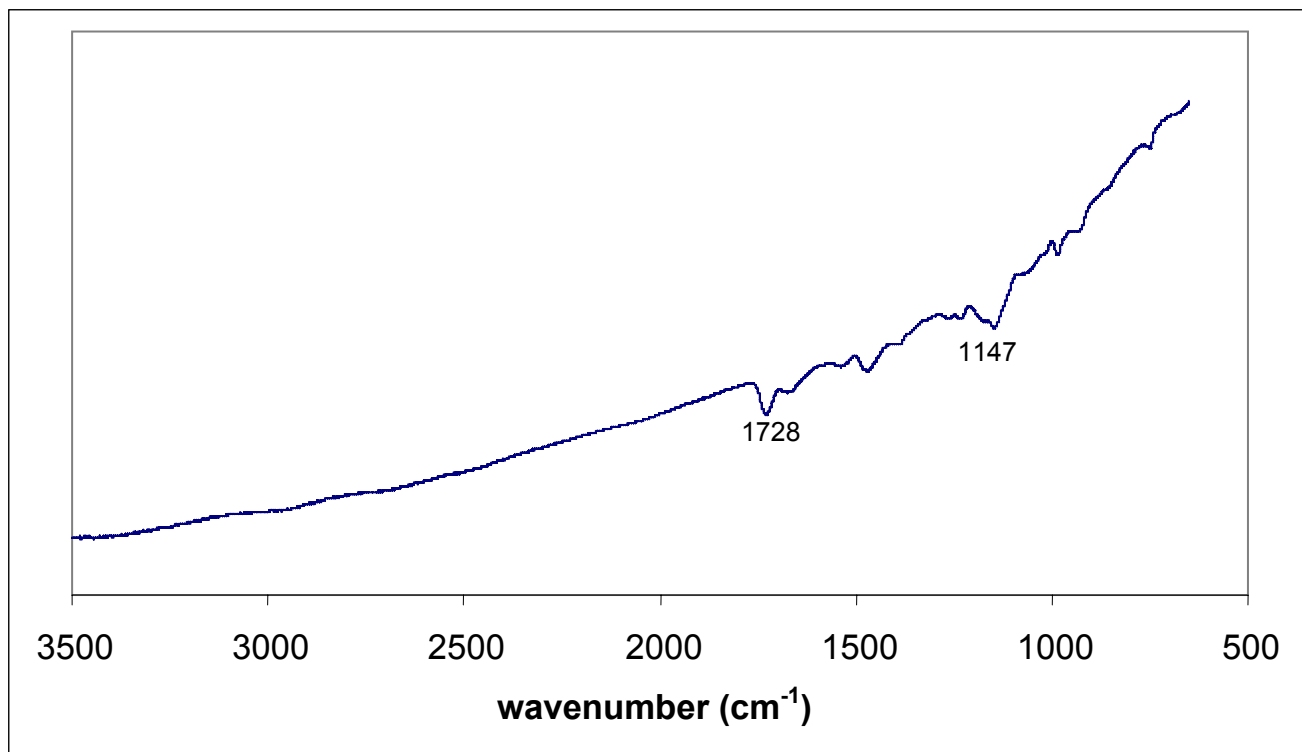


Figure 5.11: FTIR spectrum of P(DMAEMA)C polymer

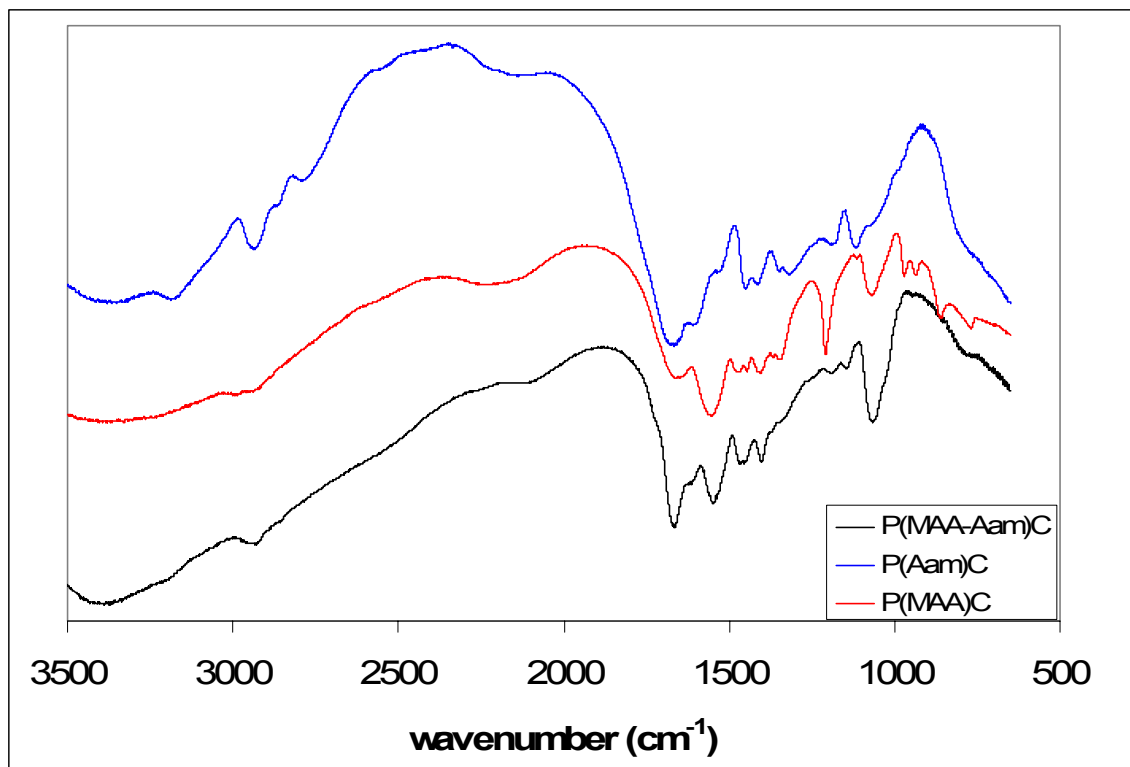


Figure 5.12: FTIR spectrum of P(MAA-Aam)C polymer with the P(Aam)C and P(MAA)C polymer spectra for reference.

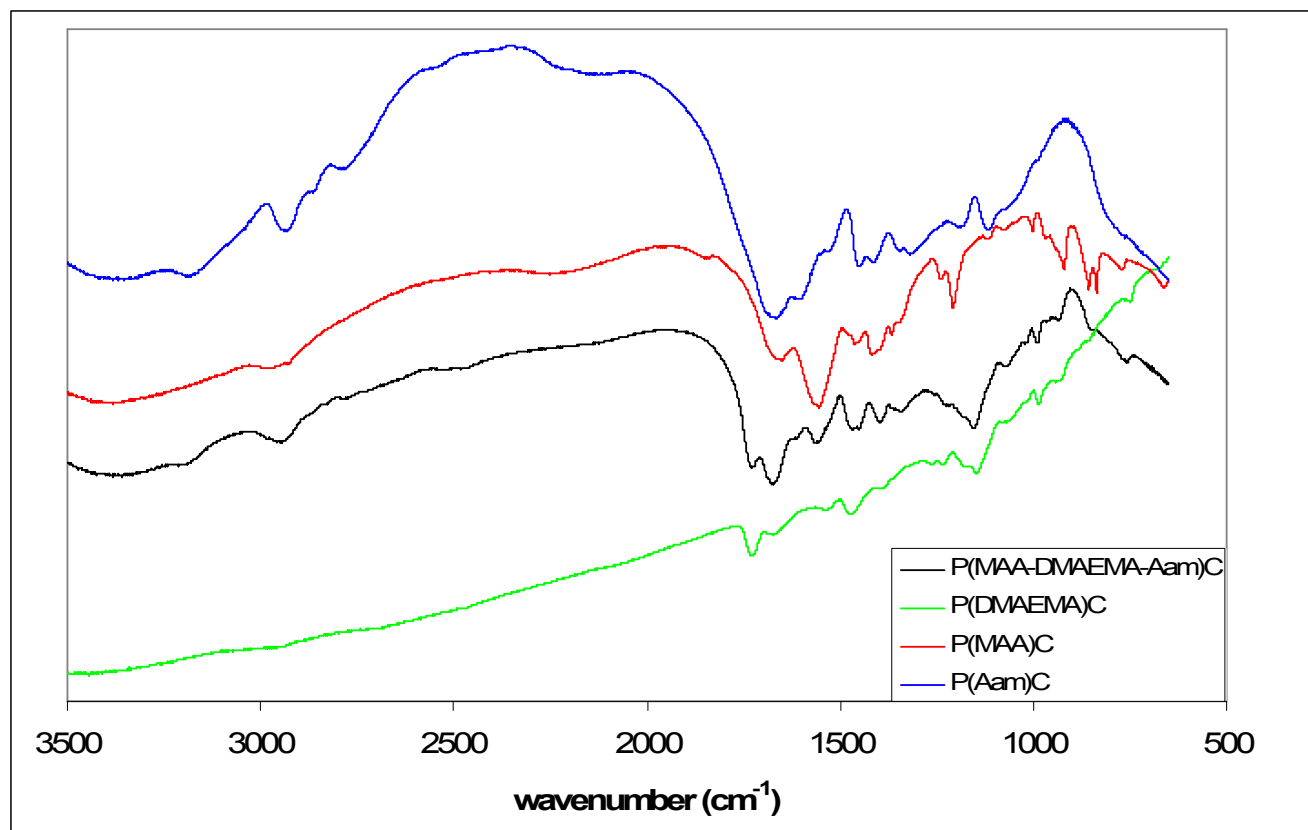


Figure 5.13: FTIR spectrum of P(MAA-DMAEMA-Aam)C polymer with P(Aam)C, P(MAA)C, and P(DMAEMA)C polymer spectra provided for reference

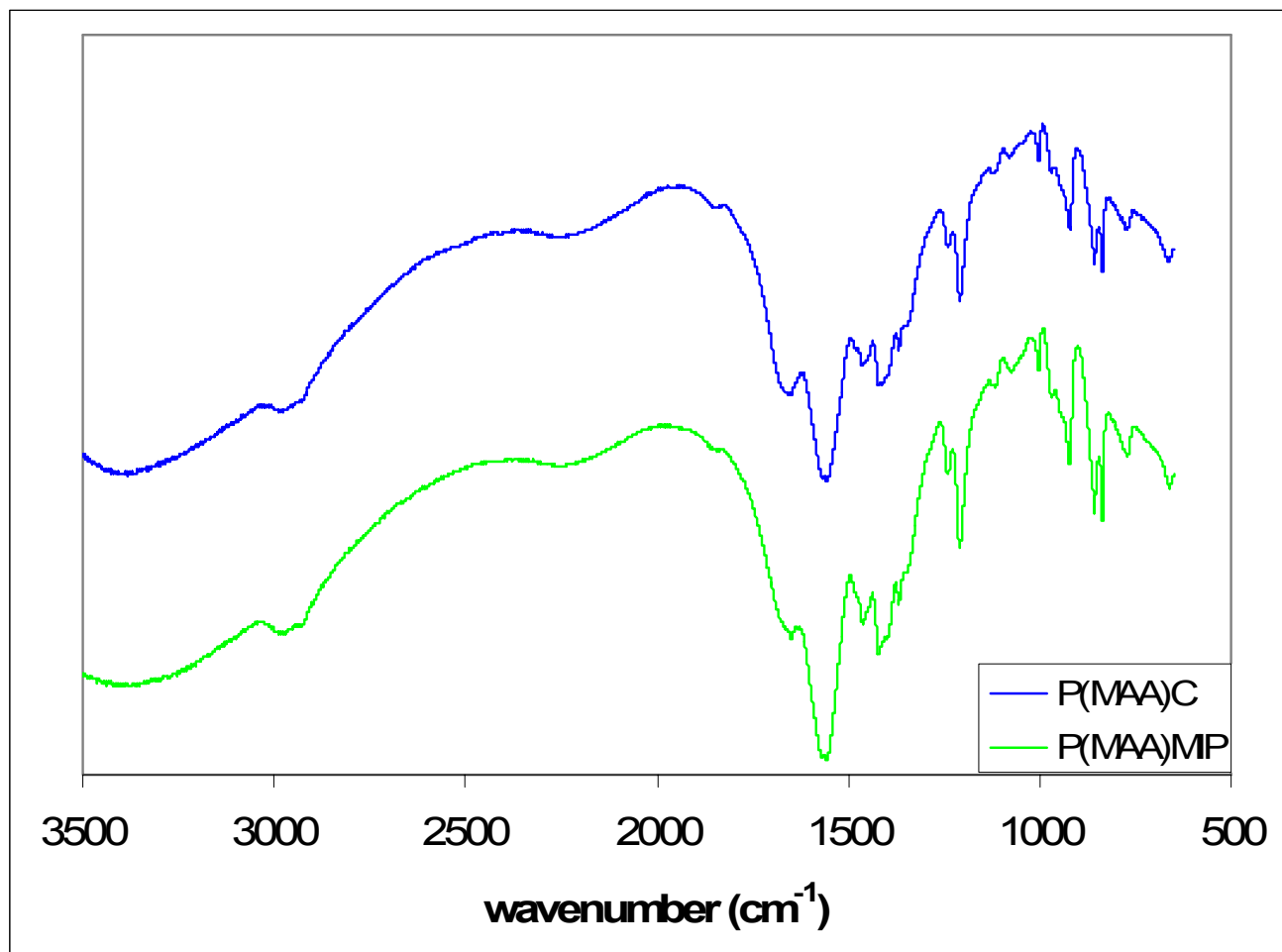


Figure 5.14: FTIR spectrum comparison between P(MAA)MIP and P(MAA)C polymers

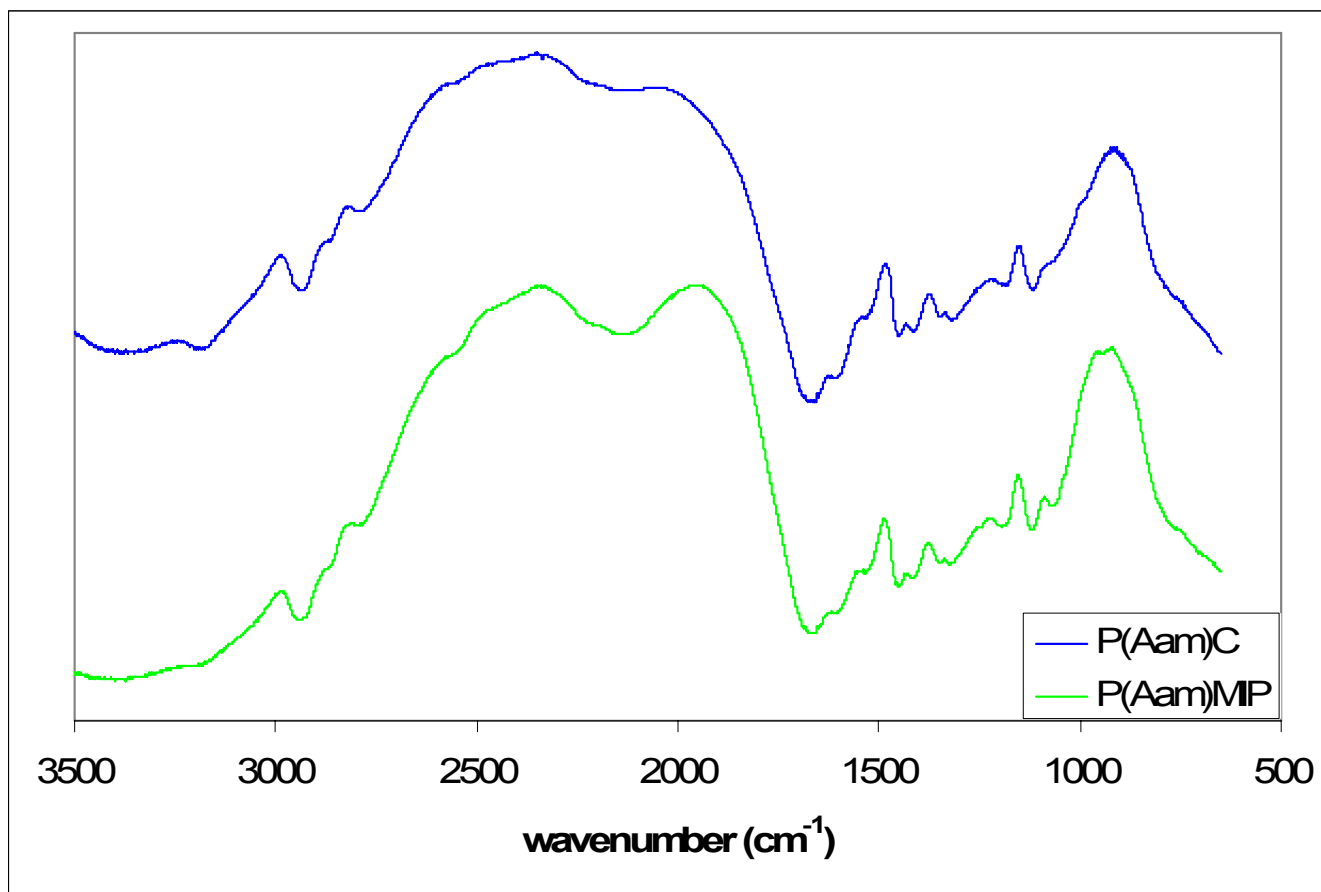


Figure 5.15: FTIR spectrum comparison between P(Aam)MIP and P(Aam)C polymer

Polymer Type	T _{g0} (°C)	MIP T _g (°C)	Control T _g (°C)
P(Aam)	165	238.2	235.7
P(MAA)	228	not observed	not observed
P(DMAEMA)	19	107.9	109.5
P(MAA-Aam)	194	246.1	253.0
P(DMAEMA-Aam)	48	102.9	98.1
P(MAA-DMAEMA-Aam)	93	198.9	195.7

Table 5.1: T_g values from the DSC analysis for the MIP and control polymers

No discernible difference in T_g was observed between MIP polymers and control polymers. Thus, an effect of imprinting on polymer network arrangement could not be concluded from DSC analysis.

Polymer	wt fraction	X	T _{g0} (°C)	M _r (g/mol)	\overline{M}_c^* (g/mol)	$\overline{M}_{c, th}$ (g/mol)
P(Aam)	n/a	0.05123	165	71.08	544	694
P(MAA)	n/a	0.06205	228	86.09	n/a	694
P(DMAEMA)	n/a	0.11330	19	157.21	435	694
P(MAA-Aam)	0.4964 M 0.5036 A	0.05608	194	78.53	702	700
P(DMAEMA-Aam)	0.7310 D 0.2690 A	0.08545	48	134.04	744	784
P(MAA-DMAEMA-Aam)	0.1967 M 0.4413 D 0.3320 A	0.07076	93	110.72	374	782

using an average T_g value for the MIP and control polymers

Table 5.2: The theoretical and experimental molecular weight between crosslinks results for the different polymer types

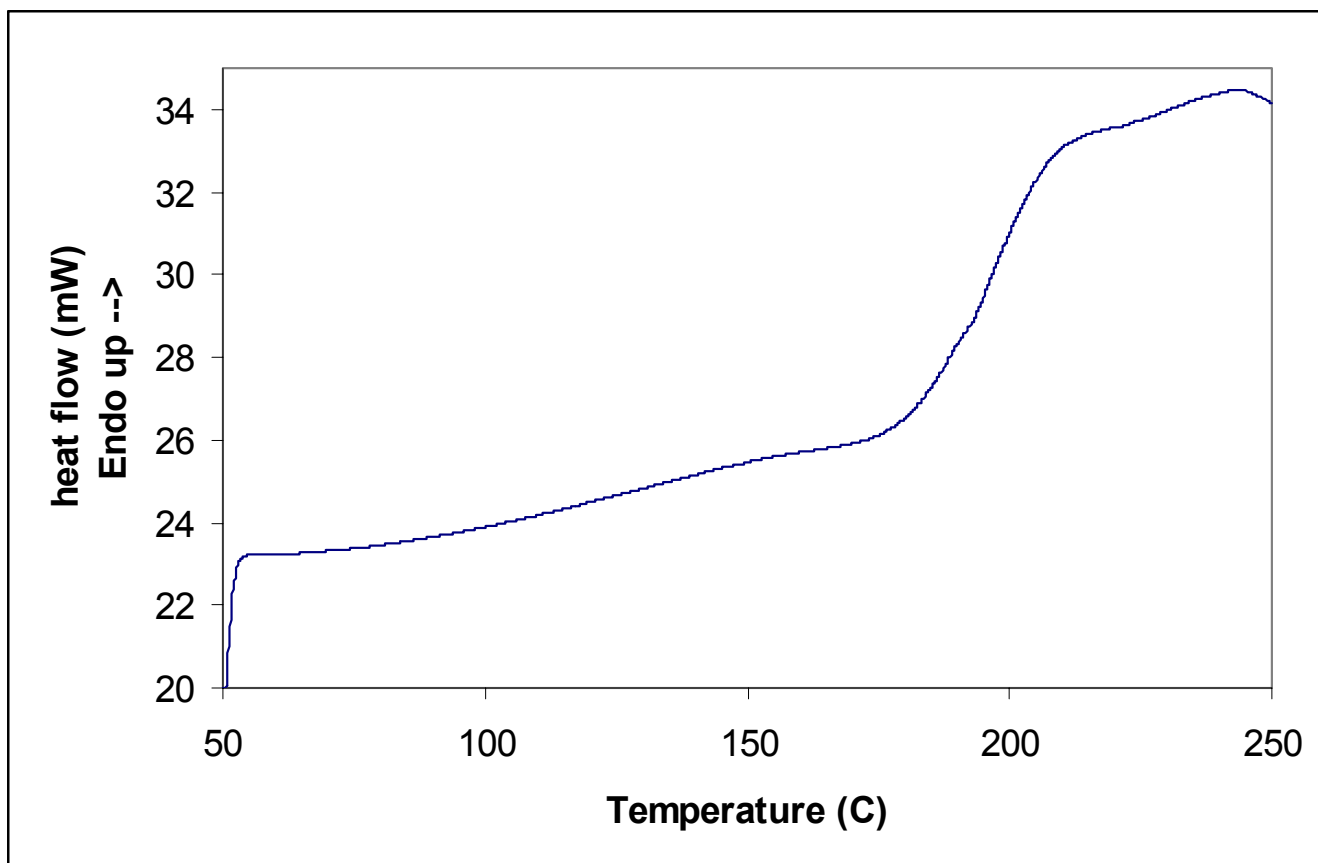


Figure 5.16: DSC scan for P(MAA-DMAEMA-Aam)C at 10°C/min indicating a T_g of 195.7°C

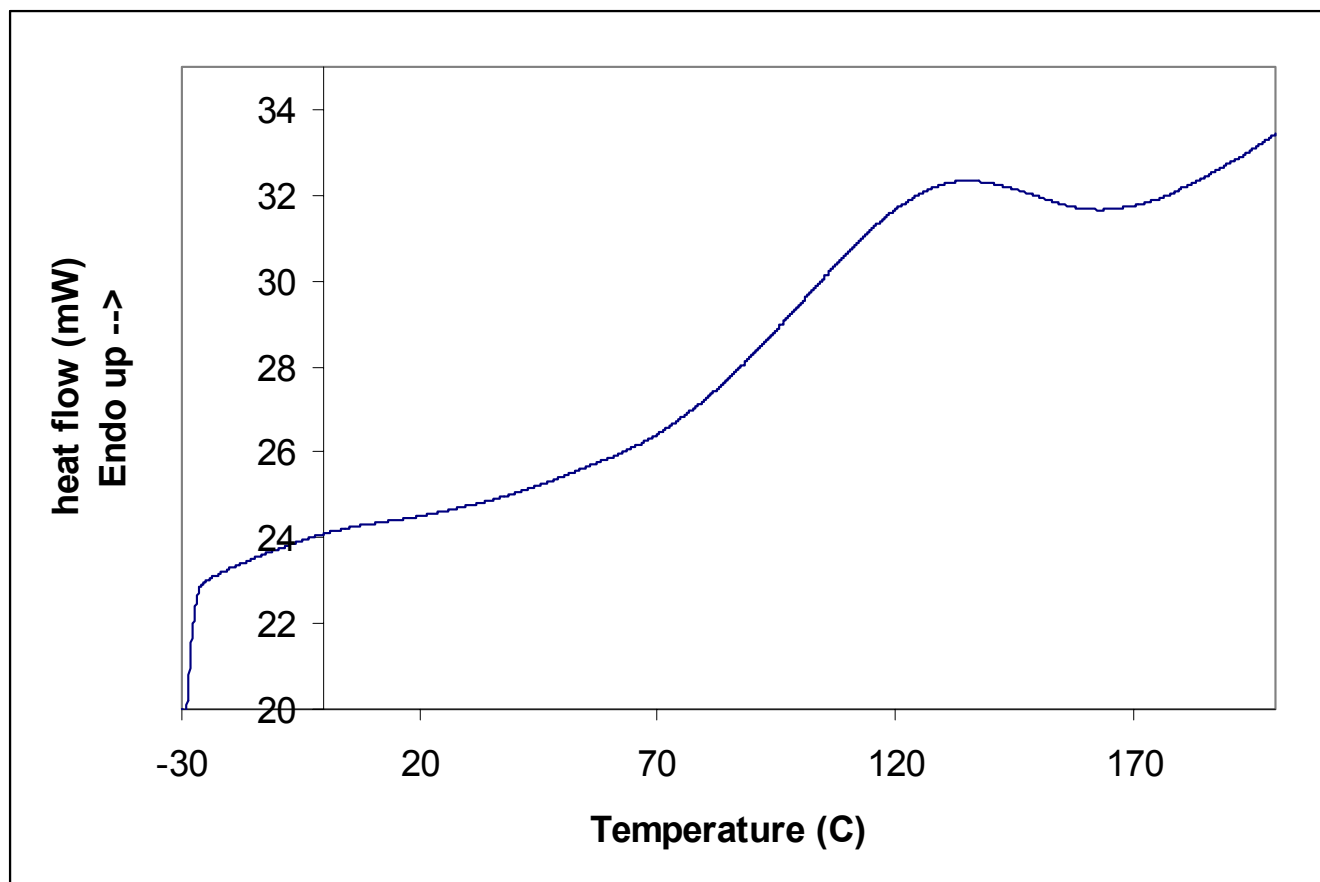


Figure 5.17: DSC scan of P(DMAEMA)C at 10°C/min indicating a T_g of 109.5°C

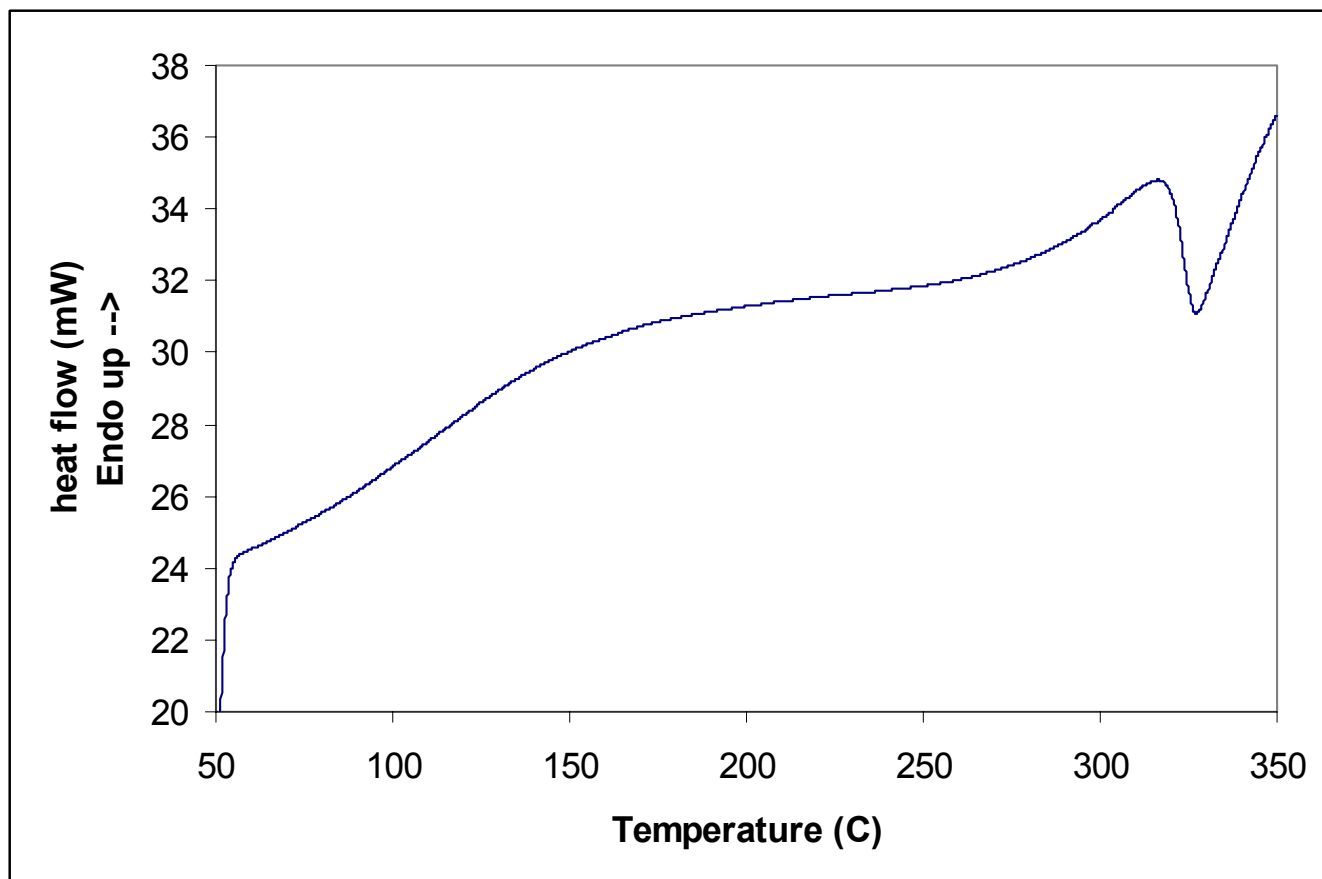


Figure 5.18: DSC scan of P(MAA)C at 10°C/min showing the exothermic thermal degradation peak interfering with the calculation of the T_g

5.5 References Cited

1. Chandler, G. W.; Seraphin, S., Scanning Electron Microscopy. In *Characterization of Materials*, Kaufman, E. N., Ed. Wiley: New Jersey, 2003; Vol. 2, pp 1050-1062.
2. Ruchel, R.; Brager, M. D., Scanning Electron Microscopic Observations of Polyacrylamide Gels. *Anal. Biochem.* **1975**, 68, 415-428.
3. Grimaud, E.; Lecoq, J. C.; Boschetti, E.; Corgier, M., Comparison of Gels Used for Molecular Sieving of Proteins by Electron Microscopy and Pore Parameters Determinations. *J. Chromatogr. A* **1978**, 166, (1), 37.
4. Patras, G.; Qiao, G. G.; Solomon, D. H., Characterization of the Pore Structure of Aqueous Three-Dimensional Polyacrylamide Gels with a Novel Cross-Linker. *Electrophoresis* **2000**, 21, (17), 3843-3850.
5. Blank, Z.; Reimschuessel, A. C., Structural Studies of Organic Gels by SEM. *J. Mater. Sci.* **1974**, 9, 1815-1822.
6. Charlionet, R.; Machour-Merlet, N.; Leclerc, S.; Malandain, J., Oriented Macroporous Polyacrylamide Gels. *Electrophoresis* **1997**, 18, 1133-1135.
7. Hsu, T.-P.; Cohen, C., Observations on the Structure of a Polyacrylamide Gel from Electron Micrographs. *Journal of Analytical Chemistry* **1983**.
8. Ismail, L. F. M.; Maziad, N. A.; Abo-Farha, S. A., Factors Affecting the Adsorption of Cationic Dyes on Polymeric Hydrogels Prepared by Gamma Irradiation. *Polym. Int.* **2005**, 54, (1), 58-64.

9. Rai, B.; Teoh, S. H.; Hutmacher, D. W.; Cao, T.; Ho, K. H., Novel PCL-Based Honeycomb Scaffolds as Drug Delivery Systems for rhBMP-2. *Biomaterials* **2005**, 26, (17), 3739-3748.
10. Palmer, R. R.; Lewis, A. L.; Kirkwood, L. C.; Rose, S. F.; Lloyd, A. W.; Vick, T. A.; Stratford, P. W., Biological Evaluation and Drug Delivery Application of Cationically Modified Phospholipid Polymers. *Biomaterials* **2004**, 25, (19), 4785-4796.
11. Zhang, X.-Z.; Wu, D.-Q.; Chu, C.-C., Synthesis, Characterization and Controlled Drug Release of Thermosensitive IPN-PNIPAAm Hydrogels. *Biomaterials* **2004**, 25, (17), 3793.
12. Li, M.; He, P.; Zhang, Y.; Hu, N., An Electrochemical Investigation of Hemoglobin and Catalase Incorporated in Collagen Films. *Biochimica et Biophysica Acta (BBA) - Proteins & Proteomics* **2005**, 1749, (1), 43.
13. Park, Y.-J.; Liang, J.; Yang, Z.; Yang, V. C., Controlled Release of Clot-Dissolving Tissue-Type Plasminogen Activator from a Poly(Glutamic Acid) Semi-Interpenetrating Polymer Network Hydrogel. *J. Controlled Release* **2001**, 75, (1-2), 37.
14. Zhang, R.; Tang, M.; Bowyer, A.; Eisenthal, R.; Hubble, J., A Novel pH- and Ionic-Strength-Sensitive Carboxy Methyl Dextran Hydrogel. *Biomaterials* **2005**, 26, (22), 4677.
15. Takahara, Y. K.; Ikeda, S.; Ishino, S.; Tachi, K.; Ikeue, K.; Sakata, T.; Hasegawa, T.; Mori, H.; Matsumura, M.; Ohtani, B., Asymmetrically Modified

Silica Particles: A Simple Particulate Surfactant for Stabilization of Oil Droplets in Water. *J. Am. Chem. Soc.* **2005**, 127, (17), 6271-6275.

16. Ulbricht, M.; Malaisamy, R., Insights into the Mechanism of Molecular Imprinting by Immersion Precipitation Phase Inversion of Polymer Blends Via a Detailed Morphology Analysis of Porous Membranes. *J. Mater. Chem.* **2005**, 15, (14), 1487-1497.

17. Wang, H. Y.; Xia, S. L.; Sun, H.; Liu, Y. K.; Cao, S. K.; Kobayashi, T., Molecularly Imprinted Copolymer Membranes Functionalized by Phase Inversion Imprinting for Uracil Recognition and Permselective Binding. *J. Chromatogr. B Analyt. Technol. Biomed. Life Sci.* **2004**, 804, (1), 127-134.

18. Byrne, M. E.; Oral, E.; Hilt, J. Z.; Peppas, N. A., Networks for Recognition of Biomolecules: Molecular Imprinting and Micropatterning Poly(Ethylene Glycol)-Containing Films. *Polymers for Advanced Technologies* **2002**, 13, (10-12), 798-816.

19. Byrne, M. E.; Park, K.; Peppas, N. A., Molecular Imprinting within Hydrogels. *Adv. Drug Deliv. Rev.* **2002**, 54, (1), 149-161.

20. Piletsky, S. A.; Matuschewski, H.; Schedler, U.; Wilpert, A.; Piletska, E. V.; Thiele, T. A.; Ulbricht, M., Surface Functionalization of Porous Polypropylene Membranes with Molecularly Imprinted Polymers by Photograft Copolymerization in Water. *Macromolecules* **2000**, 33, (8), 3092-3098.

21. Nicholls, I. A.; Rosengren, J. P., Molecular Imprinting of Surfaces. *Bioseparation* **2002**, 10, 301-305.

22. Lu, Y.; Li, C.; Wang, X.; Sun, P.; Xing, X., Influence of Polymerization Temperature on the Molecular Recognition of Imprinted Polymers. *J. Chromatogr. B* **2004**, 804, (1), 53.
23. Screenivasulu Reddy, P.; Kobayashi, T.; Abe, M.; Fujii, N., Molecular Imprinted Nylon-6 as a Recognition Material of Amino Acids. *Eur. Polym. J.* **2002**, 38, (3), 521.
24. Roorda, W. E.; Bouwstra, J. A.; de Vries, M. A.; Junginger, H. E., Thermal Behavior of Poly Hydroxy Ethyl Methacrylate (pHEMA) Hydrogels. *Pharm. Res.* **1988**, 5, (11), 722-725.
25. Righetti, P. G.; Gelfi, C., Electrophoresis Gel Media: The State of the Art. *J. Chromatogr. B Biomed. Sci. Appl.* **1997**, 699, (1-2), 63.
26. Righetti, P. G., Macroporous Gels: Facts and Misfacts. *J. Chromatogr. A* **1995**, 698, (1-2), 3.
27. Guinta, P. R. Fabrication and Characterization of Novel Nanocomposite Materials. Florida State University, 2005.
28. Guinta, P. R.; Washington, R. P.; Campbell, T. D.; Steinbock, O.; Stiegman, A. E., Preparation of Mesoporous Silica Monoliths with Ordered Arrays of Macrochannels Templated from Electric-Field Oriented Hydrogels. *Angew. Chem., Int. Ed. Engl.* **2004**, 43, 1505-1507.

29. Righetti, P. G.; Caglio, S.; Saracchi, M.; Quaroni, S., 'Laterally Aggregated' Polyacrylamide Gels for Electrophoresis. *Electrophoresis* **1992**, 10, 587-595.
30. Yu, S.; Chow, G. M., Carboxyl Group (-CO₂H) Functionalized Ferrimagnetic Iron Oxide Nanoparticles for Potential Bio-Applications. *J. Mater. Chem.* **2004**, 14, (18), 2781-2786.
31. Ende, M. T. A.; Peppas, N. A., Transport of Ionizable Drugs and Proteins in Crosslinked Poly(Acrylic Acid) and Poly(Acrylic Acid-co-2-Hydroxyethyl Methacrylate) Hydrogels.1. Polymer Characterization. *J. Appl. Polym. Sci.* **1996**, 59, (4), 673-685.
32. *Polymer Handbook*. 4 ed.; John Wiley and Sons, Inc.: New York, 1999.
33. Ho, B. C.; Lee, Y. D.; Chin, W. K., Thermal-Degradation of Polymethacrylic Acid. *J. Polym. Sci., Part A: Polym. Chem.* **1992**, 30, (11), 2389-2397.
34. Druzhinina, T. V.; Andrichenko, Y. D.; Erofeeva, I. V., Thermooxidation of Modified Polycaproamide Fibre Containing Graft Poly(Dimethylaminoethyl Methacrylate). *Fibre Chemistry* **2001**, 33, (3), 193-199.
35. Xiao, C. B.; Lu, Y. S.; Jing, Z. Z.; Zhang, L., Study on Physical Properties of Blend Films from Gelatin and Polyacrylamide Solutions. *J. Appl. Polym. Sci.* **2002**, 83, (5), 949-955.

Chapter 6: Investigation of Acrylamide-Based MIP Polymers as Drug Delivery Systems

Due to the high biocompatibility of the MIP polymers and their ability to recognize the lysozyme template, MIP polymers are considered to be a good means of delivering proteins as part of an implantable drug delivery system (IDDS). Thus, the loading and release of lysozyme from MIP polymers was investigated and quantified to determine if polymers exhibited sustained release of the protein and if the protein remained biologically active upon release

6.1 Introduction

Unfortunately, current drug delivery systems are often limited because they cannot respond directly to the need of a patient. Every person's physiology and pathological conditions vary slightly. Medical conditions also vary through the course of time, and many disease states often possess unpredictable episodes or unnoticeable symptoms that lead to catastrophic physiological effects.

The most predominant drug delivery methods are oral administration and injection, and although most drugs are currently formulated for this delivery, these methods are not always most efficient routes for a particular therapy. Thus, the development of numerous drugs has been limited. Injection suffers from low patient compliance and spikes in therapeutic levels that do not mimic physiological effects. Oral delivery is challenging due to breakdown of many

drugs in the intestinal tract by gastric enzymes and acids. Oral administration is especially challenging for biologic drugs such as proteins and nucleic acids which are highly susceptible to acid degradation. Thus many researchers are investigating IDDS systems as an alternative route of delivery.

Innovative drug delivery systems such as implantable controlled release devices may make it possible to use certain chemical entities or biologics that were previously impractical because of toxicities or because of administration limits. A greater therapeutic effect can also be obtained through implanted systems over conventional oral or injection routes. For example, bioerodible polymer systems have been used in the sustained delivery of chemotherapy agents directly to tumors, thus reducing systemic side effects and increasing dose effectiveness¹. In addition, researchers have had success delivering DNA and RNA therapies using IDDS².

In addition to improved dosage efficacy, IDDS offer additional advantages, such as better patient compliance. While conventional oral therapies can require administration of drugs multiple times a day, some of the implantable systems have been developed to deliver therapeutics over months or even years at a time and require minimal monitoring.

6.1.1 Hydrogels for Drug Administration

In addition to the commonly used oral and injection routes, drugs can also be administered through other means, including transdermal³, transmucosal⁴,

ocular⁵, pulmonary⁶, and implantation⁷. In all of these administration routes, polymers have been investigated as a possible platform for administration. Polymer materials exhibit several desirable properties for drug carrier use including biocompatibility, biodegradability, and functionalization capability. Through functionalization and structural manipulation of polymer materials, drug molecules can be incorporated within the polymer. Entrapping or encapsulating the drug within a polymer allows for greater control of the pharmacokinetic behavior of the active drug molecule. The drug can be released with a more ideal, near zero-order kinetic profile, which establishes a more constant flow of the drug out of the carrier. This pharmacokinetic behavior maintains more appropriate steady levels of the drug at the site of delivery.

In contrast, conventional oral drug delivery typically follows first-order release kinetics where the drug release rate is proportional to the amount of drug remaining in the drug carrier. Landgraf et al⁸ have compared the release kinetics of an anti-inflammatory agent taken orally by use of a macroporous copolymer carrier and a microporous copolymer carrier containing nanochannels. The macroporous drug carrier releases the drug with an initial burst and follows first-order release kinetics. The microporous carrier structured with nanochannels steadily releases the drug in near zero-order fashion.

6.1.2 Polymers with Ionic Functional Groups for Controlled Release

Recently, many groups have been focusing on changing the structure of polymers on the nanoscale in order to release macromolecules as part of an implantable system. In order to accomplish this result, the interactions between the polymer and macromolecule must be understood. For instance, all proteins carry an overall positive or negative charge due the chemical groups found on the amino acid sequence. Of the twenty naturally occurring amino acids found in proteins, five of them possess a charge under physiological pH values. Glutamic acid and aspartic acid are negatively charged and highly ionized at the near neutral pH values present in most biological systems *in vivo*. Lysine and arginine are positively charged and highly ionized, while histidine is positively charged (acidic) and weakly ionized. Thus, by introducing electrostatic functionalities into a polymer system, many groups hope to form weak interactions with these side groups and thus slow diffusion of the protein out of the network. This interaction can in turn cause a sustained, controlled release of the protein when part of an implantable drug delivery system.

Kwon et al.⁹ have been able to fabricate negatively charged microspheres that could be loaded with cationic proteins and drugs. Upon implantation, these polymers exhibited sustained release of therapeutic proteins. Jang and colleagues¹⁰ were able form PLGA microspheres that contained an MAA core. This MAA core was complexed via electrostatic interactions to insulin and

resulted in a sustained release *in vivo*. Of particular interest to our work are the hydrogels fabricated by Nakamae and colleagues¹¹⁻¹³ that have anionic phosphate groups that complex with the cationic protein lysozyme. With the introduction of phosphate groups, lysozyme loading is increased, and the subsequent release is sustained over a longer period of time. In addition, the lysozyme activity is retained in the lysozyme released from these polymers.

6.1.3 MIP Polymers as IDDS

Recently, MIP hydrogels have been investigated as carriers in IDDS. It is hypothesized that the imprinting effect not only increases loading of the drug into the polymer but also promotes an extended drug release compared to gels containing only electrostatic groups through the creation of cavities specific to the target drug. Sreenivasan has fabricated MIP polyurethane for ampicillin that can inhibit bacterial growth¹⁴. Ciardelli has investigated theophylline as a template as model for small molecule release^{15, 16} in clinical settings. Puoci et al have imprinted the colon-specific drug sulfasalazine, and shown sustained release of this drug as a possible IDDS¹⁷. New MIP contact lenses have shown sustained release of the blood-pressure drug timolol into the eye¹⁸⁻²⁰. In addition, sustained release of steroids^{21, 22} and other pain relievers²² have shown promise using MIP systems.

6.2 Materials and Methods

6.2.1 Loading of MIP Polymers with Lysozyme

MIP gels were fabricated as outlined in Section 3.2. Gels were lyophilized, ground, and sieved to obtain particles of 75-90 μm . The particles were then washed free of lysozyme template as outlined previously in Section 3.2. 25 mg of MIP polymers or control gels were then placed into 50 mL conical tubes containing 25 mL of a 1 mg/mL solution of lysozyme in Tris buffer (0.02M, pH 7.4). Tubes were placed on an orbital shaker for 24 hours to allow gel protein loading to reach equilibrium. Tubes were then centrifuged (5 min, 4000xg), and the supernatant was analyzed by UV-Vis spectroscopy at 280 nm. Polymer particles were lyophilized and stored at -20 °C under dessication until further use.

6.2.2 Release of Lysozyme from Hydrogels

25 mg of lysozyme loaded microparticles were placed into 50 mL tubes containing 25 mL of a Tris buffer solution (0.02M, pH 7.4) containing either 0 or 0.154M of NaCl. Tubes were again placed on an orbital shaker, and at various timepoints, the tubes were centrifuged (3 min, 4000xg). The supernatant was then analyzed by UV-Vis spectroscopy at 280 nm absorbance. Samples were then returned to the orbital shaker until the next timepoint.

6.2.3 Enzymatic Activity of Lysozyme Released

To measure the activity of lysozyme released, the loading and release studies were repeated as outlined in 6.2.1 and 6.2.2. When the release of

protein in ionized Tris buffer reached ~95% (as measured by UV-spectroscopy), 1 mL of solution was removed for the assay. In addition, a corresponding control lysozyme solution was made to match the lysozyme concentration that was released. Activity of released lysozyme and lysozyme in the control solution was measured using the EnzCheck® Lysozyme Assay Kit (Molecular Probes, Wisconsin). Fluorescent intensity was measured using a fluorescence microplate reader with standard fluorescein filters.

6.3 Results and Discussion

6.3.1 Lysozyme Loading in the Hydrogels

As shown previously in Chapter 4, the functional monomer present in the MIP polymers has a direct effect upon the recognition of the lysozyme template. For this reason, it is believed that the release of lysozyme will vary from formulation to formulation due changes in the ionic groups present across the polymer systems.

The amount of protein loaded, P_{loaded} (units of mg-protein / g-polymer), in the polymers was calculated by:

$$P_{\text{loaded}} = \frac{V(C_{\text{initial}} - C_{\text{equilibrium}})}{M_p} \quad (6.1)$$

where C_{initial} is the starting protein concentration, $C_{\text{equilibrium}}$ the final concentration of protein in supernatant after protein loading, V the volume of protein solution, and M_p the mass of polymer microparticles used.

Figure 6.1 shows the relationship between polymer composition and the amount of lysozyme loaded into the polymer. P(MAA-DMAEMA-Aam)MIP and P(MAA-Aam)MIP gels had the highest amount of loading at ~80.0 and 66.0 mg lysozyme/g polymer respectively. These results agree with the equilibrium loading experiments obtained in Chapter 4. Also in agreement were the results of loading P(DMAEMA) polymers, which showed the lowest amount of lysozyme loading. For lysozyme release, only polymers exhibiting the most loading of lysozyme—P(MAA-Aam) and P(MAA-DMAEMA-Aam)—were investigated.

6.3.2 Lysozyme Release from MIP Polymers

The MIP microparticles demonstrated an extended release time for lysozyme as compared to the control polymers when placed in only Tris buffer containing a biological ionic strength of 0.154M (Figure 6.2). Similarly, lysozyme loaded in the MIP microparticles is released at a slower rate than from the control polymers when placed only in Tris buffer with no salt, with less than 15% lysozyme released after 24 hours (Figure 6.3). The lysozyme release rates are slower in this experiment due to the absence of the salt. The presence of Na^+ and Cl^- ions compete with and ultimately displace the complexed protein, resulting in increased release at higher ionic strengths. Complexation between

ionic functional groups and lysozyme is supported by the extended release times of the protein from the MIP microparticles.

In all cases, slower release rates were observed in MIP polymers over control polymers, especially the P(MAA-DMAEMA-Aam)MIP. It is believed that the increased number of protein-polymer ionic interactions in the imprinted site leads to the slower release than the non-specific interactions that are found in the control. Water and ions in solution must overcome these interactions in order for the protein to release from the network. It is believed that the concentration of interactions in the imprinted sites leads to stronger complexation than the non-specific interactions that occur in control gels. In control gels, only a few functionalities are complexed with a lysozyme molecule, facilitating polar and ionic interactions from the environment to break these bonds. As such, the release rate is greater in control networks.

6.3.3 Ezymatic Activity of Released Lysozyme

In effective controlled release systems, the delivered agent must retain biological activity in order to achieve the desired therapeutic effect. This is especially important in drugs that require high dosages for efficacy. The activity of released lysozyme was measured using the EnzCheck® Lysozyme Assay Kit. This is a fluorescence based assay containing a suspension of fluorescently labeled *Micrococcus lysodeitikus*. The high concentration of fluorescent probe on the cell walls of these bacteria effectively quenches the dye. Lysozyme acting

on these bacteria will release the tag, and the resulting fluorescence can be measured using a microplate reader, with increasing fluorescent intensity corresponding to increased enzyme activity.

When the lysozyme activity of the protein that was initially loaded was compared to the lysozyme released from MIP gels, enzymatic activity was maintained (Table 6.1). In the P(MAA-Aam), approximately 95% of the activity was maintained, while in the P(MAA-DMAEMA-Aam)MIP the retained activity measured 90%. These results show the feasibility of using this system for the sustained release of biomacromolecules for the treatment of disease.

6.4 Conclusions

Lysozyme was successfully loaded and released from MIP hydrogel networks. In all cases, the MIP microparticles exhibited a slower, and thus more controlled, release rate of lysozyme over the control polymers. At a biological ionic strength, this release of lysozyme increased due to the competing effects of the solvating salt ions, but the lysozyme released retained enzymatic activity as detected by fluorescent assay. The successful loading and release of lysozyme from MIP polymer networks supports the idea that MIP networks can be used for the controlled release of macromolecules as part of a sustained DDS.

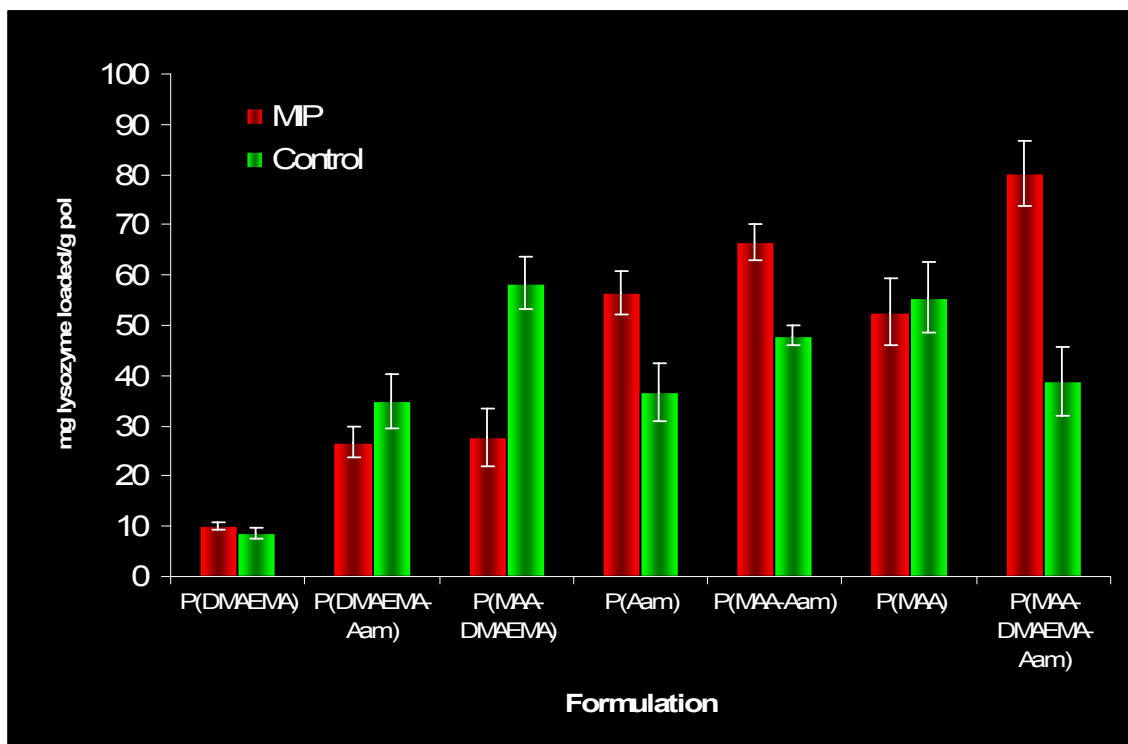


Figure 6.1: Equilibrium Lysozyme Loading in Polymer Microparticles

Microparticles were placed into solution containing a known concentration of lysozyme. After supernatant analysis, lysozyme loading was calculated. P(MAA-Aam)MIP and P(MAA-DMAEMA-Aam)MIP polymers displayed the greatest lysozyme loading. P(DMAEMA) gels displayed the least amount lysozyme loading.

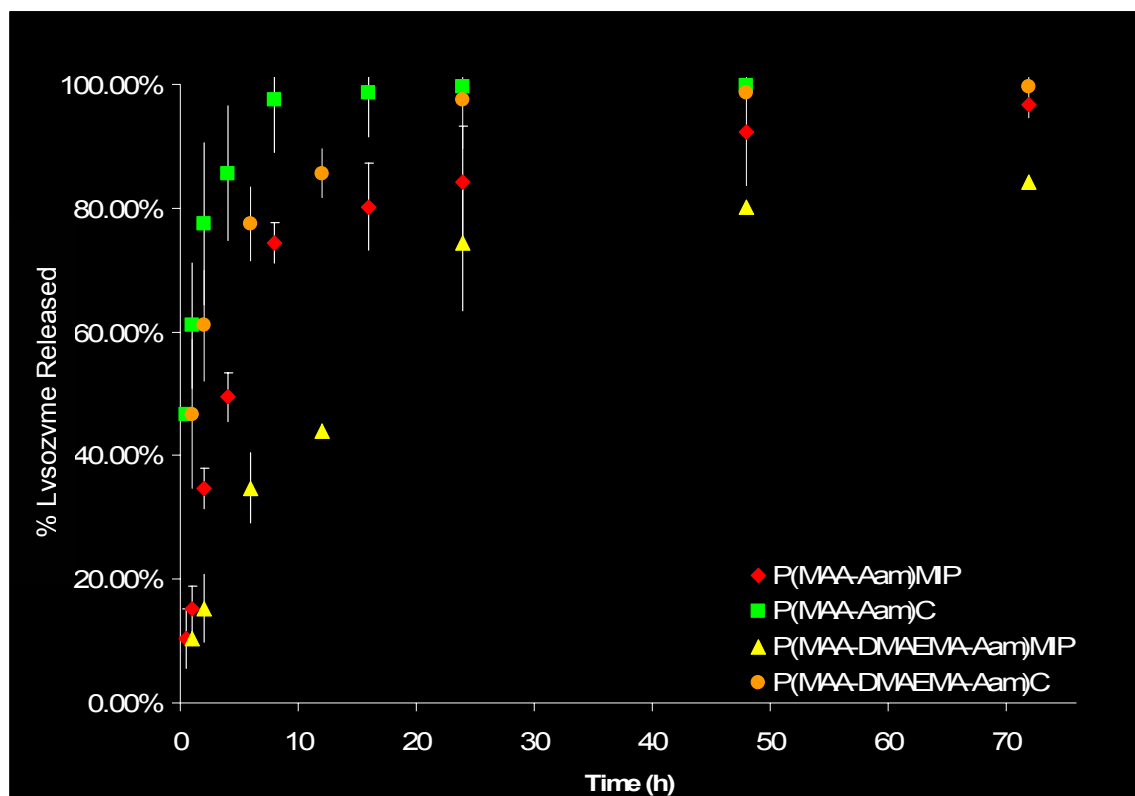


Figure 6.2: Lysozyme Release from Microparticles in ionized Tris Buffer (pH 7.4, 0.154M NaCl)

The presence of ions in the solution caused a greater release from microparticles. The MIP polymers also exhibited a slower release of lysozyme than controls. This supports the theory of imprinted sites that have a high specificity for the lysozyme template. In contrast, the control gels exhibited a rapid release, which supports the conclusion of non-specific binding.

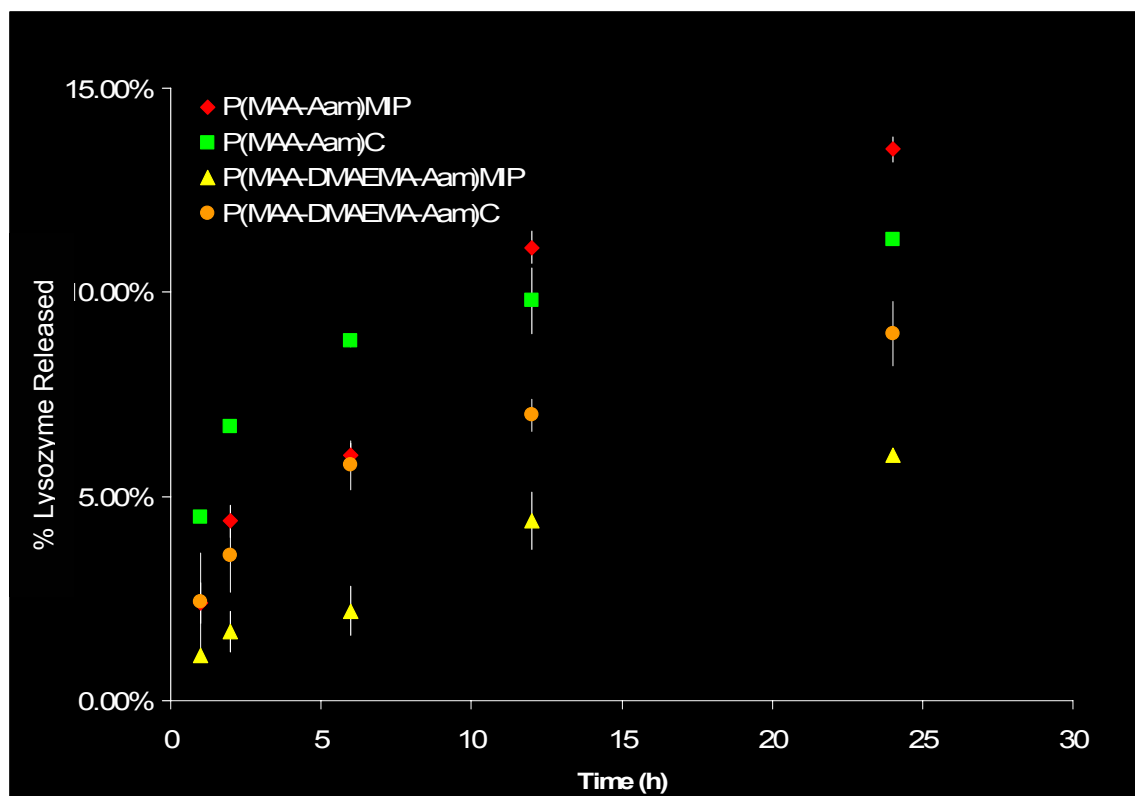


Figure 6.3: Lysozyme Release from Microparticles in Tris Buffer (pH 7.4, 0.02M)
 Microparticles carrying lysozyme exhibited a slower release of lysozyme in the absence of ions. After 24 h, less than 15% of lysozyme is released into solution across all formulations.

	Initial Lysozyme Activity (U/mg lysozyme)	Remaining Activity (U/mg lysozyme)	% Activity Maintained
P(MAA-Aam)MIP	876 \pm 45	837 \pm 36	95.6%
P(MAA-DMAEMA-Aam)MIP	943 \pm 134	845 \pm 99	89.6%

Table 6.1: Enzymatic Activity Retained upon Lysozyme Release from MIP Polymers into 0.154M Tris Buffer.

High Enzymatic Activity was maintained in both MIP formulations.

6.5 References Cited

1. El-Aneel, A., An Overview of Current Delivery Systems in Cancer Gene Therapy. *J. Controlled Release* **2004**, 94, (1), 1.
2. Bradbury, J., Beyond Pills and Jabs. *The Lancet* **2003**, 362, (9400), 1984.
3. Karande, P.; Jain, A.; Ergun, K.; Kispersky, V.; Mitragotri, S., Design Principles of Chemical Penetration Enhancers for Transdermal Drug Delivery. *Proc. Natl. Acad. Sci. U.S.A.* **2005**, 102, (13), 4688-4693.
4. Jose Alonso, M., Nanomedicines for Overcoming Biological Barriers. *Biomed. Pharmacother.* **2004**, 58, (3), 168.
5. Calvo, P.; Vila-Jato, J. L.; Alonso, M. J., Evaluation of Cationic Polymer-Coated Nanocapsules as Ocular Drug Carriers. *Int. J. Pharm.* **1997**, 153, (1), 41.
6. Cook, R. O.; Pannu, R. K.; Kellaway, I. W., Novel Sustained Release Microspheres for Pulmonary Drug Delivery. *J. Controlled Release* **2005**, 104, (1), 79.
7. Davis, M. P.; Walsh, D.; Lagman, R.; LeGrand, S. B., Randomized Clinical Trial of an Implantable Drug Delivery System. *J. Clin. Oncol.* **2003**, 21, (14), 2800-2801.
8. Landgraf, W.; Li, N. H.; Benson, J. R., Polymer Microcarrier Exhibiting Zero-Order Release. *Drug Delivery Technology* **2003**, 3.

9. Kwon, G. S.; Bae, Y. H.; Cremers, H.; Feijen, J.; Kim, S. W., Release of Proteins Via Ion Exchange from Albumin-Heparin Microspheres. *J. Controlled Release* **1992**, 22, (2), 83.
10. Jiang, H. L.; Jin, J. F.; Hu, Y. Q.; Zhu, K. J., Improvement of Protein Loading and Modulation of Protein Release from Poly(Lactide-co-Glycolide) Microspheres by Complexation of Proteins with Polyanions. *J. Microencapsul.* **2004**, 21, (6), 615-624.
11. Kato, K.; Furukawa, M.; Kanzaki, Y.; Hoffman, A. S.; Nakamae, K., Lysozyme Loading in Phosphate Carrying Hydrogels at High Density and the Controlled Release of Lysozyme. *Kobunshi Ronbunshu* **1998**, 55, (6), 353-358.
12. Nakamae, K.; Nizuka, T.; Miyata, T.; Furukawa, M.; Nishino, T.; Kato, K.; Inoue, T.; Hoffman, A. S.; Kanzaki, Y., Lysozyme Loading and Release from Hydrogels Carrying Pendant Phosphate Groups. *J. Biomater. Sci. Polym. Ed.* **1997**, 9, (1), 43-53.
13. Nakamae, K.; Nishino, T.; Kato, K.; Miyata, T.; Hoffman, A. S., Synthesis and Characterization of Stimuli-Sensitive Hydrogels Having a Different Length of Ethylene Glycol Chains Carrying Phosphate Groups: Loading and Release of Lysozyme. *J. Biomater. Sci. Polym. Ed.* **2004**, 15, (11), 1435-1446.
14. Sreenivasan, K., Surface-Imprinted Polyurethane Having Affinity Sites for Ampicillin. *Macromol. Biosci.* **2005**, 5, (3), 187-191.

15. Ciardelli, G.; Cioni, B.; Cristallini, C.; Barbani, N.; Silvestri, D.; Giusti, P., Acrylic Polymeric Nanospheres for the Release and Recognition of Molecules of Clinical Interest. *Biosens. Bioelectron.* **2004**, 20, (6), 1083-1090.
16. Silvestri, D.; Borrelli, C.; Giusti, P.; Cristallini, C.; Ciardelli, G., Polymeric Devices Containing Imprinted Nanospheres: A Novel Approach to Improve Recognition in Water for Clinical Uses. *Anal. Chim. Acta* **2005**, 542, (1), 3.
17. Puoci, F.; Iemma, F.; Muzzalupo, R.; Spizzirri, U. G.; Trombino, S.; Cassano, R.; Picci, N., Spherical Molecularly Imprinted Polymers (SMIPs) Via a Novel Precipitation Polymerization in the Controlled Delivery of Sulfasalazine. *Macromol. Biosci.* **2004**, 4, (1), 22.
18. Hiratani, H.; Fujiwara, A.; Tamiya, Y.; Mizutani, Y.; Alvarez-Lorenzo, C., Ocular Release of Timolol from Molecularly Imprinted Soft Contact Lenses. *Biomaterials* **2005**, 26, (11), 1293.
19. Hiratani, H.; Alvarez-Lorenzo, C., The Nature of Backbone Monomers Determines the Performance of Imprinted Soft Contact Lenses as Timolol Drug Delivery Systems. *Biomaterials* **2004**, 25, (6), 1105.
20. Hiratani, H.; Alvarez-Lorenzo, C., Timolol Uptake and Release by Imprinted Soft Contact Lenses Made of N,N-Diethylacrylamide and Methacrylic Acid. *J. Controlled Release* **2002**, 83, (2), 223.

21. Allender, C. J.; Richardson, C.; Woodhouse, B.; Heard, C. M.; Brain, K. R., Pharmaceutical Applications for Molecularly Imprinted Polymers. *Int. J. Pharm.* **2000**, 195, (1-2), 39.
22. Suedee, R.; Srichana, T.; Rattananont, T., Enantioselective Release of Controlled Delivery Granules Based on Molecularly Imprinted Polymers. *Drug Delivery* **2002**, 9, (1), 19-30.

Chapter 7: Investigation of Cytocompatibility of Acrylamide-Based MIP Polymers

7.1 Introduction

When designing biomaterials, it is important that the material exhibit biocompatibility when in contact with cells and tissues of the body. The materials should show a low level of toxicity while not causing a systemic rejection from the immune system. In addition, they should exhibit cytocompatibility by causing no lysis of cell membranes or cell toxicity. One of the most widely used tools to initially screen the feasibility of using polymers as biomaterials are *in vitro* assays utilizing cellular models.

7.1.1 Advantages of *in vitro* Studies.

In vitro studies offer a number of advantages over *in vivo* studies when initially determining suitable biomaterials. Because they involve cell cultures rather than animal studies, *in vitro* studies are much less expensive to perform, and the results can be obtained much more rapidly. The test material can be placed in direct contact with cells in culture, and the amount of material can also be controlled. In addition, a higher level of control of environmental factors over the course of the experiment is possible. This means the material can be examined in isolation from secondary factors that can cloud results because of variability between experiments. Factors that can be controlled include metabolic

activity, changes in pH, and changes in temperature. In this way, *in vitro* tests for cytocompatibility can provide valuable information about the initial suitability of a biomaterial.

7.1.2 Swiss 3T3 Fibroblasts and *in vitro* Cell Culture

Fibroblasts were one of the first cell lines to be cultured from vertebrate animals and, as a result, are one of the most widely utilized cell types in many cell culture studies. Fibroblasts are cells that secrete collagen, glycoproteins, glycosaminoglycans, and other ECM materials. This secretion gives rise to mesodermal tissue. Most fibroblasts develop into connective tissues such as muscles, ligaments, and tendons, but some can differentiate to become adipose tissue depending on phenotype. In culture, fibroblasts are amoeboid with branched cytoplasmic structures and a speckled nucleus (Figure 7.1).

Most studies involving fibroblasts have revolved around the study of a cell line termed the Swiss 3T3 cell line. This line was established by Todaro and Green in 1963 from disaggregated tissue of an albino Swiss mouse (*Mus musculus*) embryo¹. The 3T3 component of the name for this cell line is derived from the conditions of plating density and subculture frequency². The form of the name comes in “xTy” where “x” is the number of days between subculturing (3) and “y” is the number of cells needed for passaging in units of 10^5 cells.

Todaro and Green discovered that from passage to passage, these cells showed little change in morphology and adhesion characteristics. In addition,

these cell lines were shown to be virtually immortal from passage to passage. The cells also can be considered to be clones of each other because they do not differentiate to other tissue types³. For these reasons, 3T3 cell lines are invaluable cells for cytocompatibility assays, as the cellular characteristics can be expected to be passage independent and uniform through repeat experiments.

7.2 Materials and Methods

7.2.1 Handling Procedure for Frozen Cells

In vitro experiments were done using an NIH/3T3 murine fibroblast cell line (#CRL-1658; American Type Culture Collection (ATCC), Manassas, VA). Cells were cultured in Dulbecco's modified Eagle's medium (DMEM) with 4 mM L-glutamine adjusted to contain 1.5 g/L sodium bicarbonate and 4.5 g/L glucose (ATCC). Media was also supplemented with 10% fetal calf serum (ATCC). Until needed, the frozen cell culture was stored in the vapor phase of liquid nitrogen. When required, the cell culture vial was thawed via gentle agitation in a 37°C water bath, with a thawing time of approximately two minutes. While thawing, care was taken to keep the O-ring and cap of the vial above the water level of the bath, minimizing the possibility of cell contamination. Once the vial contents were thawed, the vial was removed from the water bath and decontaminated by dipping it in 70% ethanol solution. At this stage, all further steps were done under strictly aseptic conditions.

The vial contents were then transferred to a centrifuge tube containing 9.0 milliliters of DMEM. This mixture was spun at approximately 125 xg for 5 to 7 minutes. After aspirating the media, the resulting cell pellet was then resuspended with the complete growth medium using the culture recommended dilution ratio for each specific batch and dispensed into a 25 cm² or a 75 cm² culture flask. Before the cell pellet was added, the culture flask charged with the appropriate amount of complete growth medium was placed in the incubator for at least 15 minutes to establish the optimal pH range (7.0 – 7.6). The culture was then incubated at 37°C in a 95% humidified and 5% CO₂ atmosphere.

7.2.2 Subculturing Procedure:

After reaching ~70% confluency, the cells were ready for subculturing. During this procedure, the flask culture was removed from the incubator, and the culture medium was aspirated off as waste. The cell layer was then briefly rinsed with Dulbeccos Phosphate Buffered Saline without CaCl₂ and MgCl₂ (DPBS, Sigma, St. Louis, MO) solution to remove any remains of trypsin inhibitor containing serum. Two to three milliliters of 0.25% (w/v) Trypsin-0.53mM EDTA (Sigma) solution were added to the flask. The cells flasks were left alone for 5 to 10 minutes until the cell layer was dispersed as viewed under an inverted microscope. If the cells were not detached, the flasks were incubated to facilitate the process.

Upon cell detachment, 8 mL of DMEM were added, and the cells were gently aspirated via pipetting to break up cell clumps and detach remaining cells. A standard cell count was performed using a hemocytometer. The suspension was then centrifuged at 150xg for 5min. Upon completion, the remaining Trypsin/EDTA containing liquid was then aspirated off of the resulting cell pellet and replaced with fresh media to give a cell concentration of $3\text{-}5 \times 10^3 \text{ cell/cm}^2$. Appropriate aliquots of the cell suspension were then added to new 25 cm² or 75 cm² culture flasks. The culture flasks were incubated at 37°C under a 95% humidity and 5% CO₂ atmosphere. Care was taken to ensure that the subculturing was done at 80% confluency or less. Figure 7.2 shows fibroblasts in culture as reproduced from ATCC. The picture on the left shows cells 1 day after passaging. The image on the right shows cells at ~70% confluency and ready for subculturing. The subculture procedure was repeated approximately every third day.

7.2.3 Medium Renewal

Medium was renewed every two days. To replenish the media, used DMEM was aspirated from the flask, and 10 mL of DPBS was added. The culture flask was gently swirled to ensure removal of dead cells and leftover media. The liquid was again aspirated, and 10 mL of fresh DMEM was added.

7.2.4 Cryopreservation of 3T3 cell lines

Cells were trypsinized and counted as outlined previously. Using DMEM containing 5% (v/v) dimethylsulfoxide (DMSO, Sigma), cells were resuspended to give a cell concentration of 1.5×10^6 cells/mL. The cell suspension was then pipetted in 2 mL aliquots into cryovials. Vials were then placed into a 5100 Cryo 1°C Freezing Container (Wessington Cryogenics, Philadelphia) containing isopropyl alcohol and cooled at -1°C per min in a -80°C refrigerator overnight. Vials were then transferred to a liquid nitrogen storage unit for long-term storage.

7.2.5 Cytotoxicity Evaluation

Control and MIP microparticles were fabricated as outlined previously. Cytotoxicity studies were conducted in 96 well plates when cells reached ~90% confluency or above (3-4 days). Cell studies were performed between passages 5-10. Media was refreshed 12 hours before the experiment. At the start of the experiment, the growth medium was removed from each well. MIP microparticles were added to wells at concentrations of 0.25 mg/mL, 0.5 mg/mL, and 1.0 mg/mL suspended in DMEM. Prior to addition, the pH of each suspension was adjusted to 7.4 with NaOH. Microparticles were then incubated with the cells for either 4 or 24 hours at 37°C and 5% CO₂. The microparticle suspension was removed from each well, and the wells were rinsed three times with 200 µL Hanks Balanced Salt Solution (HBSS, Sigma) to remove

microparticles and residual phenol red, for this indicator can interfere the absorbance readings of the assay.

Cytotoxicity was measured using CellTiter 96[®] AQueous One Solution Cell Proliferation Assay (Promega, Madison, WI). This method is a cellular metabolic assay used to measure NADPH production to give an accurate count of viable cells⁴. This assay contains a tetrazolium compound, 3-(4,5-dimethylthiazol-2-yl)-5-(3-carboxymethoxyphenyls)-2-(4-sulfophenyl)-2H-tetrazolium) (MTS), and an electron coupling reagent, phenazine ethosulfate (PES). The MTS reagent is bio-reduced by cells in culture to produce a colored formazan that is released into DMEM. It is believed the mechanism of reduction is achieved by NADPH contained in dehydrogenase enzymes from metabolically active cells (Figure 7.3). The absorbance of the formazan can then be read via a plate reader and corresponded to the viable number of cells (Figure 7.4).

In 10 mL of HBSS, 2 mL of assay reagent was suspended. Then, 120 µL of the solution was added to each well and incubated with the cells for 1.5 hours at 37 °C and 5% CO₂. A UV/vis microplate reader (Bio-Tek Synergy HT, Winooski, VT) was then used to determine the absorbance in each well at 490 nm. To determine cell viability, absorbance was compared to control wells that were not incubated with microparticles but only with HBSS and the CellTiter 96[®] reagent. Background absorbance of control wells containing only cells and

HBSS was subtracted from the results. A 10% bleach solution was used as a negative control.

7.3 Results and Discussion

When absorbances of the microplates were read, it was found that no toxicity was exhibited by any of the polymer formulations. At both time points, cells were still viable (>85%) and showed no statistically significant change in absorbance when compared to controls (Figure 7.5, Figure 7.6). Wells containing bleach retained very little cell viability, as expected. These results are in accordance with other published data utilizing these studies as biomaterials, where no toxicity was shown to fibroblasts at comparable amounts. In addition, when imaged under an inverted microscope, cells retained the same morphology (Figure 7.7) as compared to cells under normal culture conditions (Figure 7.8). Although timepoints must be extended, these results are encouraging towards the use of these polymers as biomaterials.

7.4 Conclusions

MIP polymer formulations exhibited little cytotoxicity to the 3T3 fibroblast cell line. These results were in agreement with previously published data on using these materials in the human body. Although other cell lines must be studied, the low toxicity of these polymers at the chosen concentrations is encouraging.

7.5 Figures

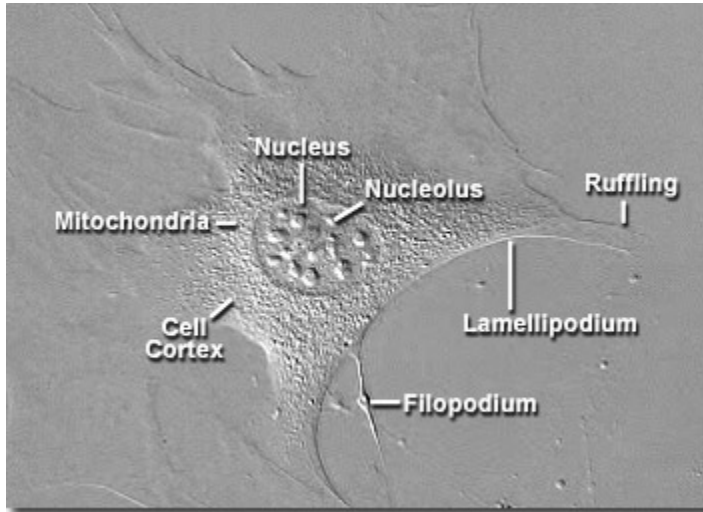
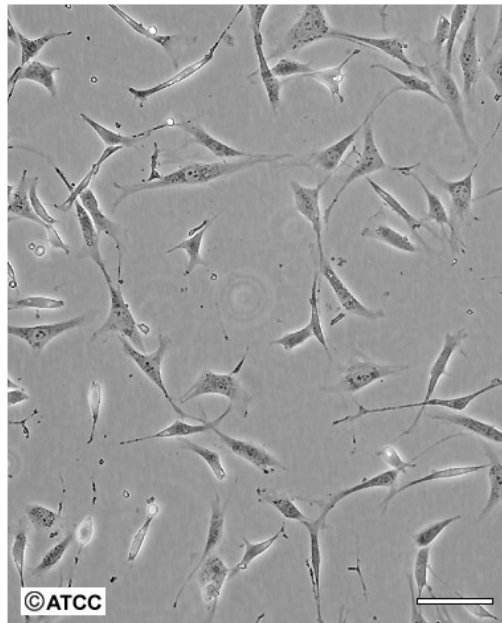


Figure 7.1: Major Structures of Fibroblast cells

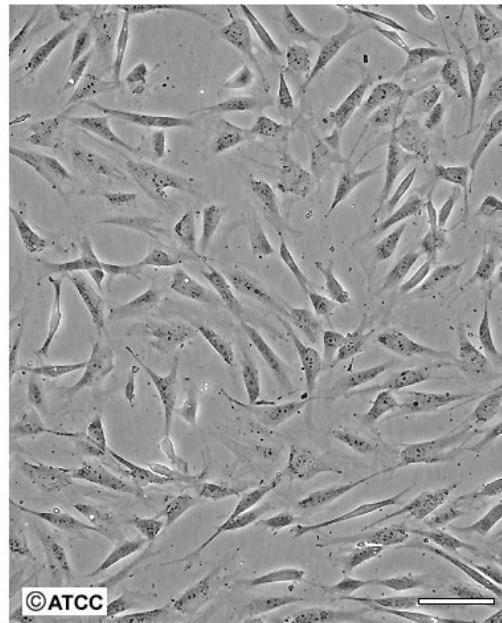
Live image of a 3T3 mouse fibroblast. Image reproduced from Nikon Online Digital Image Gallery⁵.

ATCC Number: **CRL-1658**
Designation: **NIH/3T3**



Low Density

Scale Bar = 100µm



High Density

Scale Bar = 100µm

Figure 7.2: Swiss 3T3 Cells in Culture

Inverted microscope images showing NIH/3T3 fibroblasts at 1 day (left) and 3 days in culture (right). Image reproduced from ATCC.org⁶.

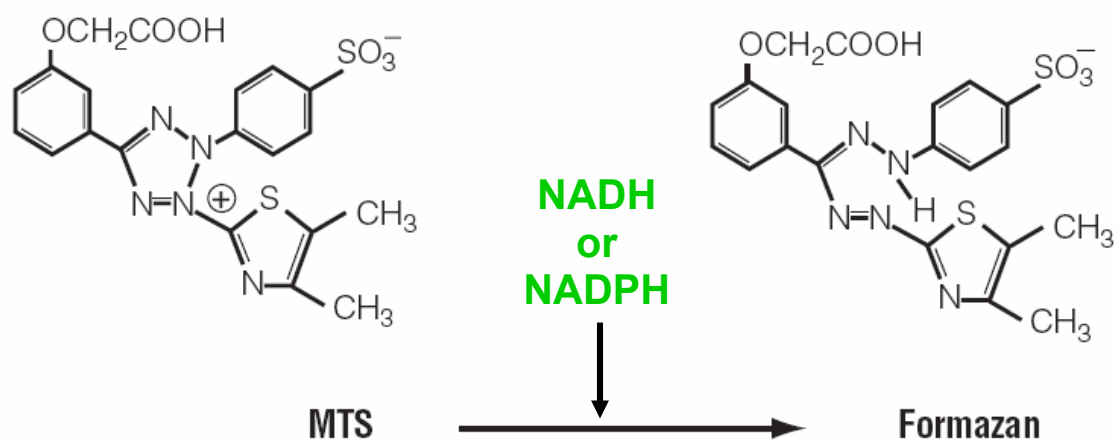


Figure 7.3: MTS Tetrazolium Salt and Its Reduction to Formazan.
 Figure modified from Promega Technical Bulletin⁴.

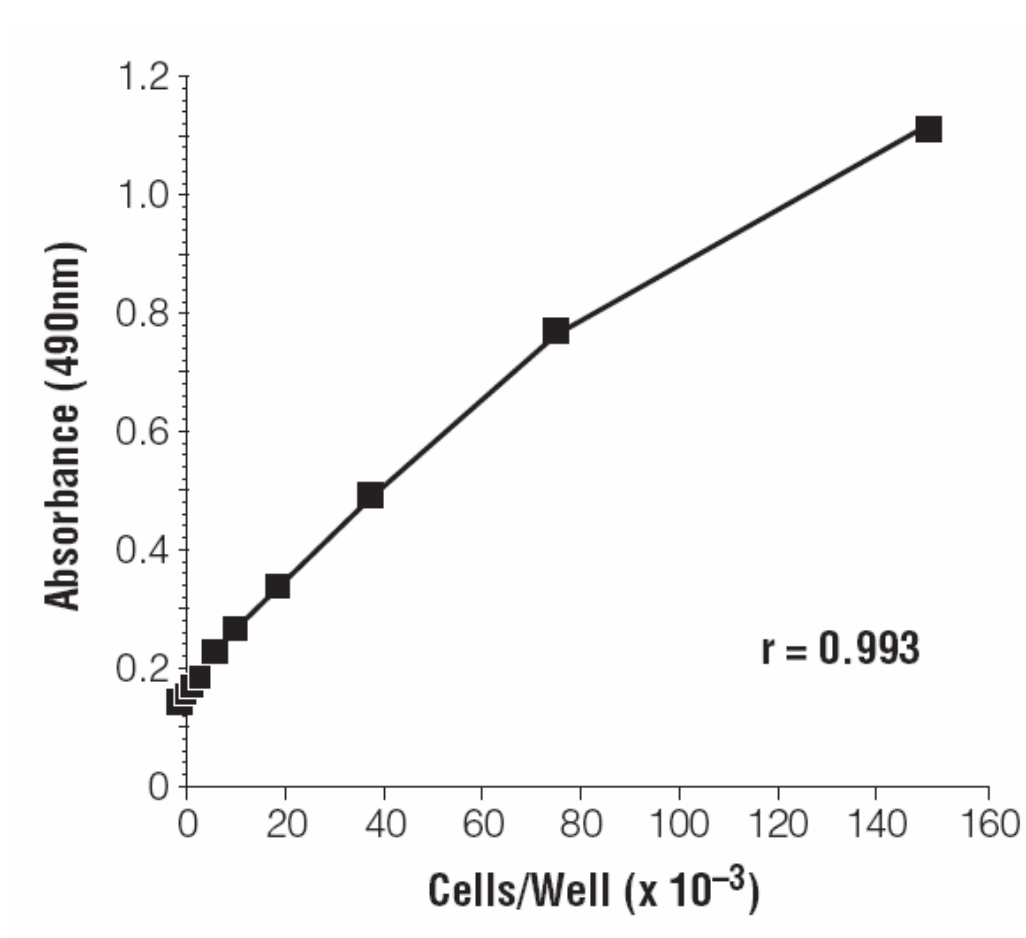


Figure 7.4: Corresponding Increase in Absorbance as an Indicator of Cell Number.
Figure reproduced from Promega⁴.

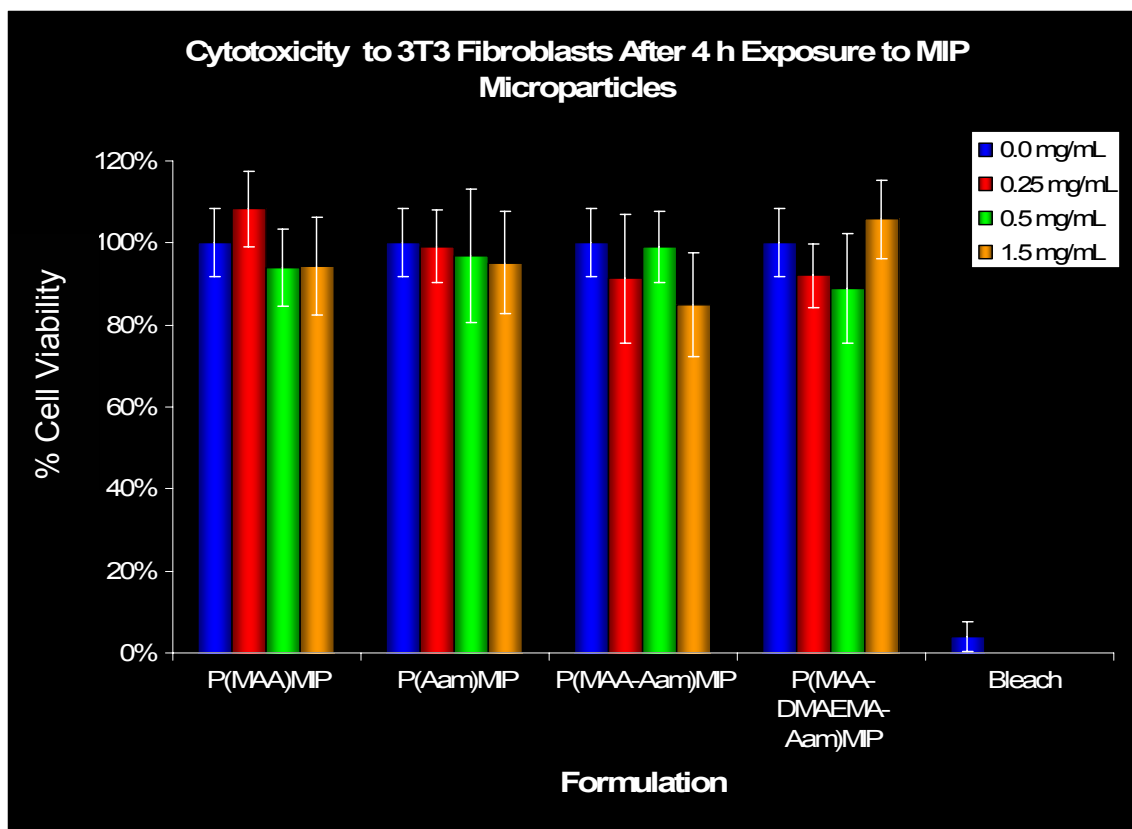


Figure 7.5: Cytotoxicity of MIP polymers to 3T3 fibroblasts after 4h

Enzymatic activity of 3T3 cells after exposure to MIP microparticles and bleach. Results are expressed as the percentage of absorbance at 490 nm for a given microparticle concentration as compared to control wells containing only cells and HBSS. Cell viability was maintained across all concentrations and formulations.

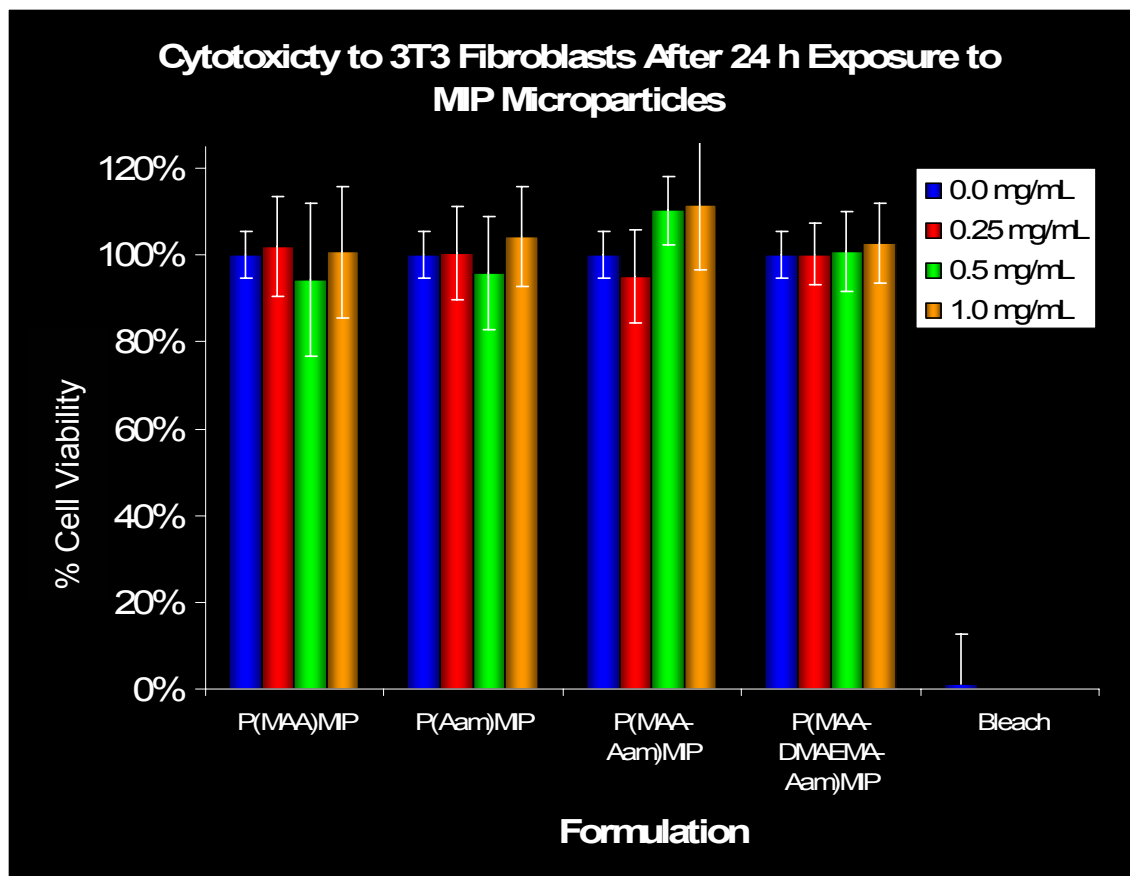


Figure 7.6: Cytotoxicity of MIP polymers to 3T3 fibroblasts after 24h.

Enzymatic activity of 3T3 cells after exposure to increasing concentrations of MIP microparticles and 10% bleach. Results are expressed as the percentage of absorbance at 490 nm for a given microparticle concentration as compared to control wells containing only cells and HBSS. Cell viability was maintained across all concentrations and formulations.

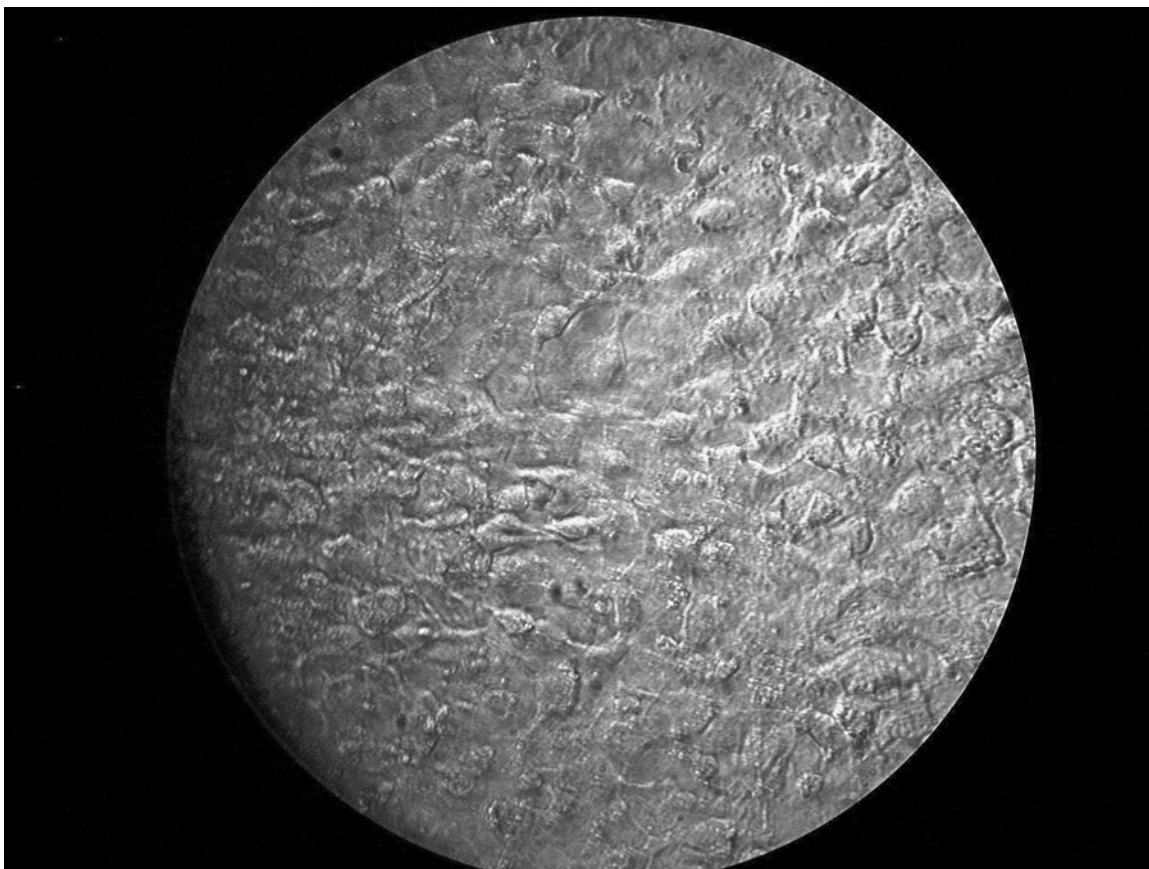


Figure 7.7: Morphology of 3T3 Cells after 24 h contact with P(MAA-DMAEMA-Aam)MIP Polymer

Inverted microscope image showing morphology of fibroblast cells after 24 h contact with poly(MAA-DMAEMA-Aam) MIP microparticles. Cells exhibited normal fibroblast morphology.

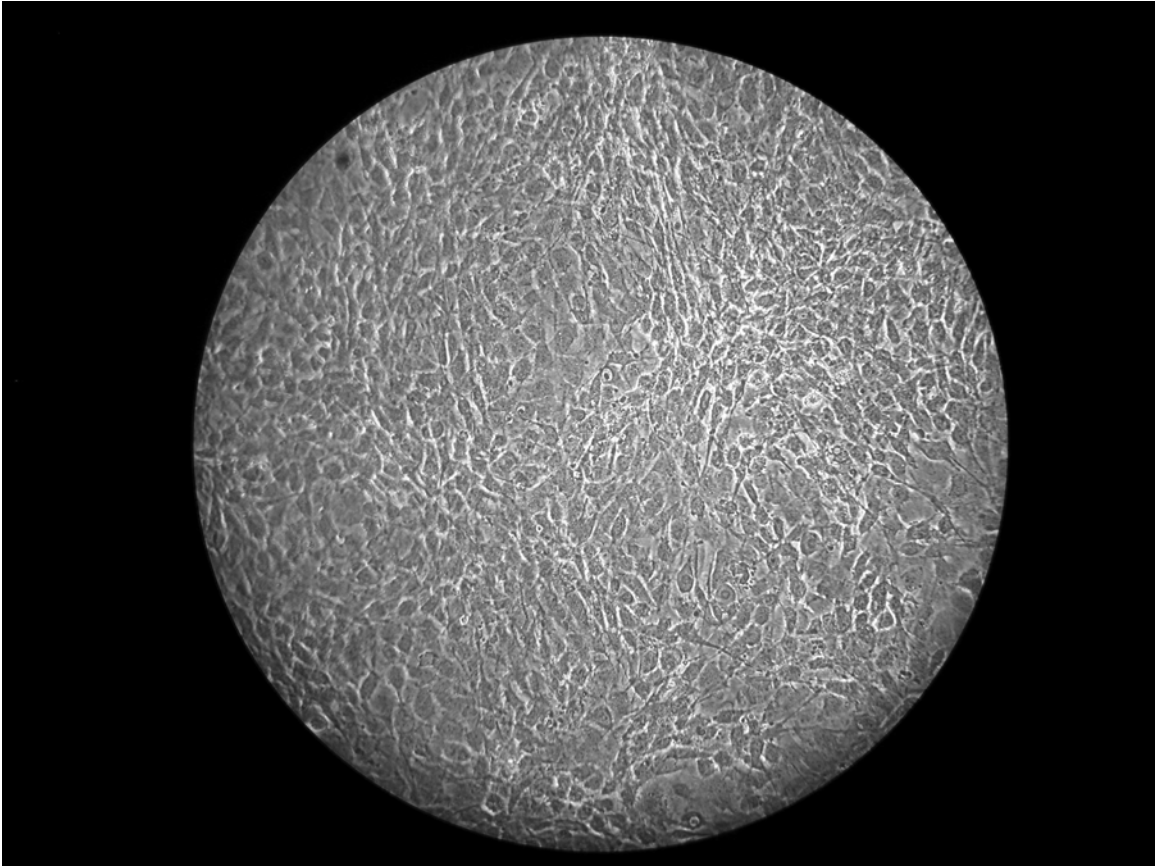


Figure 7.8: Inverted Microscope Image of Confluent 3T3 Fibroblasts after 5 Days in Culture.

7.6 References Cited

1. Todaro, G. J.; Green, H., Quantitative Studies of the Growth of Mouse Embryo Cells in Culture and Their Development into Established Lines. *J. Cell Biol.* **1963**, 17, (2), 299-313.
2. Mansbridge, J., Dermal Fibroblasts. In *Primary Mesenchymal Cells*, Koller, M. R.; Palsson, B.; Masters, J. R. W., Eds. Kluwer Academic Publishers: Boston, 2001; Vol. 5, pp 125-172.
3. Rittling, S. R., Clonal Nature of Spontaneously Immortalized 3T3 Cells. *Exp. Cell Res.* **1996**, 229, (1), 7.
4. Promega, Celltiter 96® AQueous One Solution Cell Proliferation Assay, *Technical Bulletin*. **2005**.
5. Nikon, Albino Swiss Mouse Embryo Fibroblasts (3T3 Line). <http://www.microscopyu.com/moviegallery/livecellimaging/3t3/> **2005**.
6. ATCC, Fibroblast Morphology. http://www.atcc.org/common/images/Cells/CRL-1658_mg1.jpg **2005**.

Chapter 8: Conclusions

As the depth and breadth of our society's current biomedical knowledge expands, the need for biocompatible materials that can be easily tailored to specific applications becomes readily apparent. To this end, the field of molecular imprinting in polymers has garnered more attention, as MIP polymers have shown a singular ability to be both sensitive to and selective for their target molecules. Much research has been done involving MIPs using small molecules as the templates, but less focus has been placed on using larger, more complex templates such as proteins due to such factors as inherent diffusion limitations of larger molecules and the sensitive structure/function relationship of proteins. If these factors can be overcome, applying MIP technology to proteins can have an immediate impact in the area of protein therapy, useful to treat such medical conditions as liver disease, cancer, and HIV. Because these MIPs are selective for their target protein, these polymers could also be used to filter the body of "bad" proteins, such as the incorrectly folded, infectious proteins that cause mad cow disease.

This study demonstrates the successful synthesis of crosslinked hydrogels containing various functional monomers—methacrylic acid, acrylamide, and dimethylaminoethyl methacrylate—that recognized the immunoprotein lysozyme. The specific combination of monomers was studied to determine which formulation induced the best recognition of lysozyme. The amount of

crosslinking was also investigated to produce hydrogels that maintained their physical integrity and yet allowed for sufficient diffusion of the macromolecule lysozyme.

These polymers, regardless of the specific formulation, did not demonstrate any cytotoxicity effects, indicating their biocompatible nature. In addition, the uptake of lysozyme was studied to ascertain their protein loading capabilities. The resulting protein release times were determined for both the MIPs and the control polymers, demonstrating a slower, and hence more controlled, release rate of the protein from the MIPs—a useful feature in the protein therapy realm. In addition, the released lysozyme showed no loss in function; thus, the polymer-protein interactions do not affect the structure of the target proteins.

These materials were also studied via several characterization techniques to better understand their properties. SEM was used to study the porosity and microscopic features of the MIPs. The SEM images showed that the presence of the template protein had an effect on the polymerization, forming a more porous and structured polymer as compared to the controls. FTIR was used to confirm the presence of each of the monomers in the copolymer formulations as well as to demonstrate the fact that the MIPs and control polymers are chemically identical. DSC was used to determine the glass transition temperatures of the crosslinked hydrogels and, from such information, the effective molecular weight

between crosslinks. These values were compared to the theoretical molecular weight between crosslinks to ensure the validity of the observed T_g values.

Thus, this study showed the successful creation of biocompatible MIPs that demonstrate a controlled release of the target protein. Considering that many proteins are charged entities, this technique could be readily expanded to additional proteins—especially those of therapeutic value—by simply manipulating the functional monomer ratios to provide the best selectivity and sensitivity and the crosslinking ratio to provide the best diffusional characteristics. In addition, these MIP microparticles can be anchored into another hydrogel by adding them to another hydrogel polymerization mixture, thus allowing these MIPs to be formed into different shapes and sizes. Thus, these MIPs could be made into discs (or some other solid shape) and placed at the site of the protein therapy—for instance, in close proximity to a tumor to fight cancer or near the liver to fight liver disease—to allow for a controlled release of the protein near the target organ, increasing the efficacy of the therapy.

All References Cited

1. *Polymer Handbook*. 4 ed.; John Wiley and Sons, Inc.: New York, 1999.
2. Adhikari, B.; Majumdar, S., Polymers in Sensor Applications. *Progress In Polymer Science* **2004**, 29, (7), 699-766.
3. Allender, C. J.; Richardson, C.; Woodhouse, B.; Heard, C. M.; Brain, K. R., Pharmaceutical Applications for Molecularly Imprinted Polymers. *Int. J. Pharm.* **2000**, 195, (1-2), 39.
4. Alvarez-Lorenzo, C.; Concheiro, A., Molecularly Imprinted Polymers for Drug Delivery. *J. Chromatogr. B Analyt. Technol. Biomed. Life Sci.* **2004**, 804, (1), 231-245.
5. Alvarez-Lorenzo, C.; Guney, O.; Oya, T.; Sakai, Y.; Kobayashi, M.; Enoki, T.; Takeoka, Y.; Ishibashi, T.; Kuroda, K.; Tanaka, K.; Wang, G. Q.; Grosberg, A. Y.; Masamune, S.; Tanaka, T., Polymer Gels That Memorize Elements of Molecular Conformation. *Macromolecules* **2000**, 33, (23), 8693-8697.
6. Alvarez-Lorenzo, C.; Guney, O.; Oya, T.; Sakai, Y.; Kobayashi, M.; Enoki, T.; Takeoka, Y.; Ishibashi, T.; Kuroda, K.; Tanaka, K.; Wang, G. Q.; Grosberg, A. Y.; Masamune, S.; Tanaka, T., Reversible Adsorption of Calcium Ions by Imprinted Temperature Sensitive Gels. *J. Chem. Phys.* **2001**, 114, (6), 2812-2816.
7. Alvarez-Lorenzo, C.; Hiratani, H.; Tanaka, K.; Stancil, K.; Grosberg, A. Y.; Tanaka, T., Simultaneous Multiple-Point Adsorption of Aluminum Ions and Charged Molecules a Polyampholyte Thermosensitive Gel: Controlling Frustrations in a Heteropolymer Gel. *Langmuir* **2001**, 17, (12), 3616-3622.

8. Alvarez-Lorenzo, C. H., H.; Gomez-Amoza, J.L.; Martinez-Pacheco, R.; Souto, C.; Concheiro, A., Soft Contact Lenses Capable of Sustained Delivery of Timolol. *J. Pharm. Sci.* **2002**, 91, (10), 2182.
9. Andersson, L.; Lunden, R., The Composition of Human Plasma. In Blomback, B.; Hanson, L., Eds. John Wiley and Sons: Bath, Great Britain, 1979; pp 17-21.
10. Ansell, R. J.; Kriz, D.; Mosbach, K., Molecularly Imprinted Polymers for Bioanalysis: Chromatography, Binding Assays and Biomimetic Sensors. *Curr. Opin. Biotechnol.* **1996**, 7, (1), 89-94.
11. Ansell, R. J.; Ramstrom, O.; Mosbach, K., Towards Artificial Antibodies Prepared by Molecular Imprinting. *Clin. Chem.* **1996**, 42, (9), 1506-1512.
12. Anseth, K. S.; Shastri, V. R.; Langer, R., Photopolymerizable Degradable Polyanhydrides with Osteocompatibility. *Nature Biotechnology* **1999**, 17, (2), 156-159.
13. Arshady, R.; Mosbach, K., Synthesis of Substrate-Selective Polymers by Host-Guest Polymerization. *Macromolecular Chemistry and Physics-Makromolekulare Chemie* **1981**, 182, (2), 687-692.
14. ATCC, Fibroblast Morphology. http://www.atcc.org/common/images/Cells/CRL-1658_mg1.jpg **2005**.
15. Bao, G., Mechanics of Biomolecules. *Journal Of The Mechanics And Physics Of Solids* **2002**, 50, (11), 2237-2274.

16. Bashir, R.; Hilt, J. Z.; Elibol, O.; Gupta, A.; Peppas, N. A., Micromechanical Cantilever as an Ultrasensitive pH Microsensor. *Appl. Phys. Lett.* **2002**, 81, (16), 3091-3093.
17. Beebe, D. J.; Moore, J. S.; Bauer, J. M.; Yu, Q.; Liu, R. H.; Devadoss, C.; Jo, B. H., Functional Hydrogel Structures for Autonomous Flow Control inside Microfluidic Channels. *Nature* **2000**, 404, (6778), 588-+.
18. Bergmann, N. P., N.A., Protein-Imprinted Microparticles for Tissue Engineering Application. *Transactions of the Society of Biomaterials* **2003**, 29, 457.
19. Blank, Z.; Reimschuessel, A. C., Structural Studies of Organic Gels by SEM. *J. Mater. Sci.* **1974**, 9, 1815-1822.
20. Bolisay, L. D. V.; March, J. F.; Bentley, W. E.; Kofinas, P. In *Separation of Baculoviruses Using Molecularly Imprinted Polymer Gels*, Materials Research Society, San Fransisco, 2004; Materials Research Society: San Fransisco, 2004; pp G3.1.1-G3.1.5.
21. Bradbury, J., Beyond Pills and Jabs. *The Lancet* **2003**, 362, (9400), 1984.
22. Brannon-Peppas, L. V., M., Polylactic and Polyglycolic Acids as Drug Delivery Carriers. In *Handbook of Pharmaceutical Controlled Release Technology*, Brannon-Peppas, L. K., A.M.; Langer, R.; Mikos, A.G.; Peppas, N.A.; Trantolo, D.J.; Yaszemski, M.J.; Wnek, G.E., Ed. 2000; pp 99-130.
23. Brazel, C. S.; Peppas, N. A., Synthesis and Characterization of Thermomechanically and Chemomechanically Responsive Poly(N-Isopropylacrylamide-co-Methacrylic Acid) Hydrogels. *Macromolecules* **1995**, 28, (24), 8016-8020.

24. Brem, H.; Gabikian, P., Biodegradable Polymer Implants to Treat Brain Tumors. *J. Controlled Release* **2001**, 74, (1-3), 63-67.
25. Britschgi, M.; von Greyerz, S.; Burkhart, C.; Pichler, W. J., Molecular Aspects of Drug Recognition by Specific T Cells. *Current Drug Targets* **2003**, 4, (1), 1-11.
26. Bromberg, L. E.; Klibanov, A. M., Transport of Proteins Dissolved in Organic-Solvents across Biomimetic Membranes. *Proc. Natl. Acad. Sci. U. S. A.* **1995**, 92, (5), 1262-1266.
27. Burdick, J. A.; Anseth, K. S., Photoencapsulation of Osteoblasts in Injectable RGD-Modified PEG Hydrogels for Bone Tissue Engineering. *Biomaterials* **2002**, 23, (22), 4315-4323.
28. Bures, P.; Huang, Y. B.; Oral, E.; Peppas, N. A., Surface Modifications and Molecular Imprinting of Polymers in Medical and Pharmaceutical Applications. *J. Controlled Release* **2001**, 72, (1-3), 25-33.
29. Burkoth, A. K.; Anseth, K. S., A Review of Photocrosslinked Polyanhydrides: In Situ Forming Degradable Networks. *Biomaterials* **2000**, 21, (23), 2395-2404.
30. Byrne, M. E.; Oral, E.; Hilt, J. Z.; Peppas, N. A., Networks for Recognition of Biomolecules: Molecular Imprinting and Micropatterning Poly(Ethylene Glycol)-Containing Films. *Polymers for Advanced Technologies* **2002**, 13, (10-12), 798-816.
31. Byrne, M. E.; Park, K.; Peppas, N. A., Molecular Imprinting within Hydrogels. *Adv. Drug Deliv. Rev.* **2002**, 54, (1), 149-161.

32. Calvo, P.; Vila-Jato, J. L.; Alonso, M. J., Evaluation of Cationic Polymer-Coated Nanocapsules as Ocular Drug Carriers. *Int. J. Pharm.* **1997**, 153, (1), 41.
33. Cambrosio, A.; Jacobi, D.; Keating, P., Arguing with Images: Pauling's Theory of Antibody Formation. *Representations* **2005**, 89, (1), 94-130.
34. Carrel, A., On the Permanent Life of Tissue Outside of the Organism. *J. Exp. Med.* **1912**, 15, (5), 516-528.
35. Chandler, G. W.; Seraphin, S., Scanning Electron Microscopy. In *Characterization of Materials*, Kaufman, E. N., Ed. Wiley: New Jersey, 2003; Vol. 2, pp 1050-1062.
36. Charlionet, R.; Machour-Merlet, N.; Leclerc, S.; Malandain, J., Oriented Macroporous Polyacrylamide Gels. *Electrophoresis* **1997**, 18, 1133-1135.
37. Chen, B. N.; Piletsky, S.; Turner, A. P. F., Molecular Recognition: Design of "Keys". *Comb. Chem. High Throughput Screen.* **2002**, 5, (6), 409-427.
38. Ciardelli, G.; Cioni, B.; Cristallini, C.; Barbani, N.; Silvestri, D.; Giusti, P., Acrylic Polymeric Nanospheres for the Release and Recognition of Molecules of Clinical Interest. *Biosens. Bioelectron.* **2004**, 20, (6), 1083-1090.
39. Ciardelli, G.; Silvestri, D.; Cristallini, C.; Barbani, N.; Giusti, P., The Relevance of the Transfer of Molecular Information between Natural and Synthetic Materials in the Realisation of Biomedical Devices with Enhanced Properties. *J. Biomater. Sci. Polym. Ed.* **2005**, 16, (2), 219-236.
40. Cook, R. O.; Pannu, R. K.; Kellaway, I. W., Novel Sustained Release Microspheres for Pulmonary Drug Delivery. *J. Controlled Release* **2005**, 104, (1), 79.

41. Cormack, P. A. G.; Elorza, A. Z., Molecularly Imprinted Polymers: Synthesis and Characterisation. *J. Chromatogr. B* **2004**, 804, (1), 173.
42. Cudic, P.; Behenna, D. C.; Kranz, J. K.; Kruger, R. G.; Wand, A. J.; Veklich, Y. I.; Weisel, J. W.; McCafferty, D. G., Functional Analysis of the Lipoglycopeptide Antibiotic Ramoplanin. *Chem. Biol.* **2002**, 9, (8), 897-906.
43. Cumiskey, J. M.; Melinn, M.; Mclaughlin, H., Lysozyme Levels in Sarcoidosis. *Ir. J. Med. Sci.* **1978**, 147, (3), 108-111.
44. Davies, M. P.; De Biasi, V.; Perrett, D., Approaches to the Rational Design of Molecularly Imprinted Polymers. *Anal. Chim. Acta* **2004**, 504, (1), 7-14.
45. Davis, K. A.; Burdick, J. A.; Anseth, K. S., Photoinitiated Crosslinked Degradable Copolymer Networks for Tissue Engineering Applications. *Biomaterials* **2003**, 24, (14), 2485-2495.
46. Davis, M. P.; Walsh, D.; Lagman, R.; LeGrand, S. B., Randomized Clinical Trial of an Implantable Drug Delivery System. *J. Clin. Oncol.* **2003**, 21, (14), 2800-2801.
47. DeBakey, M. S., F., Battle Injuries of the Arteries. *Am. J. Surg.* **1946**, 123, 534.
48. Dick, W.; Theilmann, L., Urinary Levels of Lysozyme in Children with Acute or Chronic Recurrent Urinary-Tract Infection. *Pediatr. Pedol.* **1980**, 15, (4), 345-350.
49. Dickert, F. L.; Lieberzeit, P.; Miarecka, S. G.; Mann, K. J.; Hayden, O.; Palfinger, C., Synthetic Receptors for Chemical Sensors--Subnano- and

Micrometre Patterning by Imprinting Techniques. *Biosensors and Bioelectronics* **2004**, 20, (6), 1040.

50. Droge, J. H. M.; Janssen, L. H. M.; Wilting, J., A Comparative-Study of Some Physicochemical Properties of Human-Serum Albumin Samples from Different Sources.1. Some Physicochemical Properties of Isoionic Human-Serum Albumin Solutions. *Biochem. Pharmacol.* **1982**, 31, (23), 3775-3779.

51. Drury, J. L.; Mooney, D. J., Hydrogels for Tissue Engineering: Scaffold Design Variables and Applications. *Biomaterials* **2003**, 24, (24), 4337-4351.

52. Druzhinina, T. V.; Andrichenko, Y. D.; Erofeeva, I. V., Thermooxidation of Modified Polycaproamide Fibre Containing Graft Poly(Dimethylaminoethyl Methacrylate). *Fibre Chemistry* **2001**, 33, (3), 193-199.

53. Dunn, M. J., *Gel Electrophoresis: Proteins*. Alden Press Ltd.: Oxford, UK, 1993.

54. El-Aneed, A., An Overview of Current Delivery Systems in Cancer Gene Therapy. *J. Controlled Release* **2004**, 94, (1), 1.

55. Elisseeff, J.; Anseth, K.; Sims, D.; McIntosh, W.; Randolph, M.; Langer, R., Transdermal Photopolymerization for Minimally Invasive Implantation. *Proc. Natl. Acad. Sci. U. S. A.* **1999**, 96, (6), 3104-3107.

56. Ende, M. T. A.; Peppas, N. A., Transport of Ionizable Drugs and Proteins in Crosslinked Poly(Acrylic Acid) and Poly(Acrylic Acid-co-2-Hydroxyethyl Methacrylate) Hydrogels.1. Polymer Characterization. *J. Appl. Polym. Sci.* **1996**, 59, (4), 673-685.

57. Enoki, T.; Tanaka, K.; Watanabe, T.; Oya, T.; Sakiyama, T.; Takeoka, Y.; Ito, K.; Wang, G. Q.; Annaka, M.; Hara, K.; Du, R.; Chuang, J.; Wasserman, K.; Grosberg, A. Y.; Masamune, S.; Tanaka, T., Frustrations in Polymer Conformation in Gels and Their Minimization through Molecular Imprinting. *Phys. Rev. Lett.* **2000**, 85, (23), 5000-5003.
58. Flynn, L.; Dalton, P. D.; Shoichet, M. S., Fiber Templating of Poly(2-Hydroxyethyl Methacrylate) for Neural Tissue Engineering. *Biomaterials* **2003**, 24, (23), 4265-4272.
59. Frenkel, S. R.; Toolan, B.; Menche, D.; Pitman, M. I.; Pachence, J. M., Chondrocyte Transplantation Using a Collagen Bilayer Matrix for Cartilage Repair. *J. Bone Joint Surg. Br.* **1997**, 79B, (5), 831-836.
60. Freshney, R. I., *Animal Cell Culture: A Practical Approach*. Oxford: Washington, D.C., 1986.
61. Gallardo, A.; Eguiburu, J. L.; Berridi, M. J. F.; San Roman, J., Preparation and *in vitro* Release Studies of Ibuprofen-Loaded Films and Microspheres Made from Graft Copolymers of Poly(L-Lactic Acid) on Acrylic Backbones. *J. Controlled Release* **1998**, 55, (2-3), 171-179.
62. Gershon, D., Microarray Technology - an Array of Opportunities. *Nature* **2002**, 416, (6883), 885-+.
63. Gitlin, G.; Bayer, E. A.; Wilchek, M., Studies on the Biotin-Binding Site of Avidin - Lysine Residues Involved in the Active-Site. *Biochem. J.* **1987**, 242, (3), 923-926.

64. Gitlin, G.; Bayer, E. A.; Wilchek, M., Studies on the Biotin-Binding Site of Avidin - Tryptophan Residues Involved in the Active-Site. *Biochem. J.* **1988**, 250, (1), 291-294.
65. Glick, B. R. P., J.J., Microbial Production of Therapeutic Agents. In *Molecular Biotechnology: Principles and Applications of Recombinant DNA*, ASM Press: Washington D.C., 1998; pp 235-237.
66. Goldbart, R.; Kost, J., Calcium Responsive Bioerodible Drug Delivery System. *Pharm. Res.* **1999**, 16, (9), 1483-1486.
67. Golub, E. S.; Green, D. R., *Immunology: A Synthesis*. Sinauer Assoc.: Sunderland, MA, 1991.
68. Green, N. M., Avidin. In *Adv. Protein Chem.*, Anfinsen, C. B., Ed. Academic Press: New York, 1975; Vol. 29.
69. Grimaud, E.; Lecoq, J. C.; Boschetti, E.; Corgier, M., Comparison of Gels Used for Molecular Sieving of Proteins by Electron Microscopy and Pore Parameters Determinations. *J. Chromatogr. A* **1978**, 166, (1), 37.
70. Guinta, P. R. Fabrication and Characterization of Novel Nanocomposite Materials. Florida State University, 2005.
71. Guinta, P. R.; Washington, R. P.; Campbell, T. D.; Steinbock, O.; Stiegman, A. E., Preparation of Mesoporous Silica Monoliths with Ordered Arrays of Macrochannels Templated from Electric-Field Oriented Hydrogels. *Angew. Chem., Int. Ed. Engl.* **2004**, 43, 1505-1507.
72. Haupt, K.; Mosbach, K., Plastic Antibodies: Developments and Applications. *Trends. Biotechnol.* **1998**, 16, (11), 468-475.

73. Hedin-Dahlstrom, J.; Shoravi, S.; Wikman, S.; Nicholls, I. A., Stereoselective Reduction of Menthone by Molecularly Imprinted Polymers. *Tetrahedron: Asymmetry* **2004**, 15, (15), 2431.
74. Hern, D. L.; Hubbell, J. A., Incorporation of Adhesion Peptides into Nonadhesive Hydrogels Useful for Tissue Resurfacing. *J. Biomed. Mater. Res.* **1998**, 39, (2), 266-276.
75. Hilt, J. Z., Nanotechnology and Biomimetic Methods in Therapeutics: Molecular Scale Control with Some Help from Nature. *Adv. Drug Deliv. Rev.* **2004**, 56, (11), 1533-1536.
76. Hilt, J. Z.; Byrne, M. E., Configurational Biomimesis in Drug Delivery: Molecular Imprinting of Biologically Significant Molecules. *Adv. Drug Deliv. Rev.* **2004**, 56, (11), 1599-1620.
77. Hilt, J. Z.; Gupta, A. K.; Bashir, R.; Peppas, N. A., Ultrasensitive BioMEMS Sensors Based on Microcantilevers Patterned with Environmentally Responsive Hydrogels. *Biomed. Microdevices* **2003**, 5, (3), 177-184.
78. Hiratani, H.; Alvarez-Lorenzo, C., The Nature of Backbone Monomers Determines the Performance of Imprinted Soft Contact Lenses as Timolol Drug Delivery Systems. *Biomaterials* **2004**, 25, (6), 1105.
79. Hiratani, H.; Alvarez-Lorenzo, C., Timolol Uptake and Release by Imprinted Soft Contact Lenses Made of N,N-Diethylacrylamide and Methacrylic Acid. *J. Controlled Release* **2002**, 83, (2), 223.
80. Hiratani, H.; Alvarez-Lorenzo, C.; Chuang, J.; Guney, O.; Grosberg, A. Y.; Tanaka, T., Effect of Reversible Cross-Linker, N,N'-Bis(Acryloyl)Cystamine, on Calcium Ion Adsorption by Imprinted Gels. *Langmuir* **2001**, 17, (14), 4431-4436.

81. Hiratani, H.; Fujiwara, A.; Tamiya, Y.; Mizutani, Y.; Alvarez-Lorenzo, C., Ocular Release of Timolol from Molecularly Imprinted Soft Contact Lenses. *Biomaterials* **2005**, 26, (11), 1293.
82. Ho, B. C.; Lee, Y. D.; Chin, W. K., Thermal-Degradation of Polymethacrylic Acid. *J. Polym. Sci., Part A: Polym. Chem.* **1992**, 30, (11), 2389-2397.
83. Hofstadler, S. A.; Griffey, R. H., Analysis of Noncovalent Complexes of DNA and RNA by Mass Spectrometry. *Chem. Rev.* **2001**, 101, (2), 377-390.
84. Hsu, T.-P.; Cohen, C., Observations on the Structure of a Polyacrylamide Gel from Electron Micrographs. *Journal of Analytical Chemistry* **1983**.
85. Hubbell, J. A. P., C.K.; Sawhney, A.S.; Amarpreet, S.; Desai, N.P.; Neil, P.; Hill-West, J.L., *Photopolymerizable Biodegradable Hydrogels as Tissue Contacting Materials and Controlled-Release Carriers*. 2001.
86. Hwang, C.-C.; Lee, W.-C., Chromatographic Characteristics of Cholesterol-Imprinted Polymers Prepared by Covalent and Non-Covalent Imprinting Methods. *J. Chromatogr. A* **2002**, 962, (1-2), 69.
87. Ismail, L. F. M.; Maziad, N. A.; Abo-Farha, S. A., Factors Affecting the Adsorption of Cationic Dyes on Polymeric Hydrogels Prepared by Gamma Irradiation. *Polym. Int.* **2005**, 54, (1), 58-64.
88. Jain, V. K.; Jamil, Z.; Shukla, O. P., Serum Lysozyme in Pulmonary Tuberculosis. *Indian. J. Chest. Dis. Allied. Sci.* **1978**, 20, (4), 168-172.

89. Janeway, C. A.; Travers, P.; Walport, M.; Shlomchik, M. J., *Immunobiology: The Immune System in Health and Disease*. Garland Publishing: New York, 2001.
90. Jiang, H. L.; Jin, J. F.; Hu, Y. Q.; Zhu, K. J., Improvement of Protein Loading and Modulation of Protein Release from Poly(Lactide-co-Glycolide) Microspheres by Complexation of Proteins with Polyanions. *J. Microencapsul.* **2004**, 21, (6), 615-624.
91. Jiang, H. L.; Zhu, K. J., Preparation, Characterization and Degradation Characteristics of Polyanhydrides Containing Poly(Ethylene Glycol). *Polym. Int.* **1999**, 48, (1), 47-52.
92. Jimenez, R.; Salazar, G.; Baldrige, K. K.; Romesberg, F. E., Flexibility and Molecular Recognition in the Immune System. *Proc. Natl. Acad. Sci. U. S. A.* **2003**, 100, (1), 92-97.
93. Jose Alonso, M., Nanomedicines for Overcoming Biological Barriers. *Biomed. Pharmacother.* **2004**, 58, (3), 168.
94. Jung, K.; Diego, J.; Strobelt, V.; Scholz, D.; Schreiber, G., Diagnostic-Significance of Some Urinary Enzymes for Detecting Acute Rejection Crises in Renal-Transplant Recipients - Alanine Aminopeptidase, Alkaline-Phosphatase, Gamma-Glutamyl-Transferase, N-Acetyl-Beta-D-Glucosaminidase, and Lysozyme. *Clin. Chem.* **1986**, 32, (10), 1807-1811.
95. Kaiserling, E.; Horny, H. P.; Geerts, M. L.; Schmid, U., Skin Involvement in Myelogenous Leukemia - Morphologic and Immunophenotypic Heterogeneity of Skin Infiltrates. *Mod. Pathol.* **1994**, 7, (7), 771-779.

96. Karande, P.; Jain, A.; Ergun, K.; Kispersky, V.; Mitragotri, S., Design Principles of Chemical Penetration Enhancers for Transdermal Drug Delivery. *Proc. Natl. Acad. Sci. U.S.A.* **2005**, 102, (13), 4688-4693.
97. Kataoka, K.; Miyazaki, H.; Bunya, M.; Okano, T.; Sakurai, Y., On-Off Regulation of Insulin-Release by Totally Synthetic Polymer Gels Responding to External Glucose Concentration. *Abstr. Pap. Am. Chem. Soc.* **1999**, 217, U564-U564.
98. Kato, K.; Furukawa, M.; Kanzaki, Y.; Hoffman, A. S.; Nakamae, K., Lysozyme Loading in Phosphate Carrying Hydrogels at High Density and the Controlled Release of Lysozyme. *Kobunshi Ronbunshu* **1998**, 55, (6), 353-358.
99. Keegan, M. E.; Whittum-Hudson, J. A.; Saltzman, W. M., Biomimetic Design in Microparticulate Vaccines. *Biomaterials* **2003**, 24, (24), 4435-4443.
100. Kobashi, T.; Matsuda, T., Fabrication of Compliant Hybrid Grafts Supported with Elastomeric Meshes. *Cell Transplant.* **1999**, 8, (5), 477-488.
101. Komiyama, M.; Toshifumi, T.; Mukawa, T.; Asanuma, H., *Molecular Imprinting: From Fundamentals to Application*. Wiley-VCH: Morlenbach, Germany, 2003.
102. Kurenkov, V. F.; Myagchenkov, V. A., Acrylamide (Polymerization and Applications). In *Polymeric Materials Encyclopedia*, Salamone, J. C., Ed. CRC Press, Inc.: Boca Raton, 1996; Vol. 1, pp 47-54.
103. Kwon, G. S.; Bae, Y. H.; Cremers, H.; Feijen, J.; Kim, S. W., Release of Proteins Via Ion Exchange from Albumin-Heparin Microspheres. *J. Controlled Release* **1992**, 22, (2), 83.

104. Lai, J. P.; Lu, X. Y.; Lu, C. Y.; Ju, H. F.; He, X. W., Preparation and Evaluation of Molecularly Imprinted Polymeric Microspheres by Aqueous Suspension Polymerization for Use as a High-Performance Liquid Chromatography Stationary Phase. *Anal. Chim. Acta* **2001**, 442, (1), 105-111.
105. Landgraf, W.; Li, N. H.; Benson, J. R., Polymer Microcarrier Exhibiting Zero-Order Release. *Drug Delivery Technology* **2003**, 3.
106. Lee, C. H.; Singla, A.; Lee, Y., Biomedical Applications of Collagen. *Int. J. Pharm.* **2001**, 221, (1-2), 1-22.
107. Leobandung, W. L.; Peppas, N. A. In *Temperature-Sensitive Particulate Systems Containing Poly(Ethylene Glycol)*, AICHE, Los Angeles, CA, 2000; Los Angeles, CA, 2000; p p 199h.
108. Li, M.; He, P.; Zhang, Y.; Hu, N., An Electrochemical Investigation of Hemoglobin and Catalase Incorporated in Collagen Films. *Biochimica et Biophysica Acta (BBA) - Proteins & Proteomics* **2005**, 1749, (1), 43.
109. Li, S. M., Hydrolytic Degradation Characteristics of Aliphatic Polyesters Derived from Lactic and Glycolic Acids. *J. Biomed. Mater. Res.* **1999**, 48, (3), 342-353.
110. Lin, T. Y.; Hu, C. H.; Chou, T. C., Determination of Albumin Concentration by MIP-QCM Sensor. *Biosens. Bioelectron.* **2004**, 20, (1), 75-81.
111. Liu, J.; Luo, G.; Gao, S.; Zhang, K.; Chen, X.; Shen, J., Generation of a Glutathione Peroxidase-Like Mimic Using Bioimprinting and Chemical Mutation. *Chem. Commun.* **1999**, 5, (2), 199.

112. Liu, T. B.; Burger, C.; Chu, B., Nanofabrication in Polymer Matrices. *Progress In Polymer Science* **2003**, 28, (1), 5-26.
113. Lowman, A. M.; Morishita, M.; Kajita, M.; Nagai, T.; Peppas, N. A., Oral Delivery of Insulin Using pH-Responsive Complexation Gels. *J. Pharm. Sci.* **1999**, 88, (9), 933-937.
114. Lu, Y.; Li, C.; Wang, X.; Sun, P.; Xing, X., Influence of Polymerization Temperature on the Molecular Recognition of Imprinted Polymers. *J. Chromatogr. B* **2004**, 804, (1), 53.
115. Lu, Y.; Li, C. X.; Liu, X. H.; Huang, W. Q., Molecular Recognition through the Exact Placement of Functional Groups on Non-Covalent Molecularly Imprinted Polymers. *J. Chromatogr. A* **2002**, 950, (1-2), 89-97.
116. Ma, P. X., Scaffolds for Tissue Fabrication. *Materials Today* **2004**, 7, (5), 30-40.
117. Mann, B. K.; Schmedlen, R. H.; West, J. L., Tethered-TGF-Beta Increases Extracellular Matrix Production of Vascular Smooth Muscle Cells. *Biomaterials* **2001**, 22, (5), 439-444.
118. Mann, B. K.; Tsai, A. T.; Scott-Burden, T.; West, J. L., Modification of Surfaces with Cell Adhesion Peptides Alters Extracellular Matrix Deposition. *Biomaterials* **1999**, 20, (23-24), 2281-2286.
119. Mansbridge, J., Dermal Fibroblasts. In *Primary Mesenchymal Cells*, Koller, M. R.; Palsson, B.; Masters, J. R. W., Eds. Kluwer Academic Publishers: Boston, 2001; Vol. 5, pp 125-172.

120. Mishra, P.; Griebenow, K.; Klibanov, A. M., Structural Basis for the Molecular Memory of Imprinted Proteins in Anhydrous Media. *Biotechnol. Bioeng.* **1996**, 52, (5), 609-614.
121. Miyata, T.; Asami, N.; Uragami, T., A Reversibly Antigen-Responsive Hydrogel. *Nature* **1999**, 399, (6738), 766.
122. Miyata, T.; Uragami, T.; Nakamae, K., Biomolecule-Sensitive Hydrogels. *Adv. Drug Deliv. Rev.* **2002**, 54, (1), 79-98.
123. Moran, J. M. B., L.J., Fabrication and Characterization of PLA/PGA Composites for Cartilage Tissue Engineering. *Tissue Eng.* **1998**, 4, S498.
124. Mosbach, K., Molecular Imprinting. *Trends Biochem. Sci.* **1994**, 19, (1), 9-14.
125. Mosbach, K., Toward the Next Generation of Molecular Imprinting with Emphasis on the Formation, by Direct Molding, of Compounds with Biological Activity (Biomimetics). *Anal. Chim. Acta* **2001**, 435, (1), 3-8.
126. Mosbach, K.; Ramstrom, O., The Emerging Technique of Molecular Imprinting and Its Future Impact on Biotechnology. *Bio/Technology* **1996**, 14, (2), 163-170.
127. Motherwell, W. B.; Bingham, M. J.; Pothier, J.; Six, Y., A Study of Some Molecularly Imprinted Polymers as Protic Catalysts for the Isomerisation of Alpha-Pinene Oxide to Trans-Carveol. *Tetrahedron* **2004**, 60, (14), 3231-3241.
128. Nakamae, K.; Nishino, T.; Kato, K.; Miyata, T.; Hoffman, A. S., Synthesis and Characterization of Stimuli-Sensitive Hydrogels Having a Different Length of

Ethylene Glycol Chains Carrying Phosphate Groups: Loading and Release of Lysozyme. *J. Biomater. Sci. Polym. Ed.* **2004**, 15, (11), 1435-1446.

129. Nakamae, K.; Nizuka, T.; Miyata, T.; Furukawa, M.; Nishino, T.; Kato, K.; Inoue, T.; Hoffman, A. S.; Kanzaki, Y., Lysozyme Loading and Release from Hydrogels Carrying Pendant Phosphate Groups. *J. Biomater. Sci. Polym. Ed.* **1997**, 9, (1), 43-53.

130. Nguyen, K. T.; West, J. L., Photopolymerizable Hydrogels for Tissue Engineering Applications. *Biomaterials* **2002**, 23, (22), 4307-4314.

131. Nicholls, I. A.; Rosengren, J. P., Molecular Imprinting of Surfaces. *Bioseparation* **2002**, 10, 301-305.

132. Nikon, Albino Swiss Mouse Embryo Fibroblasts (3T3 Line). <http://www.microscopyu.com/moviegallery/livecellimaging/3t3/> **2005**.

133. Niwa, T.; Katsuzaki, T.; Yazawa, T.; Tatemichi, N.; Emoto, Y.; Miyazaki, T.; Maeda, K., Urinary Trehalase Activity in Chronic Glomerulonephritis. *Nephron* **1993**, 63, (4), 423-428.

134. Omorain, C.; Smethurst, P.; Levi, A. J.; Peters, T. J., Biochemical-Analysis of Enzymic Markers of Inflammation in Rectal Biopsies from Patients with Ulcerative-Colitis and Crohns-Disease. *J. Clin. Pathol.* **1983**, 36, (11), 1312-1316.

135. Oral, E.; Peppas, N. A., Responsive and Recognitive Hydrogels Using Star Polymers. *J. Biomed. Mater. Res. A* **2004**, 68A, (3), 439-447.

136. Oral, E. P., N.A., Molecularly Imprinted Hydrogels with Polyfunctional Methacrylates. In *Molecularly Imprinted Polymer Science and Technology*, Brain, K. R. A., C.J., Ed. STS Publishing: Cardiff, 2000; Vol. 111.
137. O'Sullivan, C. K.; Guilbault, G. G., Commercial Quartz Crystal Microbalances - Theory and Applications. *Biosens. Bioelectron.* **1999**, 14, (8-9), 663-670.
138. Ou, S. H.; Wu, M. C.; Chou, T. C.; Liu, C. C., Polyacrylamide Gels with Electrostatic Functional Groups for the Molecular Imprinting of Lysozyme. *Anal. Chim. Acta* **2004**, 504, (1), 163.
139. Padera, R. F.; Schoen, F. J., Cardiovascular Medical Devices. In *Biomaterials Science: An Introduction to Materials in Medicine*, 2 ed.; Ratner, B. D.; Hoffmann, A. S.; Schoen, F. J.; Lemons, J. E., Eds. Elsevier, Inc.: San Diego, 2004; pp 470-493.
140. Palmer, R. R.; Lewis, A. L.; Kirkwood, L. C.; Rose, S. F.; Lloyd, A. W.; Vick, T. A.; Stratford, P. W. P. W., Biological Evaluation and Drug Delivery Application of Cationically Modified Phospholipid Polymers. *Biomaterials* **2004**, 25, (19), 4785.
141. Park, Y.-J.; Liang, J.; Yang, Z.; Yang, V. C., Controlled Release of Clot-Dissolving Tissue-Type Plasminogen Activator from a Poly(Glutamic Acid) Semi-Interpenetrating Polymer Network Hydrogel. *J. Controlled Release* **2001**, 75, (1-2), 37.
142. Parmpi, P.; Kofinas, P., Biomimetic Glucose Recognition Using Molecularly Imprinted Polymer Hydrogels. *Biomaterials* **2004**, 25, (10), 1969-1973.

143. Patras, G.; Qiao, G. G.; Solomon, D. H., Characterization of the Pore Structure of Aqueous Three-Dimensional Polyacrylamide Gels with a Novel Cross-Linker. *Electrophoresis* **2000**, 21, (17), 3843-3850.
144. Pauling, L., A Theory of the Structure and Process of Formation of Antibodies. *J. Am. Chem. Soc.* **1940**, 62, 2645-2655.
145. Peppas, N. A., Devices Based on Intelligent Biopolymers for Oral Protein Delivery. *Int. J. Pharm.* **2004**, 277, (1-2), 11-17.
146. Peppas, N. A.; Bures, P.; Leobandung, W.; Ichikawa, H., Hydrogels in Pharmaceutical Formulations. *Eur. J. Pharm. Biopharm.* **2000**, 50, (1), 27-46.
147. Peppas, N. A.; Colombo, P., Analysis of Drug Release Behavior from Swellable Polymer Carriers Using the Dimensionality Index. *J. Controlled Release* **1997**, 45, (1), 35-40.
148. Peppas, N. A.; Huang, Y.; Torres-Lugo, M.; Ward, J. H.; Zhang, J., Physicochemical, Foundations and Structural Design of Hydrogels in Medicine and Biology. *Annu. Rev. Biomed. Eng.* **2000**, 2, 9-29.
149. Peppas, N. A.; Khare, A. R., Preparation, Structure and Diffusional Behavior of Hydrogels in Controlled-Release. *Adv. Drug Deliv. Rev.* **1993**, 11, (1-2), 1-35.
150. Peppas, N. A. Z., J., Diffusional Behavior in pH- and Temperature-Sensitive Interpenetrating Networks Used in Drug Delivery. In *Biomaterials and Drug Delivery Systems Towards the New Millenium*, Park, K. D. K., I.C.; Yui, N.; Yeong, S.Y.; Park, K., Ed. Seoul, Korea, 2000; pp 87-96.

151. Piletsky, S. A.; Matuschewski, H.; Schedler, U.; Wilpert, A.; Piletska, E. V.; Thiele, T. A.; Ulbricht, M., Surface Functionalization of Porous Polypropylene Membranes with Molecularly Imprinted Polymers by Photograft Copolymerization in Water. *Macromolecules* **2000**, 33, (8), 3092-3098.
152. Pitt, C. G.; Gratzl, M. M.; Kimmel, G. L.; Surles, J.; Schindler, A., Aliphatic Polyesters.2. The Degradation of Poly(dl-Lactide), Poly(Epsilon-Caprolactone), and Their Copolymers *in vivo*. *Biomaterials* **1981**, 2, (4), 215-220.
153. Promega, Celltiter 96® AQueous One Solution Cell Proliferation Assay, *Technical Bulletin*. **2005**.
154. Pugliese, L.; Coda, A.; Malcovati, M.; Bolognesi, M., 3-Dimensional Structure of the Tetragonal Crystal Form of Egg-White Avidin in Its Functional Complex with Biotin at 2.7-Angstrom Resolution. *J. Mol. Biol.* **1993**, 231, (3), 698-710.
155. Pugliese, L.; Malcovati, M.; Coda, A.; Bolognesi, M., Crystal-Structure of Apo-Avidin from Hen Egg-White. *J. Mol. Biol.* **1994**, 235, (1), 42-46.
156. Puoci, F.; Iemma, F.; Muzzalupo, R.; Spizzirri, U. G.; Trombino, S.; Cassano, R.; Picci, N., Spherical Molecularly Imprinted Polymers (SMIPs) Via a Novel Precipitation Polymerization in the Controlled Delivery of Sulfasalazine. *Macromol. Biosci.* **2004**, 4, (1), 22.
157. Rachkov, A.; Minoura, N., Towards Molecularly Imprinted Polymers Selective to Peptides and Proteins. The Epitope Approach. *Biochimica Et Biophysica Acta-Protein Structure And Molecular Enzymology* **2001**, 1544, (1-2), 255-266.

158. Ragab, D. M.; Babiker, E. E.; Eltinay, A. H., Fractionation, Solubility and Functional Properties of Cowpea (*Vigna Unguiculata*) Proteins as Affected by pH and/or Salt Concentration. *Food Chem.* **2004**, 84, (2), 207-212.
159. Rai, B.; Teoh, S. H.; Hutmacher, D. W.; Cao, T.; Ho, K. H., Novel PCL-Based Honeycomb Scaffolds as Drug Delivery Systems for rhBMP-2. *Biomaterials* **2005**, 26, (17), 3739.
160. Rakovskaya, R. V.; Popova, I. I.; Beniaminov, V. O., Content of Lysozyme in the Blood-Serum of Patients with Pulmonary Tuberculosis and Chronic Unspecific Pulmonary-Diseases. *Vrach. Delo.* **1985**, (6), 41-42.
161. Reddy, R. P.; Kobayashi, T.; Abe, M.; Fujii, N., Molecular Imprinted Nylon-6 as a Recognition Material of Amino Acids. *Eur. Polym. J.* **2002**, 38, (3), 521.
162. Reed, A. M.; Gilding, D. K., Biodegradable Polymers for Use in Surgery - Poly(Glycolic)-Poly(Lactic Acid) Homo and Co-Polymers.2. Invitro Degradation. *Polymer* **1981**, 22, (4), 494-498.
163. Reid, L. M. Z., M.A., *Extracellular Matrix Chemistry and Biology*. Marcel Dekker: New York, 1993.
164. Reyes, D. R.; Iossifidis, D.; Auroux, P. A.; Manz, A., Micro Total Analysis Systems. 1. Introduction, Theory, and Technology. *Anal. Chem.* **2002**, 74, (12), 2623-2636.
165. Righetti, P. G., Macroporous Gels: Facts and Misfacts. *J. Chromatogr. A* **1995**, 698, (1-2), 3.

166. Righetti, P. G.; Caglio, S.; Saracchi, M.; Quaroni, S., 'Laterally Aggregated' Polyacrylamide Gels for Electrophoresis. *Electrophoresis* **1992**, 10, 587-595.
167. Righetti, P. G.; Gelfi, C., Electrophoresis Gel Media: The State of the Art. *J. Chromatogr. B Biomed. Sci. Appl.* **1997**, 699, (1-2), 63.
168. Rittling, S. R., Clonal Nature of Spontaneously Immortalized 3T3 Cells. *Exp. Cell Res.* **1996**, 229, (1), 7.
169. Roorda, W. E.; Bouwstra, J. A.; de Vries, M. A.; Junginger, H. E., Thermal Behavior of Poly Hydroxy Ethyl Methacrylate (pHEMA) Hydrogels. *Pharm. Res.* **1988**, 5, (11), 722-725.
170. Ruchel, R.; Brager, M. D., Scanning Electron Microscopic Observations of Polyacrylamide Gels. *Anal. Biochem.* **1975**, 68, 415-428.
171. Salins, L. L. E.; Deo, S. K.; Daunert, S., Phosphate Binding Protein as the Biorecognition Element in a Biosensor for Phosphate. *Sens. Actuators, B* **2004**, 97, (1), 81-89.
172. Santini, J. T.; Cima, M. J.; Langer, R., A Controlled-Release Microchip. *Nature* **1999**, 397, (6717), 335-338.
173. Saraydin, D.; Unver-Saraydin, S.; Karadag, E.; Koptagel, E.; Guven, O., In Vivo Biocompatibility of Radiation Crosslinked Acrylamide Copolymers. *Nucl. Instrum. Methods Phys. Res., Sect. B* **2004**, 217, (2), 281.
174. Schoen, F. J.; Mitchell, R. N., Tissues, the Extracellular Matrix, and Cell-Biomaterial Interactions. In *Biomaterials Science: An Introduction to Materials in*

Medicine, 2 ed.; Ratner, B. D.; Hoffmann, A. S.; Schoen, F. J.; Lemons, J. E., Eds. Elsevier, Inc.: San Diego, 2004; pp 260-281.

175. Schoning, M. J.; Poghossian, A., Recent Advances in Biologically Sensitive Field-Effect Transistors (BioFETs). *Analyst* **2002**, 127, (9), 1137-1151.

176. Sellergren, B., Noncovalent Molecular Imprinting: Antibody-Like Molecular Recognition in Polymeric Network Materials. *Trac-Trends In Analytical Chemistry* **1997**, 16, (6), 310-320.

177. Sepaniak, M.; Datskos, P.; Lavrik, N.; Tipple, C., Microcantilever Transducers: A New Approach to Sensor Technology. *Anal. Chem.* **2002**, 74, (21), 568A-575A.

178. Sherwood, R. L.; Lippert, W. E.; Goldstein, E., Effect of 0.64 ppm Ozone on Alveolar Macrophage Lysozyme Levels in Rats with Chronic Pulmonary Bacterial-Infection. *Environ. Res.* **1986**, 41, (2), 378-387.

179. Shi, H. Q.; Tsai, W. B.; Garrison, M. D.; Ferrari, S.; Ratner, B. D., Template-Imprinted Nanostructured Surfaces for Protein Recognition. *Nature* **1999**, 398, (6728), 593-597.

180. Shin, H.; Jo, S.; Mikos, A. G., Biomimetic Materials for Tissue Engineering. *Biomaterials* **2003**, 24, (24), 4353-4364.

181. Silvestri, D.; Borrelli, C.; Giusti, P.; Cristallini, C.; Ciardelli, G., Polymeric Devices Containing Imprinted Nanospheres: A Novel Approach to Improve Recognition in Water for Clinical Uses. *Anal. Chim. Acta* **2005**, 542, (1), 3.

182. Slade, C. J., Molecular (or Bio-) Imprinting of Bovine Serum Albumin. *J. Mol. Catal., B Enzym.* **2000**, 9, (1-3), 97-105.

183. Sreenivasan, K., Surface-Imprinted Polyurethane Having Affinity Sites for Ampicillin. *Macromol. Biosci.* **2005**, 5, (3), 187-191.
184. Sternberg, M. H., D., Separation of Proteins with Polyacrylic Acids. *Biochemica et Biophysica Acta (BBA) - Protein Structure* **1974**, 342, (1), 195-206.
185. Suedee, R.; Srichana, T.; Rattananont, T., Enantioselective Release of Controlled Delivery Granules Based on Molecularly Imprinted Polymers. *Drug Delivery* **2002**, 9, (1), 19-30.
186. Sundberg, E. J.; Mariuzza, R. A., Molecular Recognition in Antibody-Antigen Complexes. *Protein Modules and Protein-Protein Interactions* **2003**, 61, 119-160.
187. Takahara, Y. K.; Ikeda, S.; Ishino, S.; Tachi, K.; Ikeue, K.; Sakata, T.; Hasegawa, T.; Mori, H.; Matsumura, M.; Ohtani, B., Asymmetrically Modified Silica Particles: A Simple Particulate Surfactant for Stabilization of Oil Droplets in Water. *J. Am. Chem. Soc.* **2005**, 127, (17), 6271-6275.
188. Takeda, K.; Kobayashi, T., Bisphenol A Imprinted Polymer Adsorbents with Selective Recognition and Binding Characteristics. *Science and Technology of Advanced Materials* **2005**, 6, (2), 165.
189. Thorsen, T.; Maerkl, S. J.; Quake, S. R., Microfluidic Large-Scale Integration. *Science* **2002**, 298, (5593), 580-584.
190. Todaro, G. J.; Green, H., Quantitative Studies of the Growth of Mouse Embryo Cells in Culture and Their Development into Established Lines. *J. Cell Biol.* **1963**, 17, (2), 299-313.

191. Tong, D.; Hetenyi, C.; Bikadi, Z.; Gao, J. P.; Hjerten, S., Some Studies of the Chromatographic Properties of Gels ('Artificial Antibodies/Receptors') for Selective Adsorption of Proteins. *Chromatographia* **2001**, 54, (1-2), 7-14.
192. Tulinsky, A., Molecular Interactions of Thrombin. *Semin. Thromb. Hemost.* **1996**, 22, (2), 117-124.
193. Uchimura, E.; Otsuka, H.; Okano, T.; Sakurai, Y.; Kataoka, K., Totally Synthetic Polymer with Lectin-Like Function: Induction of Killer Cells by the Copolymer of 3-Acrylamidophenylboronic Acid with N,N-Dimethylacrylamide. *Biotechnol. Bioeng.* **2001**, 72, (3), 307-314.
194. Ulbricht, M., Membrane Separations Using Molecularly Imprinted Polymers. *J. Chromatogr. B* **2004**, 804, (1), 113-115.
195. Ulbricht, M.; Malaisamy, R., Insights into the Mechanism of Molecular Imprinting by Immersion Precipitation Phase Inversion of Polymer Blends Via a Detailed Morphology Analysis of Porous Membranes. *J. Mater. Chem.* **2005**, 15, (14), 1487-1497.
196. Vaidya, A. A.; Lele, B. S.; Kulkarni, M. G.; Mashelkar, R. A., Thermoprecipitation of Lysozyme from Egg White Using Copolymers of N-Isopropylacrylamide and Acidic Monomers. *J. Biotechnol.* **2001**, 87, (2), 95-107.
197. Vakkalanka, S. K.; Brazel, C. S.; Peppas, N. A., Temperature- and pH-Sensitive Terpolymers for Modulated Delivery of Streptokinase. *J. Biomater. Sci. Polym. Ed.* **1996**, 8, (2), 119-129.
198. Venton, D. L.; Gudipati, E., Influence of Protein on Polysiloxane Polymer Formation: Evidence for Induction of Complementary Protein-Polymer

Interactions. *Biochimica et Biophysica Acta (BBA) - Protein Structure and Molecular Enzymology* **1995**, 1250, (2), 126.

199. Vlatakis, G.; Andersson, L. I.; Muller, R.; Mosbach, K., Drug Assay Using Antibody Mimics Made by Molecular Imprinting. *Nature* **1993**, 361, (6413), 645-647.

200. Vogel, V.; Thomas, W. E.; Craig, D. W.; Krammer, A.; Baneyx, G., Structural Insights into the Mechanical Regulation of Molecular Recognition Sites. *Trends. Biotechnol.* **2001**, 19, (10), 416-+.

201. Voorhees, A. B. J., A.; Blakemore, A.H., The Use of Tubes Constructed from "Vinyon" N Cloth in Bridging Arterial Defects. *Ann. Surg.* **1952**, 135, 332.

202. Wang, H. Y.; Xia, S. L.; Sun, H.; Liu, Y. K.; Cao, S. K.; Kobayashi, T., Molecularly Imprinted Copolymer Membranes Functionalized by Phase Inversion Imprinting for Uracil Recognition and Permselective Binding. *J. Chromatogr. B Analyt. Technol. Biomed. Life Sci.* **2004**, 804, (1), 127-134.

203. Ward, J. H.; Bashir, R.; Peppas, N. A., Micropatterning of Biomedical Polymer Surfaces by Novel UV Polymerization Techniques. *J. Biomed. Mater. Res.* **2001**, 56, (3), 351-360.

204. Whang, K.; Goldstick, T. K.; Healy, K. E., A Biodegradable Polymer Scaffold for Delivery of Osteotropic Factors. *Biomaterials* **2000**, 21, (24), 2545-2551.

205. Whitcombe, M. J.; Rodriguez, M. E.; Villar, P.; Vulfson, E. N., A New Method for the Introduction of Recognition Site Functionality into Polymers Prepared by Molecular Imprinting - Synthesis and Characterization of Polymeric Receptors for Cholesterol. *J. Am. Chem. Soc.* **1995**, 117, (27), 7105-7111.

206. Wizeman, W. J.; Kofinas, P., Molecularly Imprinted Polymer Hydrogels Displaying Isomerically Resolved Glucose Binding. *Biomaterials* **2001**, 22, (12), 1485-1491.
207. Wulff, G.; Grobeeinsler, R.; Vesper, W.; Sarhan, A., Enzyme-Analogue Built Polymers.5. Specificity Distribution of Chiral Cavities Prepared in Synthetic-Polymers. *Makromolekulare Chemie-Macromolecular Chemistry and Physics* **1977**, 178, (10), 2817-2825.
208. Wulff, G.; Knorr, K., Stoichiometric Noncovalent Interaction in Molecular Imprinting. *Bioseparation* **2001**, 10, (6), 257-276.
209. Wulff, G.; Vesper, W.; Grobeeinsler, R.; Sarhan, A., Enzyme-Analogue Built Polymers.4. Synthesis of Polymers Containing Chiral Cavities and Their Use for Resolution of Racemates. *Makromolekulare Chemie-Macromolecular Chemistry and Physics* **1977**, 178, (10), 2799-2816.
210. Xiao, C. B.; Lu, Y. S.; Jing, Z. Z.; Zhang, L., Study on Physical Properties of Blend Films from Gelatin and Polyacrylamide Solutions. *J. Appl. Polym. Sci.* **2002**, 83, (5), 949-955.
211. Yoshikawa, M., Molecularly Imprinted Polymeric Membranes. *Bioseparation* **2001**, 10, (6), 277-286.
212. Yu, S.; Chow, G. M., Carboxyl Group (-CO₂H) Functionalized Ferrimagnetic Iron Oxide Nanoparticles for Potential Bio-Applications. *J. Mater. Chem.* **2004**, 14, (18), 2781-2786.
213. Zhang, J.; Peppas, N. A., Molecular Interactions in Poly(Methacrylic Acid)/Poly(N-Isopropyl Acrylamide) Interpenetrating Polymer Networks. *J. Appl. Polym. Sci.* **2001**, 82, (5), 1077-1082.

214. Zhang, R.; Tang, M.; Bowyer, A.; Eienthal, R.; Hubble, J., A Novel pH- and Ionic-Strength-Sensitive Carboxy Methyl Dextran Hydrogel. *Biomaterials* **2005**, 26, (22), 4677.
215. Zhang, X.-Z.; Wu, D.-Q.; Chu, C.-C., Synthesis, Characterization and Controlled Drug Release of Thermosensitive IPN-PNIPAAm Hydrogels. *Biomaterials* **2004**, 25, (17), 3793.
216. Zhang, Z. H.; Li, H.; Liao, H. P.; Nie, L. H.; Yao, S. Z., Influence of Cross-Linkers' Amount on the Performance of the Piezoelectric Sensor Modified with Molecularly Imprinted Polymers. *Sensors And Actuators, B: Chemical* **2005**, 105, (2), 176-182.
217. Zhou, Y. X.; Yu, B.; Levon, K., Potentiometric Sensor for Dipicolinic Acid. *Biosens. Bioelectron.* **2005**, 20, (9), 1851-1855.

Vita

Nicole Marie Bergmann was born in Belleville, Illinois on May 12, 1979. After completing high school in Columbia, Illinois, she began pursuing a Bachelor of Science Degree in Biomedical Engineering at St. Louis University. She completed her degree in 2001. Following graduation, she received an NSF/IGERT Graduate Fellowship from Purdue University, and subsequently began work towards a Doctorate in Biomedical Engineering. Her project on molecularly imprinted hydrogels was supervised by Professor Nicholas A. Peppas. She transferred to the University of Texas at Austin with Professor Peppas in January of 2003. She completed her doctoral degree in August 2005 before moving on to post-doctoral work at Rice University. She thinks it is nifty that at least one person is reading this right now.

Permanent Address: 12345 Alameda Trace #218, Austin, TX 78727

This dissertation was typed by the author.